GLACIOCHEMICAL STUDIES OF DOKRIANI GLACIER, CENTRAL HIMALAYA, INDIA: IMPLICATION OF SOLUTEACQUISITION PROCESSES

A thesis submitted to the
University of Petroleum and Energy Studies

For the Award of
Doctor of Philosophy
in
Petroleum Engineering and Earth Sciences

BY
Shipika Sundriyal

July 2022

SUPERVISOR (s)

Dr. Uday Bhan
Dr. D P Dobhal

UPES
UNIVERSITY OF TOMORROW

Department of Petroleum Engineering & Earth Sciences
School of Engineering
University of Petroleum & Energy Studies
Dehradun-248007: Uttarakhand

GLACIOCHEMICAL STUDIES OF DOKRIANI GLACIER, CENTRAL HIMALAYA, INDIA: IMPLICATION OF SOLUTEACQUISITION PROCESSES

A thesis submitted to the
University of Petroleum and Energy Studies

For the Award of
Doctor of Philosophy
in
Petroleum Engineering and Earth Sciences

BY
By Shipika Sundriyal
(SAP ID 500033392)

July 2022

Internal Supervisor

Dr. Uday Bhan
Senior Associate Professor
Department of Petroleum Engineering & Earth Sciences
University of Petroleum & Energy Studies

External Supervisor

Dr. D P Dobhal
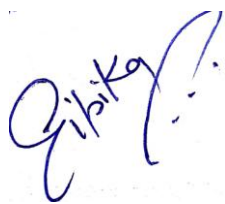Retired Scientist 'F'
Wadia Institute of Himalayan Geology,Dehradun

UPES
UNIVERSITY OF TOMORROW

Department of Petroleum Engineering & Earth Sciences
School of Engineering
University of Petroleum & Energy Studies
Dehradun-248007: Uttarakhand

DECLARATION

I declare that the thesis entitled "**GLACIO CHEMICAL STUDIES OF DOKRIANI GLACIER, CENTRAL HIMALAYA, INDIA: IMPLICATION OF SOLUTE ACQUISITION PROCESSES**" has been prepared by me under the guidance of Dr. Uday Bhan, Senior Associate Professor, Department of Petroleum Engineering and Earth Sciences, University of Petroleum and Energy Studies, Dehradun and Dr D P Dobhal, Scientist F (Retired), Centre for Glaciology, Wadia Institute of Himalayan Geology, Dehradun. No part of this thesis has formed the basis for the award of any degree or fellowship previously.

Shipika Sundriyal

Department of Petroleum Engineering and Earth Sciences

University of Petroleum and Energy Studies

Dehradun-248007

DATE: 20/07/2022

THESIS COMPLETION CERTIFICATE

I certify that Shipika Sundriyal (SAP ID 500033392) has prepared her thesis entitled **"Glacio chemical studies of Dokriani Glacier, central Himalaya, India: Implication of solute acquisition processes"** for the award of PhD degree of the University of Petroleum and Energy Studies, under my guidance. She has carried out the work at the Department of Petroleum Engineering and Earth Sciences, University of Petroleum & Energy Studies.

Internal Guide

Dr. Uday Bhan   18/07/2022

Senior Associate Professor

Energy Cluster [Department of Petroleum Engineering & Earth Sciences]

School of Engineering, University of Petroleum & Energy Studies (UPES)

Village & Post -Bidholi, Via Premnagar

Dehradun

Ph- 8765432128,

Email: ubhan@ddn.upes.ac.in

Place: Dehradun

Date: 18/07/2022

Energy Acres: Bidholi Via Prem Nagar, Dehradun - 248 007 (Uttarakhand), India T: +91 135 2770137, 2776053/54/91, 2776201, 9997799474 F: +91 135 2776090/95
Knowledge Acres: Kandoli Via Prem Nagar, Dehradun - 248 007 (Uttarakhand), India T: +91 8171979021/2/3, 7060111775

NEW

ENGINEERING I COMPUTER SCIENCE I DESIGN I BUSINESS I LAW I HEALTH SCIENCES AND TECHNOLOGY I MODERN MEDIA I LIBERAL STUDIES

WADIA INSTITUTE OF HIMALAYAN GEOLOGY
(An Autonomous Institution of Department of Science & Technology Govt. of India)
33, General Mahadeo Singh Road, Dehra Dun –248 001 (UK.)

Dr. D.P.DOBHAL
Scientist 'F' (Retired) and
Former Group Head
Geomorphology & Environmental Geology,
Centre for Glaciology

THESIS COMPLETION CERTIFICATE

I certify that Shipika Sundriyal (SAP ID 500033392) has prepared her thesis entitled **"Glacio chemical studies of Dokriani Glacier, central Himalaya, India: Implication of solute acquisition processes"** for the award of PhD degree of the University of Petroleum and Energy Studies, under my guidance. She has carried out the work at the Department of Petroleum Engineering and Earth Sciences, University of Petroleum & Energy Studies.

External Guide

(Dr. D P Dobhal)

Place: Dehradun

Date: 20.07.2022

ABSTRACT

The glacier chemistry in the snow/ice has been originated since the glacier formation and established in forms of chemical weathering. The present study is an effort to understand the regional ionic stoichiometry as major chemical weathering problem and explains the interaction between water- rock interactions. The present work is mainly concentrating on chemical weathering mechanism through solute acquisition and provenance by using multi statistical and modelling approach. The study has presented the conceivable explanations for carbonate/silicate weathering pattern at the precipitation dominated central Himalaya and plausible mechanism which regulates the short to long term climatic setting. The Himalayan glaciers receive its nourishment from interaction of WD and ISM. Since, central Himalayan glacier is equally affected by both precipitation patterns therefore central Himalayan glacier is more suitable for studies. We have quantified the atmospheric deposition in snow/ice in Dokriani Glacier valley of central Himalaya and correlated with the melt water data by statistical approach and modelling. To estimate the ions in meltwater and quantify rate by carbonate and silicate weathering in glacier melt water carried out field for 4 years during 2015 to 2018. Other than this a well-established modelling is opted to resolving the relationship between atmospheric and terrestrial chemistry. Based on these measurements results divided into 3 season early, peak and late ablation. The aim of this study is examine the solute acquisition processes of Dokriani Glacier to the changing climate through the observations of chemical weathering and solute apportioning model. As part of my work, total

260 samples were taken from the accumulation, ablation, Supraglacial Lake, snow pit, englacial channel, snout and melt water from the discharge sites of Dokriani glaciers. The pH and EC of these meltwater are found to be under 7 and conductivity in between 22-128 μS cm^{-1}. Results show the Ca^{+2} is the most dominant cation whereas a SO_4^{-2} was observed the most dominating anion. High ratio of Ca+Mg vs TZ^+ and Ca+Mg vs Na+K elucidate that the Dokriani glacier melt water is mainly controlled by a carbonate weathering. Detailed geochemical studies were taken through combined measurements of major ions and trace elements in melt water. Under such terrain and lithology, water rock interaction along with sediment and debris has the possibility to produce more ions found in the meltwater. This indicate that the meltwater that solute chemistry have a significant controls in term of lithology and atmospheric deposition.

The major ion concentration of melt water between the years 1994–2015 has been reassessed to infer the glacial/subglacial weathering induced ionic release from Dokriani glacier system. The results from meltwater data collected during ablation period shows that Ca^{+2} is more dominant cation followed by Mg^{+2}, K^+, Na^+ and SO_4^{-2} is most dominant anion followed by HCO_3^- and Cl^-. Ca + Mg vs total cations shows the overall dominance of carbonate weathering whereas Na+K vs total anions shows high positive relation suggesting domination of both carbonate and silicate weathering. By comparison, the ionic concentration of the study period with previous published data suggests a significant increase since 1994; however, the discharge weighted concentrations could provide more detailed estimates. An increasing trend in major cations viz. calcium (Ca^{+2}) and magnesium (Mg^{+2})

while the bicarbonate (HCO_3^-), sulphate (SO_4^{-2}) and nitrogen (NO_3^-) has been observed as major anion. Further, the source of Cl^-, NH_4^+, and NO_3^- in the meltwater stream is mainly derived from the atmospheric precipitation, anthropogenic, and weathering process.

An attempt is also made to understand the atmospheric deposition and transport at the Himalaya on induce glacier melting. Investigated trace elements (TEs) concentration and depositional pattern at Dokriani Glacier, central Himalaya to understand their levels, dynamics, and potential effects. The results of analyzed trace metals (Al, Cr, Mn, Fe, Sr, Co, Ni, Cu, Zn, Cd, As, and Pb) showed high enrichment values for Zn, Cr, Co, Ni and Mn compared to other parts of the Himalayan region, suggesting the influence of anthropogenic emissions (e.g., fossil fuel, metal production, and industrial processes) from urbanized areas of South Asia. Our results also revealed the possible health effects related to the enrichment of Zn and Cd, which may be responsible for skin-related diseases in Uttarakhand region. In order to understand and quantify the composition of major ions and its contribution in water resources, a long term database is required that provides the local as well as global knowledge and database with respect to climatic conditions. Geochemical studies concerning wet precipitation over glaciers are limited throughout the world. In the shallow snow pit from Dokriani Glacier was undertaken for the pre-monsoon season to understand the cycling of major ions from atmosphere to solute acquisition process. The intimating connections of ions cycling in snow and its temporal behavior was observed and analyzed through various statistical tests. Among major ions, the SO_4^{2-} has the highest concentration among anions on an average considered as

14.21% in 2013 and 29.46% in 2015. On the other side Ca^{2+} is the dominant cation contributing 28.22% in 2013 and 15.3% in 2015 on average. The average ratio of Na^+/Cl^- was higher in 2013 whereas lower in 2015. The backward trajectory analysis suggests the possible sources of the ions transported from Central Asia through the Western Disturbance (WD) as a prominent source of winter precipitation mainly in the Central Himalaya.

Therefore, it is concluded that the chemical weathering regulates the chemistry of glacier and enhanced the melting process. Overall results suggest that 20% of atmospheric pollution contributes in the glacier and rest 80% significantly contributes the weathering ions in the glacier. These results imply that the in glacier the controlling factor which regulates the melt water of the glacier is chemical weathering. Therefore, it is concluded that the in early ablation is weathering rate is high and gradually decreasing in peak ablation season.

In the studied area, covering only little bit part of Central Himalayan glacier yielded the weathering rate in the range of (42.3, 46.6 and 15.7 t km^{-2} y^{-1} for early, peak and late ablation season respectively). Further, it is comparatively unpolluted and reusable in nature and hence becoming a preferred choice for an alternative energy resources worldwide. Possibly, the significant contribution of trace elements and weathering rate of the Dokriani Glacier will have an impact on the local public lived in the locality and economy with reformation for mountaineering training and tourism on this glacier becoming much more difficult in future. In addition, the results of present study on Dokriani Glacier provide base line information on how central Himalayan glaciers respond in present scenario.

ACKNOWLEDGEMENTS

Indeed during my journey to the mountains, I met numerous people who helped unconditionally and provided support every time I need. I would like to express my deep gratitude to all of them.

First of all, I would like to thanks Centre for Glaciology, Wadia Institute of Himalayan Geology, Department of Science and Technology (DST), for providing funding and research facilities. I am thankful to the Director, Wadia Institute of Himalayan Geology (WIHG), Dehra Dun, and National Institute of Hydrology, Roorkee, India for providing facilities and ample support to carry out this work. Beside, this I would also like to express my gratitude to Department of Science and Technology, New Delhi women scientist scheme (WOSA) (DST/WOSA/EA-44/2016) for giving me financial support for my research work.

Foremost, I would like to thanks my external guide, **Dr. D.P. Dobhal**, for introducing me to the Himalayan glaciers. His deepest knowledge in the field always push me inspired me to work. His unconditional support and motivation at every phase illuminate my career as a glacio-chemist.

I would like to express my deepest gratitude to my internal Guide, **Dr. Uday Bhan**, for his valuable unwavering guidance to understand dynamics of complex Himalaya and its climate.

To all the former and present post docs, senior researchers and professors during my time as a researcher, I would like to thank Dr. Rajesh Singh, Dr. Manish Mehta, Dr. S K Bartarya, Dr M K Sharma, Dr R J Thayyen, Dr Pradeep Srivastava, Dr Rajita Shukla, Dr.Amit Kumar, Dr

Table of Contents

LIST OF ACRONYMS AND ABBREVATIONS

AAR- Accumulation Area Ratio

ABC- Advance Base Camp CC–

Carbonate Carbonation CD–

Carbonate Dissolution CDR–

Chemical Denudation Rate

CWR–Chemical Weathering rate

DKD- DraupadiKaDanda EA–

Early Ablation

EF- Enrichment Factor

ELA- Equilibrium Line Altitude

GHG–Green House Gases

GPS - Global Positioning system

HHC- higher Himalayan Crystalline

HYSPLIT- Hybrid Single-particle Lagrangian Integrated Trajectory model

ICP-MS- Inductively coupled plasmamass spectrometry

IGP–Indo Gangetic plain

IHR- Indian Himalayan Region

ISM–Indian summer monsoon

LA- Late Ablation

LLM- Left Lateral Moraine

MCT- Main Central Thrust

NE- North East

NIH - National Institute of Hydrology

NNW- North Northwest wards

NOAA- National Oceanic and atmospheric Administration

PA -Peak Ablation

PCA- Principal Component Analysis

RLM- Right Lateral moraine SHC–

Simple hydrolysis of carbonates

SMF–Sulphate mass fraction

SO- Sulphide Oxidation SRM–

Snowmelt runoff model SSL–

Suspended Sediment LoadSW-

South West

SWR–Silicate weathering rate

TEs–Trace elements

TSS–Total Suspended Sediment

UCC- Upper Continental Crust

WDs–Western Disturbance

WGMS- World Glacier Monitoring Service

WIHG - Wadia Institute of Himalayan Geology

WWN- West West-Northwards

List of Figures

standards-II, product no-057590) traceable to National Institute of
Standard (NIST).

List of Tables

CHAPTER 1

INTRODUCTION

Earth's climate and habitability were long being linked with tectonic uplift, accompanied by increase in physical erosion rates (Hren et al., 2007), and chemically constrained nutrients transfers from high altitudes to oceans (Ramyo and Ruddiman, 1992; Lanord and Derry,1997; Gaillardet et al., 1999; Hilton and West, 2020). Studies have enabled an improved understanding for the effect of physical and chemical erosion over orogenic belts of the Earth and highlighted the role of atmosphere-rock-water interactions and nutrient cycling over shorter (10^0– 10^1) to longer (10^3-10^5) time scales (Hilton and West, 2020 and references therein). One such system is present at the Himalayas which extend up to ~ 2400 km from North West to South i.e. from Karakoram to Indo-Gangetic Plain (IGP) by connecting five countries i.e. India, Nepal, Bhutan, China and Pakistan of southern Asia. The Himalaya (also known as "water towers of the Asia") contain approximately 2955 to 4737 km^3 of ice volume spread over 40,800 km^2 of area (Frey et al.,2014, Bolch et al.,2012, Raina & Srivastava., 2008, SAC, 2014) and regarded youngest among different orogenic systems on Earth. The mountain ranges of mighty Himalayas are heavily glacierized at the top and provide melt water for the downstream people in addition to the rainfall generating streamflow in rivers (Singh & Bengtsson, 2004; Immerzeel et al., 2010; Thayyen & Gergan, 2010).The total glacier melt in Ganges, Brapmputra and Indus rivers contributed by using snowmelt runoff model (SRM) are ~ 10%, 12%, and 14% respectively (Immerzeel et al., 2010). While the contribution of rainfall accounts for 30-66% and found to be a major source to river runoff (Lutz et al., 2016). Overall, the Himalayan glaciers receive the precipitation (both rainfall and snowfall) principally throughout earth systems i.e., the Indian summer monsoon (ISM) and

Western Disturbance (WDs). In central Himalaya nourishment taken place by both ISM as well as WDs but higher precipitation ensue from western disturbance in winter (Dobhal et al., 2008; Thayyen & Gergan, 2010) while eastern to western Himalaya nourished by ISM precipitation (Wagon et al., 2013; Azam et al., 2014).This categorize the Western, Karakorum, Trans Himalaya and Tibetan glaciers as winter accumulation type, whereas southern and eastern Himalayan glacier as summer accumulation type. The Himalayan system feeding the largest river basin system i.e. the Brahmaputra, the Indus, the Ganga contains one of the largest number of glacier such as Indus basin houses ~7997 glaciers, whereas Ganga and Brahmaputra contains about 968 and 610 glaciers respectively (Raina and Srivastava, 2008). According to the recent Himalayan glaciers inventory the accountability of small glacier (<1%) falls around 66%, which covers12% of the total glacierized area and only 4% of the total ice volume, in contrast large glaciers comprises 0.1% in number with 13% of glacierized area and 27% of the total ice volume (Sangewar &Shukla, 2009) (Table 1). The large glacier lies upto 3800 m a.s.l. whereas small glacier lies above 4500 m a.s.l .and characterized with cold climate of the glacial valley system. They are known for its water storage capacity as glaciers and freshwater supply which is foremost required to sustain environmental and human water demands downstream (Viviroli et al., 2007; Immerzeel et al., 2010) with its dynamics controlled through micro-climate variability, topography and hydrological balance. Himalayan glacier although comesunder "temperate glacier systems" as they exists at the freezing point throughout. With its typical feature for presence of water at the glacier bed and capability of eroding them, it has received significant attention from geochemist, as these conditions typically favor the conditions for chemical weathering. Previous studies from Himalayan glaciated basins concerning solute fluxes suggest the chemistries lie above the global mean rate (Gaillardet et al., 1999; Torres et al., 2017). However, that speculation leaves abroad scope for determination of chemical weathering sources driven by water discharges from glacial basins.

1.1 Chemical weathering of glacier systems

The process of chemical weathering influences the atmospheric composition by ionicrelease from minerals by altering the alkalinity and redox condition of the system (Gaillardet et al., 1999; Torres et al., 2017). The glaciers, which are known as active agents of chemical weathering has got significant attention in this regard, as it holds the potential to act both aspositive and/or negative feedback to climate (Tranter et al., 1996; Sharp et al., 1995; West et al., 2000). In general, glaciers release ions through silicates and carbonate mineral dissolution processes coupled to the formation of acids through drawdown of atmospheric CO2 and release of protons through snowmelt (Tranter et al., 1993; Appelo and Postma, 2005).

However, there is significant gap in the understanding for the combination between geo-chemical reactions in proglacial and subglacial environments and nature and type of reactions which release ions during ablation season. Also, the release of glacial solute fluxes largely driven by water discharge and non-silicate sources (Anderson et al., 1997) further complicates the origin and effects of ionic release from glacierized basins of the Himalayas. The process of chemical weathering is broadly divided into two important components i.e. silicate and carbonate mineral dissolution. In general, ionic stoichiometry of glacial meltwater suggests the domination of carbonation (dissolution through carbonic acids) of silicate and carbonate mineral in generating ions from glacierized catchments (Sharp et al., 1995, Hindshaw et al., 2011, Hodson et al., 2000).

Table 1: Presents the summary of glaciers numbers, area and ice volume respected basin and sub basins of the Himalaya system. Table modified from Raina & Srivastava (2008) and Sangewar & Shukla (2009).

Basin Name	No. of glaciers	Glacierized area (km^2)	Volume (km^3)
Indus Basin			
Ravi	172	193	8.04
Chenab	1,278	3,059	206.30
Jhelum	133	94	3.30

Beas	277	579	36.93
Satluj	926	635	34.94
Indus	1,796	8,370	73.58
Shyok	2,454	10,810	601.71
Nubra	204	1,536	204.55
Kishanganga	222	163	5.93
Gilgit	535	8,240	---
Total	**7,997**	**33,679**	**1,175.30**
Ganga Basin			
Yamuna	52	144	12.21
Bhagirathi	238	755	67.02
Alaknanda	407	1255	90.75
Ghagra	271	730	43.77
Total	**968**	**2884**	**213.70**
Brahmaputra Basin			
Teesta	449	706	39.61
Brahmaputra	161	223	9.96
Total	**610**	**929**	**49.57**
Indus + Ganga + Brahmaputra	**9575**	**35338**	**1268.60**

Conversely, in process the weathering of non-silicate minerals (such as sulfide oxidation) as major solute source were majorly neglected much likely due to its minor presence in catchment rocks. Recent studies (Torres et al., 2014; 2017; Shukla et al., 2018) have although highlighted the role of oxidative weathering in solute fluxes draining glacierized catchments. The presence of sulfide and carbonate minerals in most rocks are considered to below in abundance, however, their dissolution rates are orders of magnitude faster (for pyrite log rates value are −6 to −10, and for silicate minerals are −10 to −16) than silicate minerals (Williamson and Rimstidt; 1994; White and Brantley; 2003). This current a strong case for weathering of these trace stages primarily as "limited supply" in nowadays, and present every possibility to supply more minerals for reaction if discharge increases. However, silicate and carbonate weathering is not constantly supply partial and dominated the ionic chemistries of glacierized basins. Therefore, the relative significance of carbonation and/or sulfide oxidation as a sourcefor ionic release in glacial basins needs detailed investigation in terms of its inputs through atmosphere and from underlying bedrocks. Additionally, in

glacierized basins chemical weathering also depends on several other factors like precipitation, snowpack chemistry, microbial processes, organic matter content and groundwater input (e.g. Mitchell and Brown,2008), contributing towards ionic release throughout the ablation season.

1.2   Controls of chemical weathering

Also the basin with valley type characteristics effects the seasonal concentration of major ionic release from glacial basins. For example, due to the sudden opening of subglacial conduits congested by ice/snow dams which inhibiting them from dominates in variance percolation of snowpack-derived solutes (mainly Na^+, Cl^-) in early ablation period, prevents them from exhausting the glacier proficiently (Wadham et al., 2010; Huang et al., 2010; Irvine-Fynn et al., 2011). As the melting increases, an additional channelized system develops and the effect of long resistance time over ionic concentration diminishes (Tranter et al., 2002). In transport dominated or channelized systems carbonation of silicate and carbonates usually dominates, whereas, the weathering of non-silicate minerals (i.e. sulfide oxidation and organic carbon oxidation) presents an important characteristic for distributed (weathering-dominated) systems (Tranter et al., 2002). As the ablation progresses the difference in ionic chemistries become visible and links to be tied with subglacial channel connectivity and biogeochemical processes operating inside the glacial system (Wadham et al., 2000; Cooper et al., 2002; Kristiansen et al., 2013). Therefore, the difference in between chemical process and characteristics in both proglacial and subglacial zones in a glacierized basin are needed for consideration. During the whole ablation period the chemical processes in subglacial and proglacial system. The chemical processes in the proglacial and subglacial drainage systems concern with these to snow and ice ablation rates during the whole ablation period. Also the dominant reactions like silicate vs non-silicate weathering needs detailed investigate onto ascertain the fate of ionic release from glacierized basins of the Himalayas.

1.3   Motivation of the research

Rainfall-runoff assessment of rivers originating from High Mountain Asia suggests upto 10% increase in runoff until 2050 (Lutz et al., 2014). Main highlighting has been sited on warming induced glacial retreat (Bolch et al., 2012), but solute fluxes from glaciated areas are also projected to change with continuous warming due to increases in discharge as a result of a longer melting season. The systematic efforts presented till now have inferred the seasonal pattern of meltwater chemistry relying on the interpretation of ionic release by chemical mass balance stoichiometry of Himalayan glacierized basins. Until recently, studies has proposed the dominance of either carbonate or silicate weathering reactions based on seasonal meltwater chemistries of the Himalayan glacierized basins; however, rarely any study has examined the prominent role of H^+ in Himalayan glacierized catchments in different ablation periods, despite the in prove influence over organic matter cycling, precipitation/snowpack chemistry and chemical weathering reactions (Singh and Hasnain,1999; Mitchell & Brown, 2008; Shukla et al., 2020). This has now become an emerging area of glacial geochemical weathering research over last two decades from glacial basins. Still it is unclear about the mechanism and favorable environment at which sulphide oxidation proceeds (Wadham et al., 2007, 2010). Hence, it seems appropriate explanations how chemical weathering reactions in different ablation periods affect the meltwater chemistry which is more varying than previously explained. Here we extend the present understanding of chemical weathering at Himalayan glacierized basins by combining the existing literature with new meltwater chemistry dataset from a precipitation dominated glacial system (Dokriani glacier basin) by studying the ionic deposition pattern as snow fall and release with glacial melt.

1.4   Objectives

This thesis is motivated by a set of research questions explained in previous sections that aim to further enhance our understanding of the environmental processes that affects the solute acquisition processes of a glacierized basin of the Himalaya. Thematically, these questions can be

separated into three main objectives, which are detailed below:

- To study the ionic compositions of snow, ice and melt-water streams in the glacial environment.
- To study the contribution of natural and anthropogenic sources in the solute acquisition processes.
- To identify the source mechanism of ionic release in glacial meltwater.

1.5   Outline of the thesis chapters

The outline of the thesis commenced into chapters and each chapter which is presented by section, subsection and paragraphs.

Chapter1 Introduction briefly discusses the Himalayan glaciers, their distribution, nourishment and climatic setting over the high altitude Himalayan basin and their importance in cryosphere studies. The chapter also briefly introduced about the behavior of chemical weathering in glacier system and what are the forces which regulate the chemical weathering. Besides this, the chapter also deliberates the research gap and the motivation of research on approved topic, objectives of the research which highlights the solute acquisition processes in the glacier meltwater by using chemically and empirically based equation.

Chapter2 Literature review provides the extensive background and understanding of previous studies on the glacio-hydrochemistry, trace elements and process regulating the solute chemistry carried out in the Indian and other part of Himalaya on which thesis is focused. This chapter also highlights the gap area and its need for fulfillment.

Chapter3 Study Area describes the physio-geographical setting, climatic setting, and geology, geomorphological and glacial features of Din-Gad catchment. Further, characteristic features of glacier, and discharge site are explained with pictorial map and figures taken during fieldwork.

Chapter 4 Methodology chapter includes detailed description of the in-situ

instruments and lab instrument used for the study of physical and chemical parameters along the Din-Gad valley. Chapter includes the extensive field remarks of both zone accumulation as well as ablation zone. The field work divided into the 3-part early ablation, mid ablation and late ablation. Furthermore, data acquisition scheme, data gap and accuracy assessment in data collection are also presented. The chapter deals with the analysis of collected water and snow/ice samples. In broader view, the chapter provides the seasonal as well synoptic variations in solute chemistry along the glacier valley.

Chapter5 Result and Discussion includes the seasonal variation of meltwater in the catchment and their influences on weathering processes in the central Himalaya. Future, atmospheric pollutant at snowpit has been computed. Besides this diurnal water samples were collection to show temporal solute variations in Dokriani Glacier. First time, enrichment factor of trace elements to show the dominance of natural *versus* anthropogenic over the glacier has been conceptualized.

Chapter 6 Conclusion and Future Implications concludes by discussing major findings and future implications. The conclusion of this chapter presents the overall goal, the present day understandings of chemical characteristics for the central Himalayan glaciers. Furthermore, emphasis is given to address future opportunities for its contentment for benchmarks glaciers monitoring programme in the Indian Himalaya.

CHAPTER 2

LITERATURE REVIEW

Dissolved ionic chemistry of natural water provides an important information about landscape characteristics like as sets of minerals contemporary, exposed area of surface, flow paths of solute, vegetation, and climatic parameters such as temperature, solar radiation, precipitation and water flux. Appreciated efforts has been done over glacial system of the Himalayas to simulate the kinetics of particular mineral weathering, controlled through mineralogy, temperature, pH, and solution saturation states (Singh et al., 2002, 2017a,b,2015a,b,2014,2018; Thayyen and Hasnain, 1999). Studies so far, have put the focus on geochemical studies over glaciated regions two-fold. Primarily, the deposition and transportation mechanism of glacial meltwater were established by ionic concentrations and their respective ratios which is followed by establishing the chemical denudation rates (CDR) of glacial meltwater (Singh et al., 2001; Ramanathan et al., 2000; Souchez and Lorrain, 1975, 1978). On the other hand the influence of chemical weathering over global systems were connected with atmospheric process which effects the cycling of ionic release from minerals that ultimately alter the alkalinity and redox state of the ocean–atmosphere system (Torres et al., 2017 and references therein). Particularly, the alkalinity production through weathering of silicate and carbonate minerals and removal of atmospheric carbon dioxide were responsible for acid production and subsequent ionic release. This process is widely recognized as chemical weathering perspective of small and big glacier systems of different orogenic systems of world.

2.1 Globally chemical weathering perspective

9

Glacial catchments worldwide have experienced an almost 1.2-4 times higher Chemical Denudation Rate (CDR) (the rate at which net dissolved mass loss in the solution) compared to global mean which includes glacial and non-glacial catchments and an artifact of lithology and modern climate differences (Anderson et al.,1997; Tranter et al., 2002; Wadham et al., 2010).The nonglaciated catchments which inclined to from lower latitude thus seemingly to represent warmer climates that will have larger chemical weathering rates. The most recent estimates of cation fluxes presented by Torres et al. (2017) suggests that in glacier catchments the mean cation weathering yield is high (21.5 $tkm^{-2}yr^{-1}$), compared to world's largest rivers (18 $tkm^{-2}yr^{-1}$). These variations are linked with 5.8 time's high runoff of glacial catchments than global river runoff. Concerning the weathering yields from the Himalayan glacier catchments (35.93 $tkm^{-2}yr^{-1}$), is even higher than global glacial catchments. The details of fluxes from Himalayas and global fluxes and their comparison are presented in Table 2.1.

The global estimates presented for glacial basins were attributed by strong seasonal discharge (Tipper et al., 2006b; Bookhagen and Burbank, 2010) and rapid retreat (Bolch et al., 2012), which contribute an increase in CO_2 concentration and solute yield (West et al., 2002). Changes in atmospheric inputs such as atmospheric pollutant deposition, evapotranspiration, forest cover reduction, change in energy budget, and change in greenhouse gasses (GHG) concentration would considerably change the precipitation and moisture availability for temperate glacier systems worldwide (Gaffen and Ross, 1999; Duan and Yao, 2003; Tranter, 2006). These climatic constrain alter the weathering pattern along with the temperature in the region, which generates a negative feedback mechanism of climate weathering system (Gabet et al., 2010).

2.2 Chemical weathering perspective of Himalayan Glaciers

The most comprehensive estimate of Himalayan Glaciers was generated from 18 glacial catchments covering ~702.7 km^2 area and approximately 32.6%

glacial cover (Table 2.1). The lithological control of ionic flux presented from carbonate rich, silicate rich lithologies are found to be 7.8 % to 9.3% respectively. However, these fluxes are attributed to Metamorphic (59.2%), carbonate rich sediment(7.80%) and plutonic rocks (23.7%) present in catchment rocks. Climatologically, they receive their inputs from two weather systems i.e. Indian summer monsoon (ISM) and Western Disturbances (WDs). Upon them majority of the precipitation (~80%) commenced from ISM during monsoonal months (i.e. May-September) (Burbank et al., 2012; Bookhagen and Burbank, 2010). The long term data available from Himalayan Glaciers were majorly limited to few glacier systems of central and western Himalaya such as Chotta Shigri, Bada Shigri, Patsio, Dokriani, Gangotri, Satopanth, Bagni, Kafni and Batal Glaciers.

They shows the melt water availability at circum-neutral pH conditions and controlled by majorly carbonate weathering process (Shukla et al., 2018 and references therein). The detailed chemistries of western and central Himalayan Glaciers are as follows:

Table 2.1: Summary statistics for glaciated catchments by region, and comparison to literature values of global attributes (Modified after Torres et al., 2017).

Attribute	Northern Latitudes	New Zealand	Alps	Himalayas	Rocky Mountains	Andes	Kilimanjaro	Iceland	Globe
Number of catchments	20	13	8	18	18	10	1	7	95
Number of samples	4241	35	638	568	2018	34	1	161	7696
Catchment area (km^2)	82.6	231.2	26.1	702.7	3071.2	40.1	11.3	3137.9	1002
Glacial cover	62.9%	27.4%	59.7%	35.6%	28.1%	39.3%	4.0%	15.9%	39.40%
Distance from snout (km)	0.70	14.10	0.60	5.10	12.60	2.60	8.60	51.10	9.60
Ca conc. (μmolL^{-1})	179.60	235.90	72.10	429.20	320.80	502.50	22.30	74.70	276.90
Mg conc. (μmolL^{-1})	71.60	27.20	11.40	174.90	103.40	210.20	12.60	40.30	97.70
Na conc. (μmolL^{-1})	82.10	51.40	6.68	45.00	18.30	56.70	306.10	230.20	63.00
K conc. (μmolL^{-1})	10.70	25.60	8.72	29.50	6.55	8.78	54.90	10.30	15.60

Ca / cation flux (mol%)	56.0%	68.9%	58.0%	59.8%	68.0%	63.3%	5.60%	21.10%	58.60%
Mg / cation flux (mol%)	21.40%	8.10%	10.60%	17.90%	20.00%	27.70%	3.20%	11.30%	17.50%
Na / cation flux (mol%)	18.90%	15.90%	14.80%	11.30%	7.90%	7.70%	77.30%	64.70%	17.40%
K / cation flux (mol%)	3.70%	7.20%	16.60%	11.00%	4.10%	1.30%	13.90%	2.90%	6.50%
Carbonate-rich sed.	58.90%	29.40%	14.00%	7.80%	25.80%	50.00%	0.00%	0.00%	29.20%
Siliciclastic sediment	6.60%	8.50%	2.40%	9.30%	31.30%	0.00%	0.00%	0.00%	10.40%
Metamorphic	27.70%	61.60%	33.10%	59.20%	22.00%	0.00%	0.00%	0.00%	32.40%
Volcanic rocks	6.70%	0.00%	2.80%	0.00%	12.80%	50.00%	100.00%	99.80%	17.80%
Plutonic rocks	0.20%	0.50%	47.70%	23.70%	8.00%	0.00%	0.00%	0.20%	10.10%
Runoff (mm yr^{-1})	1090		2401	1517	2162	2771		2182	1733
Weathering yield (t km^{-2}yr^{-1})	14.7		6.37	35.93	20.26	36.1		21.13	21.39

2.2.1 Chemical status-quo of western Himalayan Glaciers

Western Himalayan (WH) Glaciers cover~8943 km^{2}of glacierized area (415-895 km^3 volume) with a mean elevation of 5155 m a.s.l. (Bolch et al., 2012). In winter season the western Himalayan receives the precipitation from westerlies and in summer season from Indian summer monsoon (Yadav et al.,2011). The glacial systems were studied for various glaciological aspects such as mass balance, hydrology, energy balance but few glaciers has been systematically studied from meltwater hydrochemistry. These glaciers include Chotta Shigri, Bada Shigri, Patsio and, Batal glacier systems. Geologically the main rock type of the region is Central Crystalline Zone of the Pir Panjal range the valley is all along exposed with limestone group (Srikantia and Padhi, 1963). In Bara Shigri, Chhota Shigri, Patsio, Kafni, Dudu, Batal Glaciers various types of rock such as granite, milky-white muscovite equartzite, augen gneiss, schistose gneiss, muscovite-biotite-schist and granitic gneiss are reported (Singh et al., 2016; Rai et al., 2016; Kumar et al., 2019; Sharma et al., 2013).The hydrogeochemical aspect studied so far from western Himalayan Glaciers have presented variability in ionic fluxes. Estimates presented from different glacier systems suggests that HCO_3^- was the most dominant anion and Ca^{+2} was the most dominant cation among total ionic concentration. While the other ions follows the trend such as $HCO_3^- > SO_4^{-2} > NO_3^- > Cl^-$ in anion whereas in cation $Ca^{+2} > Mg^{+2} > Na^+ > K^+$. The chemical characteristics of melt water draining Western Himalaya shows range of variability. The average concentration of physical parameters ranges between 6.3-7.2 and $13.6 - 156$ μScm^{-1} for pH and electrical conductivity (EC) respectively. However, the major cation concentration (from high to low) follows the following trend: Ca^{+2} (74.4-1035) > Mg^{+2} (48.9-305) > Na^+ (18-50.2) > K^+ (26.6-51.7) $\mu E\ L^{-1}$. Similarly, the trend of anionic concentration are as follows: HCO_3^- (52.3-800) > SO_4^{-2} (66.4-541) > NO_3^- (1.5-20.8) > Cl^- (5-16.3) $\mu E\ L^{-1}$. Glacier meltwater dissolved ionic chemistry of is mainly controlled by the interaction between atmospheric deposition, water-rock interaction, physical and chemical erosion, englacial channels and meltwater runoff (Sundriyal et al., 2021; Hasnain et al, 1999). Although the studies has suggested suspended sediment load (SSL)

highly controls the ratios of (Ca+Mg) vstotal cations and also shows higher contribution of (Ca+Mg) over (Na+K) in solute acquisition processes. The SSL concentrations for studies western Himalayan glaciers vary between 48.8-28.1 for Patsio glacier, ~370 for Chhota Shigri and 7592-1014 mg L^{-1} for Bada Shigri Glacier. During monsoon season (July-August) ~80% of SSL releases by following the discharge pattern respective glacier systems. Studies has suggested highest concentration of SSL in the month of August much likely due to the higher input of incoming solar insolation, high accessibility of unconsolidated material and distended cross section area near the discharge site (Singh et al., 1998; Kumar et al., 2004; Pratap et al., 2002). Overall the chemistry of western Himalayan glaciers is dominated by the carbonate weathering with subordinate inputs from sulphuric acid mediated weathering reactions (Singh et al., 2013, 2014, 2015, 2020; Sharma et al., 2013). For example, high concentration of (Ca +Mg) to TZ^{+} ratio coupled to the dominance of (Ca + Mg) over (Na + K) (Fig. 2.1) corroborated that the hydro-chemistry of meltwater of Western Himalayan glaciers are primarily controlled by carbonate weathering (Pandey et al., 1999; Khadka and Ramanathan, 2013). Further, high ratio of (Ca+Mg) over (Na + K) similarly high contribution of Ca+Mg with respect to TZ^{+}, and very low input of (Na + K) to the total cations (TZ^{+}) demonstrate that Batal Glacier meltwater chemistry is mainly regulated by carbonate weathering and little input from silicate weathering. The carbonate weathering rate (CWR) and silicate weathering rate (SWR) observed at Chhota Shigri Glacier accounts for 97.4 and 22.8 t $km^{-2}y^{-1}$ also suggests the high weathering rate of carbonate over silicate (Singh et al., 2016, 2018). Proton (H^{+} ion) is mainly dominated by sulphide oxidation mechanism for weathering in all studied glacial systems. In continuation pCO_2 value is calculated to understand the kinetic phenomena and active state of productivity of river (Zhu et al., 2013). The average value of pCO_2 in Bara Shigri glacier meltwater is $10^{-2.6}$ (Singh et al., 2018) which is higher than the observed atmospheric pCO_2 i.e. $10^{-3.5}$atm (Jacobson and Langmuir, 1970). Bara Shigri glacier provides a dominance of open and carbonate weathering favorable condition for high pCO_2 values of the meltwater (Jacobson and Langmuir, 1970).

2.2.2 Chemical status-quo of Central Himalayan Glaciers

Compared to western Himalayan Glaciers, glaciers of Central Himalaya (CH) covers ~9940 km^2 of glacierized area (647-1128 km^3 volume) with a mean elevation of 5600 m a.s.l. (Bolch et al., 2012). The Central Himalaya region has similar precipitation trend which is dominated by westerlies during in winter months and Indian summer monsoon during summer months (Yadav, 2011). The glacial systems of central Himalaya include Gangotri, Dokriani, Satopanth, Chaturangi and, Pindari Glaciers. Geologically,the main rock type of the region is Central Crystalline Zone of the Himalaya and contains major metamorphic and granitic rocks types
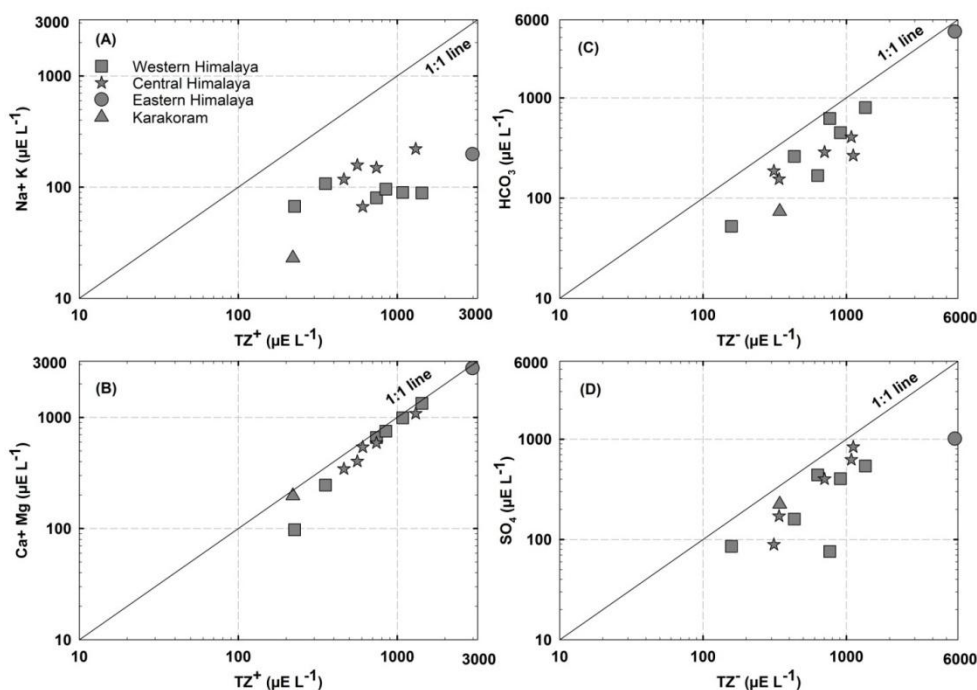
Fig.2.1: Scatter plot of average ionic concentration from Western, Central, Eastern and Karakorum Himalaya. The solid black line represents a 1:1 correlation line. A) Na+K ion against total cationic (TZ$^+$) concentration B) Ca+Mg ion against vs TZ$^+$ C) HCO$_3$ion against total anionic concentration(TZ$^-$) D) SO$_4$ ion against TZ$^-$

For eg granite, muscovite quartzite, augen gneiss, schistose gneiss, muscovite-biotite schist and granitic gneiss (Valdiya, 1999, Shukla et al.,2020) are reported in Dokriani, Gangotri, Satopanth and Pindari glaciers. The

hydrogeochemical aspect studied so far from central Himalayan Glaciers suggest that SO_4^{-2} was the most dominant anion and Ca^{+2} was the most dominant cation among total ionic concentration. While the other ions follows the trend such as SO_4^{-2}> HCO_3^-> NO_3^-> Cl^- in anion while in cation Ca^{+2}> Mg^{+2}>K^+>Na^+. The chemical characteristics of melt water draining Central Himalaya shows range of variability. The average concentration of physical parameters ranges between 5.8-7.6 and 55–122 μScm^{-1} for pH and electrical conductivity respectively. However, the major cation concentration (from high to low) follows the following trend: Ca^{+2} (206-680) > Mg^{+2} (50.8-405) >K^+ (45.7-116) >Na^+ (21-105) $\mu E\ L^{-1}$. Similarly, the anionic concentration trends are as follows: SO_4^{-2} (88.9-837) > HCO_3^- (155-406) >NO_3^- (1.9-35) >Cl^- (11.2-16) $\mu E\ L^{-1}$. The largest (in area) glacier in central Himalaya studied so far is Gangotri Glacier. The hydrogeochemical characteristics of Gangotri glacier suggest its pH ranging from 6.38 to 8.5 whereas in diurnal variation ranges from 5.5 to 8.6. However, the EC varies between 37.3 to 125.6 $\mu S\ cm^{-1}$ in Goumukh and 28.5 to 143.2 $\mu S\ cm^{-1}$ in Bhojwasa. The most dominant cation is Ca^{+2} & Mg^{+2} ranging from 24 to 1106 $\mu E\ L^{-1}$ and 6.6-353 $\mu E\ L^{-1}$ respectively whereas in Gomukh the ranges varies from 40.8-92.7% and 3.7-31.4% of total cation. In case of anions SO_4^{-2} ranges in between 23 and 1095 $\mu E\ L^{-1}$ followed by Bicarbonate lies 12-726 $\mu E\ L^{-1}$. The results shows that decrease in concentration of Ca^{+2}, Mg^{+2}, Na^+ and K^+ which results from the cation exchange, carbonate silicate weathering, subglacial water resources would affect the hydrochemistry of proglacial stream in higher altitude (Sharma et al., 2019). Author also focuses on the altitudinal effect that would decrease the composition of ions and physical characteristics due to the dilution effect produced by augmentation of freshly monsoonal recharged groundwater and downstream area (Ahmad et al., 2019). The average range of total suspended sediment (TSS) lies in between 0.054 to 4.383 g l^{-1}. Daily discharge 4 km downstream from the snout varies from 3.9 to 199.2 m^3s^{-1} during the whole ablation period of the year 2014, 2015 and 2016 respectively. The trend of concentrations of major ions are as follows Ca^{+2}>Mg^{+2}>Na^+>K^+ and SO_4^{-2}>HCO_3^->Cl^->NO_3^-. During early ablation (EA) season the concentration of sulphate ion accounts 75.4%, peak ablation (PA) season

shows the 75.2% and 77.9% in late ablation (LA) season. Other anion like bicarbonate shows 21% during early ablation, 22% in peak flow and 20% late ablation of total anions. Sharma et al., (2019) said that the lowest pH value in glacier sites may be insightful dominance of sulphide oxidation which contributes H^+ ions. In the year 2015, as compared with other years supraglacial and englacial channels may limit the production of H^+ ion and resulting pyrite oxidation which thus increases pH. In another study by Singh et al., 2012 the decreasing (high to low) trend of major anion is $SO_4^{-2}>HCO_3^->Cl^->NO_3^-$ whereas in major cations $Ca^{+2}>Mg^{+2}>Na^+>K^+$ in meltwater of Gangotri Glacier. High contribution of Ca+Mg vs TZ^+ high Ca+Mg /Na+K ratio is 2.63 and Na+Kvs TZ^+ show low ratio i.e. 0.29 indicate the governance of sulphide oxidation and carbonation are the main source of providing H^+ ions and carbonate weathering is the main source for providing ions in the meltwater (Fig. 2.1). The Chaturangi Glacier is also tributary glacier of Gangotri Glacier Singh et al., (2014) conducted study to determine the melt water chemistry of Glacier. The results show that the Ca^{+2}, Mg^{+2}, SO_4^{-2} is the dominant ions followed by the other ions. The ratio of Ca+Mg/TZ^+ average range from 0.79 to 0.86 with 0.82 ± 0.02 showed the largeinput of Ca^{+2} and Mg^{+2} to the total cations (TZ^+). Ca+Mg/Na+K ratio vary from 3.77 to 6.33 with an average value of 4.77±0.79. C ratio is nearby 0.5 which shows the Chaturangi Glacier is mainly dominated by the sulphide oxidation and proton producing mechanism (Fig. 2.1). The Ca+Mg/ SO_4 ratio indicates that the dissolution of silicatic rocks is one of the major sources of sulphate which dominated by the carbonate weathering.

Similar to Gangotri Glacier, Dokriani Glacier system has been studied for its hydrogeochemical characteristics. Previous studies (Thayyen et al., 1994, Tiwari et al., 2018, Sundriyal et al., 2021) suggested Ca^{+2} and Mg^{+2} is the most dominant major cation while sulphate and bicarbonate are the dominant major anion. The order of concentration of major ions in decreasing order (high to low) was observed to be as follows: $SO_4^{-2}>HCO_3^->NO_3^->Cl^->F^-$ for cations and $Ca^{+2}>Mg^{+2}>Na^+>K^+$ for anions respectively. Ca^{+2} and SO_4^{-2} contribute 81% to 67% of the total ions and the bicarbonate show 35% of total

anions respectively. A relative high contribution of Ca+Mg vs TZ$^+$ and Ca+Mg vs Na+K indicate that the carbonate weathering is the major source of ions (Fig. 2.1). The lower ratio of Na+K/TZ$^+$ suggests the minor contribution of silicate weathering in dissolved ions. The ratio between Ca+Mg and HCO$_3$+SO$_4$ attributes that SO$_4$+HCO$_3$ derived from silicate rock weathering. Ca^{+2}, Mg^{+2}, SO$_4^{-2}$ derived from the CaSO$_4$ and MgSO$_4$ contribute the major source of ions in meltwater. In diurnal pattern subglacial solute rich depend on the dissolved ions concentration in meltwater that minimum runoff was observed in early morning and maximum runoff observed in evening. The C ratio strongly exhibits the sulphide oxidation is the major source of SO$_4^{-2}$. Here the scientist is able to find out only reaction involved in regulating the ions in melt water draining from Dokriani glacier but still more clarification and more explanation is required to show a clear view on the status of chemical composition over the glacier.

In central Himalaya other glaciers like Bhagirathi Kharak and Satopanth Glacier. The physical parameter like pH, EC, discharge in Satopanth and Bhagirathi glacier show the following results i.e. EC is in between the range from 11.4 µS cm^{-1}to 26.9 µS cm^{-1} in the year 1989 and 30µS cm^{-1} and 45µScm^{-1} during 1991 (Chauhan and Hasnaian., 1993). The dissolved load concentration in the respective year is 1989 is lower as compared with 1991. However total solute load in 1989 is three times greater than the 1991. However, the major cation concentration (from high to low) follows the following trend: Ca^{+2} (146-294) > Mg^{+2} (47-50) > K$^+$ (25.5-60.3) >Na$^+$ (33.0-57) µE L^{-1}. Correspondingly, the trend of anionic concentration observed: SO$_4^{-2}$ (33.5-88.9) > HCO$_3^-$ (107.9-186.8) > Cl$^-$ (36.6-88.9) µE L^{-1}. The dominant solute concentration in both years are Ca^{+2} in between 146 and 294 µE L^{-1} in cation while in anion bicarbonate varies from 107.9to 186.8 µE L^{-1}however, the daily cationic yield is -7.4 to 11.2% acquired by the hourly mean. The cationic denudation rates were 5.8 mEm^{-2}day^{-1} throughout period in 1989 and 5.57 mEm-^{2}day^{-1} in 1991. The solute load suggests the high flow in 1989 suggest small supply of ions in meltwater. Thus the dominance of these

ions shows that $CaCO_3$ dissolution is the major process in solute acquisition (Fig. 2.1).

2.2.3 Chemical status-quo of Eastern Himalayan Glaciers and Karakorum

Compared to western and central Himalayan Glaciers, a very few glaciers has been studied in Eastern and North-western Himalaya including Karakorum. The Khangari Glacier located at the Eastern Himalaya which is located in the west Kameng district of Arunachal Pradesh. The monsoon pattern is same as discussed in other part of the Himalayan glaciers. The geology of Eastern Himalayan mainly comprises the metasedimentary type of rock like granitic gneiss and tourmaline near the snout (Bhattacharjee and Nandy, 2017; Bakliwal and Das, 1971). There are five type of rock type encountered consecutively are (1) Biotite containing pink granite; (2) Carbonate rich shale/slate; (3) Schist/Quartz; (4) Micaceous sandstone and (5) Leucogranite. Metamorphosed shales and slates consisting porphyroblasr of quartz and calcite, metasedimentary rocks carbonate rich sediments have biotitie (15-17%), feldspar (10-12%), calcite (25-42%), and other like ilmenite+hematite+apatite (~2%). The average concentration of physical parameter of meltwater samples are as follows: pH value are in a range between 6.71 to 7.07, EC ranges from 101.5 to 110.9 μScm^{-1}, Total dissolved solids (TDS) value vary from 51.82 to 56.72 mgL^{-1} (Bisht et al., 2018).The hydrochemical characteristics of meltwater draining from Khangri Glacier shows the dominance of Mg^{+2} in cations whereas HCO_3^- in anion. The average ionic concentration of Khangri Glacier melt water (from high to low) follows the following trend: Mg^{+2} (1623.5) > Ca^{+2} (1152.2) > Na^+ (145.7)> K^+ (52.4); HCO_3^- (4578.2) > SO_4^{-2}(1014.3) > NO_3^- (99.0) > Cl^-(16.7) μEL^{-1}. The higher concentration of $Mg^{+2}$and Ca^{+2} in the meltwater of Khangari Glacier is due to the water dissolution with calcite and Ca feldspar and biotite (Bisht et al., 2018). The high concentration ratio in between Ca+Mg/TZ$^+$ (8.8 ± 0.04 mg L^{-1}) and Ca+Mg/Na+K (7.91±0.39 mg L^{-1}) indicate that carbonate weathering followed by silicate weathering is regulating the ionic chemistries in KhangriGlacier meltwater (Fig. 2.1) (Bisht et al., 2018). In Khangari Glacier

high concentration of HCO_3^- shows the disassociation of atmospheric CO_2 and dissolution of carbonatic rocks (Sharma et al., 2013). The C ratio 0.85 ± 0.01 , which shows the evidence in Khangari lacier is mainly controlled by the carbonation reaction whereas the average value of S ratio (0.1 ± 0.01) indicate that in meltwater chemistries in Khangari Glacier is controlled by carbonate reaction. A comprehensive study has been done in the western part of Himalaya. The western Himalaya climate is moist and moderate. The mean annual precipitation receives is 1100 mm, which generally dominated from south west monsoon. Geologically, the valley is stemming from Triassic, Kinestone, Limestone, Quaternary Karewas, Permo-Carboniferous Panjal Traps and alluvium (Jeelani 2005). The average concentration of physical parameter of meltwater samples are as follows pH value are in a range between 9.21-11, EC ranges in between 50-88 μS cm^{-1} respectively. The most dominated cations in meltwater are Ca^{+2}(157.2) followed by Mg^{+2} (40.0)>Na^+(21.7)>K^+(1.4) μE L^{-1} and in anion most dominated HCO_3^- (321.2) followed by SO_4^{-2}(225.6)>Cl^-(43.4)μE L^{-1} (Jeelani et al., 2011). The most common water type found in the melt water chemistries of Kashmir valley is Ca-HCO_3, Ca-Mg-HCO_3, Na-HCO_3,Ca-SO_4 type is resulted from the configuration of dissolution of carbonate lithology. Due to shorter residence time for water rock interaction and short route flow to dissolution of carbonate mineral the Ca-HCO_3, Ca-SO_4 and Ca-Mg-HCO_3, Na-HCO_3 water type found. Na-HCO_3 water form suggests the contact of water with silicate type lithology. The ion chemistries of Kashmir valley as a result of ion exchange processes and silicate carbonate weathering (Fig. 2.1) (Jeelani et al., 2011).Beside Eastern Himalayan glaciers and Karakorum glaciers, few studies have been done in the North eastern Himalayan region like Zemu glacier, Lhonak River there is a lack of dataset availability in this region.

CHAPTER 3

STUDY AREA

This chapter provides details of the study area comprising parts of Bhagirathi Basin, Central Himalaya was selected. The detailed description such as physiography, geology, geomorphology, climatic conditions etc. are given in the following sections. The study area is situated in the vicinity of Dingad basin, sub-basin of Bhagirathi basin, central Himalaya India. The glacier system lies in Dingad basin are named as Dokriani glacier, which is a trunk glacier system of the valley along with Hurra Glacier and Draupadi Ka Danda glacier system. Detailed chapters of study area are as follows:

3.1   Physiographyof thestudyarea

Dokriani glacier (30^0 48′ to 30^0 53′ N to 78^0 39′ to 78^0 51′ E) is a valley type glacier system formed by the intersection of two cirques, one is situated at the northern slope named as "Draupadi Ka Danda (DKD)" (5716 m a.s.l.) and other at the western slope named as"Janoli" (6632 m a.s.l) glacier systems (Sundriyal et al., 2019; Dobhal et al., 2010) (Fig. 3.1). The central flow direction of the glacier system is north-north westwards (NNW) for the 2.0 km from top to the base of the ice fall from and then it turns towards west-west-northwards (WWN) direction and flow till 3.0 km downwards with an average slope of 12° before its termination at snout (3945 m a.s.l.). A meltwater stream emerges from Dokriani Glacier system is known as "DinGad" (a tributary of the Bhagirathi River) (Pratap et al., 2015) (Fig. 3.1). The total catchment covers is ~77.8 km^2 and the elevation ranges from 1760 m a.s.l at convergence point of Dingad to Bhagirathi River and extends up to 6632 m a.s.l. Total glaciated area of the Glacier catchment is 15.7 km^2, out of which ~7.0 km^2 area is glacierized. Three-fourth of the ablation area is covered by thick

supraglacial debris. The glacier has an accumulation and ablation area of ~4.7 km^2 and ~1.9 km^2 respectively, and the total length is 5.4 km with an elevation ranging from3940–6200 m a.s.l. The average air temperature is 2.3°C, and the total rainfall was ~1200 mm (Shukla et al., 2018). The annual Equilibrium Line Altitude (ELA) of the glacier lies approximately on ~5055 m a.s.l. The glacier receives ~80% of the precipitation during the monsoon season. As the temperature rises to 0 °C, the surface snows start to melt, resulting in meltwater leaving the subglacial source and other valley stream sources. The stream emerges out from the snout of the glacier is called Dingad (3950 m a.s.l.) and merges into the Bhagirathi River basin. The mean annual catchment wide runoff from the Dokriani is 1.56±0.10 m^3 s^{-1} the detailed salient features of Dokriani Glacier are summed up in Table 3.1. The Dokriani Glacier is the benchmark glacier and it is monitored since 1991 in the Indian Himalayan Region (IHR) and by fulfilling the World Glacier Monitoring Service (WGMS) standards and norms established for long term glacial monitoring. This glacier is ideal for various studied glacierized area for eg. mass balance (Dobhal et al., 2008), Snout recession, length area and volume estimation (Gergen et al.,1999: Dobhal & Mehta, 2007), meteorology (Kesherwani et al., 2012), hydrology (Singh et al., 2007: Thayyen & Hasnain., 1994, 1999), meltwater chemistry (Sundriyal et al., 2018, 2019, 2021), paleoclimate (Shukla et al., 2018) and debris cover studies (Yadav et al.,2019, Pratap et al. 2016).

3.1   Climatic settings of the study area

The climatic settings of the Dokriani Glacier system is mainly characterized by the moist temperate in summer season and dry cold in winter season. The area receives precipitation (rainfall and snowfall) from 2 moisture source i.e. first Indian Summer Monsoon (ISM) that occur between June-September months and through Western disturbance (WD) falls as winter precipitation between December–March (Thayyen & Gergan, 2010; Dobhal et al., 2004; Owen et al., 2002). The detailed long term climatic records are unavailable from the high altitudes of the basin.
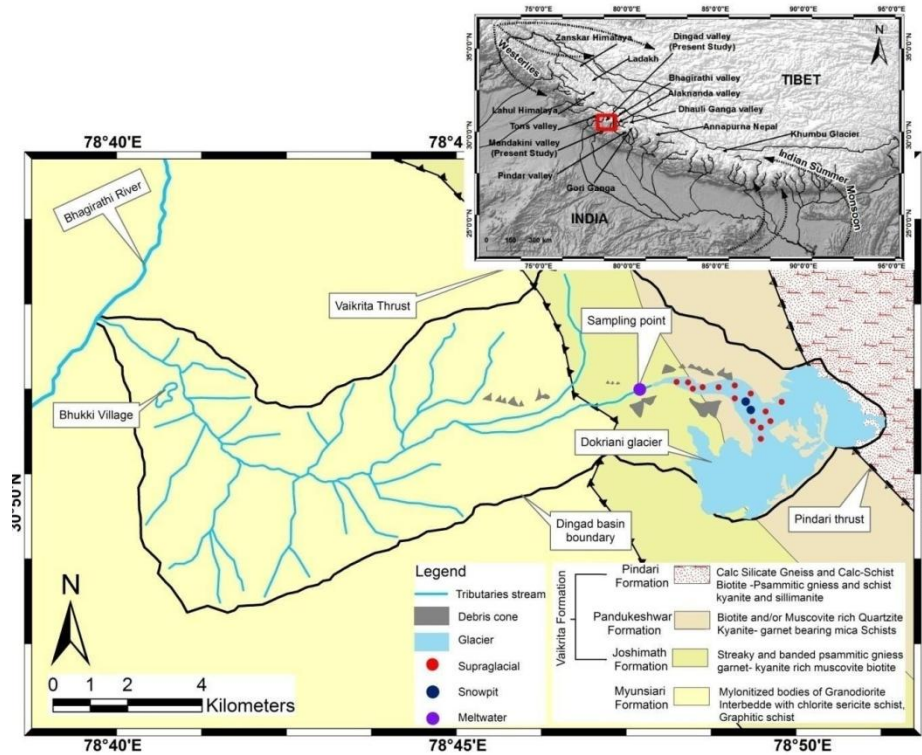
Fig. 3.1: Simplified location site map of the Din-Gad basin along with studied glacier systems in the present study (inset). The black line shows the catchment area, blue line shows the tributary stream and light blue patches shows the glacier area. The purple circle shows the sampling location i.e. meltwater samples taken from snout of the glacier, red circle shows the sample taken from supraglacial stream, dark blue circle shows the samples taken from snowpit.

24

Table 3.1: Salient features of the Dokriani Catchment (modified after Azam et al., 2020).

Parameter	Characteristics
Basin	Bhagirathi
Sub-Basin	Dingad
Location	Uttrakhand (state), India
Major glacier systems	Dokriani (main trunk), Dropadi ka Danda, Hurra
Dingad catchment characteristics	
Latitude/Longitude	$30^0$53'N / $78^0$51'E
Catchment area	15.71 km^2
Catchment outlet	3820 m a.s.l.
Maximum altitude	6632 m a.s.l.
Catchment outlet	3820 m a.s.l.
Total Glacierized area	7.35 km^2
Dokriani Glacier characteristics	
Glacier area	7.03 km^2
Debris covered area	0.94 km^2
Glacier length	~ 5 km
Snout position	4050 m a.s.l.
Mean orientation	North-West
Max altitude	6632 m a.s.l.
Mean annual catchment wide runoff	1.56±0.10 m^3 s^{-1} (1979-2018)
Mean annual mass balance (MB)	-0.25± 0.37 m w.e. (1979-2018)
Cumulative MB	-9.64± 2.32 m w.e. (1979-2018)
Mean summer MB	-0.97± 0.32 m w.e. (1979-2018)
Mean winter MB	-0.72± 0.05m w.e. (1979-2018)
Mean ELA	5309 m a.s.l. (1979-2018)
Mean AAR	46% (1979-2018)
MB gradient for debris cover ablation area	0.70 mw.e. (100m)$^{-1}$
MB gradient for clean ice ablation area	0.91 mw.e. (100m)$^{-1}$
MB gradient for accumulation area	0.28 mw.e. (100m)$^{-1}$
Annual temperature	3.1 $^{\circ}$C
Summer temperature	7.4 $^{\circ}$C
Winter temperature	-1.2 $^{\circ}$C
Annual precipitation	1616 mm w.e. (100%)
Summer precipitation	1242 mm w.e. (77%)
Winter precipitation	374 mm w.e. (23%)

In the central Himalayan region, it is observed that the monsoon period generally fall nearby June 25th and month end of the September (Raghavan, 1973; Das, 1988; Thayyen et al., 2015a). An elevation above 3760 m a.s.l the average ranges of precipitation falls between 1000-1300 mm. The winter snow accumulation is estimated in the month of May through snow pits and it is amounted about 200-250 cm at an altitude of 4400-4500 m a.s.l. Dokriani Glacier receives maximum precipitation from November to March through western disturbance is prevailing the area during this period (Dobhal et al., 2004; Mehta et al., 2012; Shukla et al., 2018) while inmelting season starts from May to September (Kumar et al., 2014). Total average rainfallobserved in Dokriani Glacier during melting season is 1041.0 mm for the years 1995-1998,1370.0 mm for the year 2010-2011 1351.8 and 1463.6 mm during period 2010 and 2011, respectively (Kumar et al., 2014). In addition, mean monthly maximum and minimum temperature were 13.2, 13.2, 13.3, 12.6 and 10.7 ^{o}C and 2.3, 5.1, 5.4, 2.5, and -3.0 ^{o}C during year 2010 and 2011 in the month of June-October, respectively. Therefore, glacier is nourished by winter precipitation i.e. from December to March more dominated in this area as it moves eastward over North India by western disturbance and summer precipitation by April to November by ISM (Thayyen & Gergan, 2010). Dobhal et al. (2008) the Dingad basin is nourished by the winter precipitation so that it melts on the summer season and plays a dominant role in sustaining stream and river runoff. The sustainability ofthe river and stream flow depends upon the orography and climatic settings that control the glacier mass wasting. In situ observation, showed that the solid precipitation was observed at high reaches in the month of summer, follow through significant melting in the ablation area (Hasnain et al., 2000; Singh et al., 2002).

3.2   Geology of the study area

The present area of investigation is located south west (SW) of Main Central Thrust (MCT) and Trans Himadri Fault (THF) in the North East (NE) contain subdivision of central crystalline rock (> 20 km). The MCT called the Munsiari thrust by Valdiya (1980), is the major structural discontinuity that separated the Lesser Himalaya from Central Himalaya and exposed at ~ 1.5

km south west of Dingad in Bhagirathi basin (Fig 3.2). The entire area of Dingad comes under the Vaikrita group of rocks from Munsairi formation and passes throughout Vishnuprayag north of Joshimath. The other major regional structure, known as Pindari Formation which crosses the river Alakndanda and evident by the sudden slope change of river course (Valdiya, 1999) (Fig 3.2). It is further noticed that this structural discontinuity differentiate the upper V-shaped glaciated valley (Dokriani) to the lower U-shaped Dingad basin. The rocks of study area are clubbed under Munsiari group of higher Himalaya (Valdiya, 1973; Valdiya et al., 1999). The detailed geological study area map is presented in figure 3.2 and geological sequence is tabulated in Table 3.2.The rocks of Munsiari Formation belong alternative band of quartzites, biotite rich fine grain gneisses, mylonitic augen gneisses, deformed amphibolites, patches of calc-silicate lenses, and phyllonites mineral assemblages. The rocks lying in between Gujjar hut and Base camp are laid over the Joshimath formation that consist banded and streaky genesis, kyanite rich muscovite-biotite, phyllonites, garnet, schist (Valdiya, 1998). This rock formation is wellexposed in between accumulation zone and GHC of the Dokriani Glacier. Consequently, the Dokriani Glacier debris cover is the dominant composition of gneisses, granite and schist. Mineral stoichiometry helps us to identify the mineral sources to calculate weathering fluxes (Table 3.4). Mineral mass balance calculation calculated weathering fluxes to source on the basis of local mineral stoichiometry (Garrels and Mackenzie, 1967; Velbel, 1985; Blum et al., 1998).
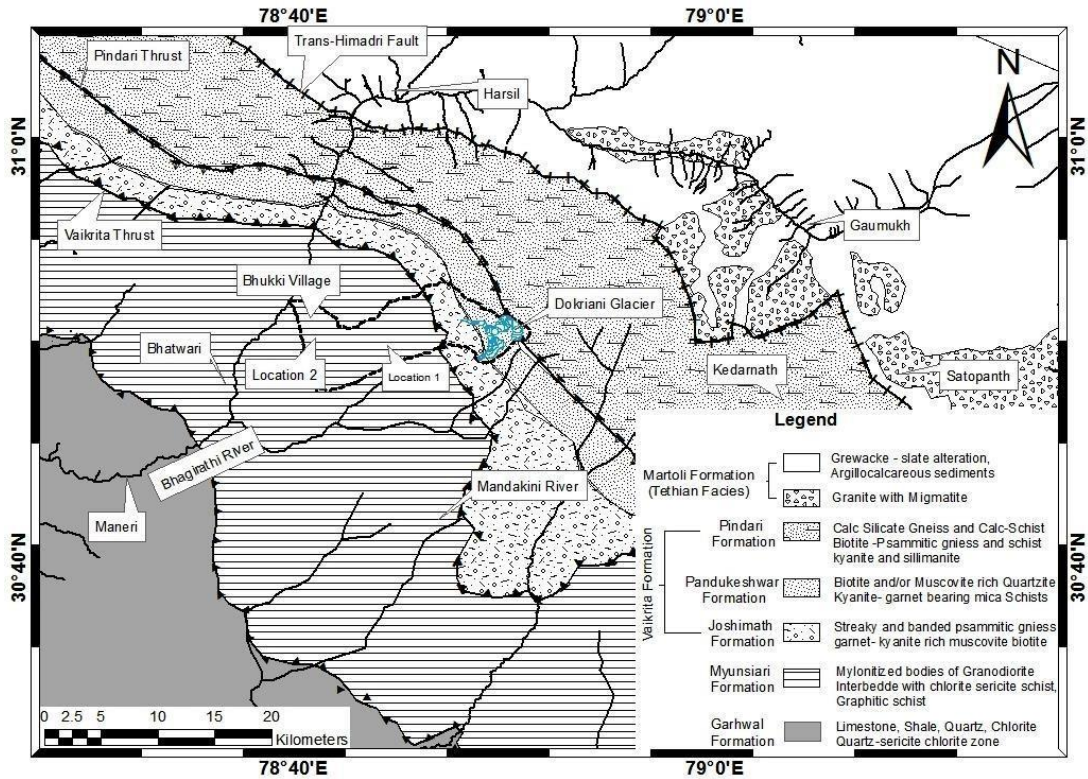
Fig 3.2: Geological map setting of Himalayan system (modified after Valdiya. 1998).

Table 3.2: Average stoichiometry of bed load mineral phase (modified after West et al., 2002 and Metcalfe, 1993).

Average stoichiometry of Bed Load Mineral	VaikritaGneisses
Mineral Phase	
Plagioclase	$Ca_{0.14}Na_{0.85}Al_{1.14}Si_{2.85}O_8$
K-Feldspar	$Na_{0.1}K_{0.9}AlSi_3O_8$
Biotite	$K_{0.82}(Fe_{1.24}Mg_{1.07}Ti_{0.11})(Al_{1.67}Si_{2.75})O_{10}(OH)_2$
Muscovite	$K_{0.89}(Mg_{0.12}Fe_{0.14}Al_{2.54}Si_{3.18})O_{10}(OH)_2$
Quartz	SiO_2
Kyanite	NotReported
Sphene	NotReported
Gamet	$(Ca_{0.32}Mg_{0.45}Fe_{2.13})(Al_{2.02})Si_3O_{12}$
Tourmalite	NotReported
Clays	NotReported
Talc	NotReported
Chlorite	NotReported

3.3 Geomorphological features

The region has well developed erosional and depositional geomorphic landforms and features throughout the valley. Geomorphologically, study area can broadly be divided into three zones according to the influence of geomorphic agency resulting in craving the landform. Such zones are generally distributed according to the elevation. The lower section is dominated by a riverine environment followed by both river and glaciers and the upper parts (>3000 m) have mainly glaciated landforms and features (Dobhal et al., 2008; Hasnain and Thayyen, 1999). The Geomorphological features like moraines and paleo-lakes tell us about the process of past glaciations (i.e. extension and stages) to unfurl the past glacial history of Himalaya, and generate information to understand paleoclimate and in modelling climate changes near future. In DGC the landforms formed by the past glaciations display four glacial stages with a retreating intensities and number of minor advances in different spans of interval (Dobhal et al., 2004; Shukla et al., 2018). The depositional and erosional features are well formed by the glacier and left trails of their past glacial extent and their volume (Fig 3.3).A succession of lateral moraines which seen near the jungle camp (2840 m a.s.l) indicating the past glaciations stages of Dokriani Glacier. On the basis of geomorphology, the entire valley area could be divided into three zones:

I.   Glacial zone: The area which lying in between 3700 and 4500 m a.s.l. are well exposed by the glacial processes, where mostly glacial and periglacial landform emerges out.

II.   Glacio-fluvial zone: It comes under the elevation range ~2800-3700 m a.s.l. where depend upon the intensities glacial fluvial action modified the glacial deposits in various stages. This area is categorized by the moraines, outwash gravel, debris flow, and erratic boulders (Fig.3).

III.   Fluvial zone: The area below 2800 m a.s.l, where U shaped valley prevails V shaped due to fluvial processes between Jungle camp to Bhukki village. On geomorphological map (Scale1:12,500) several landforms features

29

have been illustrated. The valley consists of many depositional features like talus cone, dead ice-mounds, river terraces, avalanche fans, Lacustrine deposits, proglacial boulders, lateral, medial, terminal, ground moraine as a debris deposit. (Fig 3.3).

3.4 Glacier characteristic and feature

Glacier are the huge mass of ice body formed by the accumulation of snow at higher elevation and flow downwards under own gravity. The constructing and shaping of glacier depends upon various processes like erosional and depositional which are substantial to know the dynamic activities of a glacier. The glacier feature is:

I.   **Equilibrium Line Altitude (ELA):** A imaginary line separates out the accumulation and ablation zone determining the attitude of 0 mass balance is called equilibrium line altitude (Fig.3.4)

II.   **Accumulation zone:** The zone lying in between Bergschrund and ELA receives the maximum masses through snowfall is called accumulation. The glacier is surrounded by cirque basin around the accumulation zone (Dobhal et al., 2010) (Fig 3.4).

III.   **Ablation zone:** The area among the snout (lower part of glacier) and ELA loses the mass through evaporation, melting, calving and refreezing is known as ablation zone. The ablation zone of the Dokriani Glacier is highly debris covered (Fig3.4)

IV.   **Snout:** It is known as the terminus of the glacier which is bare as ice wall and debris from where glacier meltwater originates. Currently, the snout of the glacier is 75-80 m wide, bounded by steep valley walls (Fig.3.4).

V.   **Englacial channel:** The channel at which the meltwater produced by the ablation process enter the surface and sub-surface channel and often appears as a stream. Such channels through ablation process are well exposed by rock fragment or debris. Meltwater drain through Crevasses and Moulin construct the subglacial and englacial drainage system in the glaciers.

I N D E X

Catchment boundary	Moulin	Moraine of last glacial period
Spot height 4147	Glacial table	Crevasses
Glacier	Ogives	Rock cliff
Snout	Bergschrund	Lateral moraine
Ice Cliff	Supra glacial dump moraine	End moraine

Medial moraine	Active avalanche track	Glacio-fluvial fan
Erratic field	Paleo-avalanche track	Terrace
Erratic train	Debris cone	Cliff base
Lacustrine deposit	Old moraine deposit	Edge of degraded moraine ridge
Marshland	Lake	Contour

Camp site	
Streams	
Din gad (stream)	
Bridge (discharge site)	
Supra glacial channels	

VI.

Fig.3.3: Detailed map of Geomorphological feature of Dokriani Glacier (modified after technical report of WIHG, 1995)

31

VII.   Supra glacial channels: Supraglacial water stream are formed in the ablation zone in summer season meltwater erode from the glacial surface give rise the supraglacial stream. The volume of these stream increases with rise in temperature. There are several processes operating in subglacial environment which increases melting as well nutrients in the melt water. During the monsoon and summer season these stream these channels are more active and act as an active melting agent whereas in winter season these channels are covered with snowcover.

VIII.   Bergschrund: At the head of the glacier a series of crevasses often found is known as bergschrund.

IX.   Cirque: A bowl shaped or amphitheater kind of structure placed at the head of the glacier formed by the erosion process is called cirque. Dokriani Glacier is in between two type of cirque on the western slope is Janoli (6632 m a.s.l) and on northern slope DKD (6000 m a.s.l).

X.   Moraines: Moraines are the unconsolidated deposition of glacial debris i.e. soil and rock which ensue in past glaciated regions and present glaciated regions. This debris is may due to the results of frost wedging and plucking, abrasion of glacial flour in glaciated surface. The size of the moraine can be varying from silt sized to boulders. Depends on the size the Dokriani glacier having irregular round shaped debris, the glacial valley has preserved several loop so lateral and end moraines. The lateral moraine is divided into two forms Left Lateral Moraine (LLM) and Right Lateral Moraine (RLM). The RLM is originated from Jaonli peak at an elevation of ~4500 m a.s.l and LLM is originated from DKD.
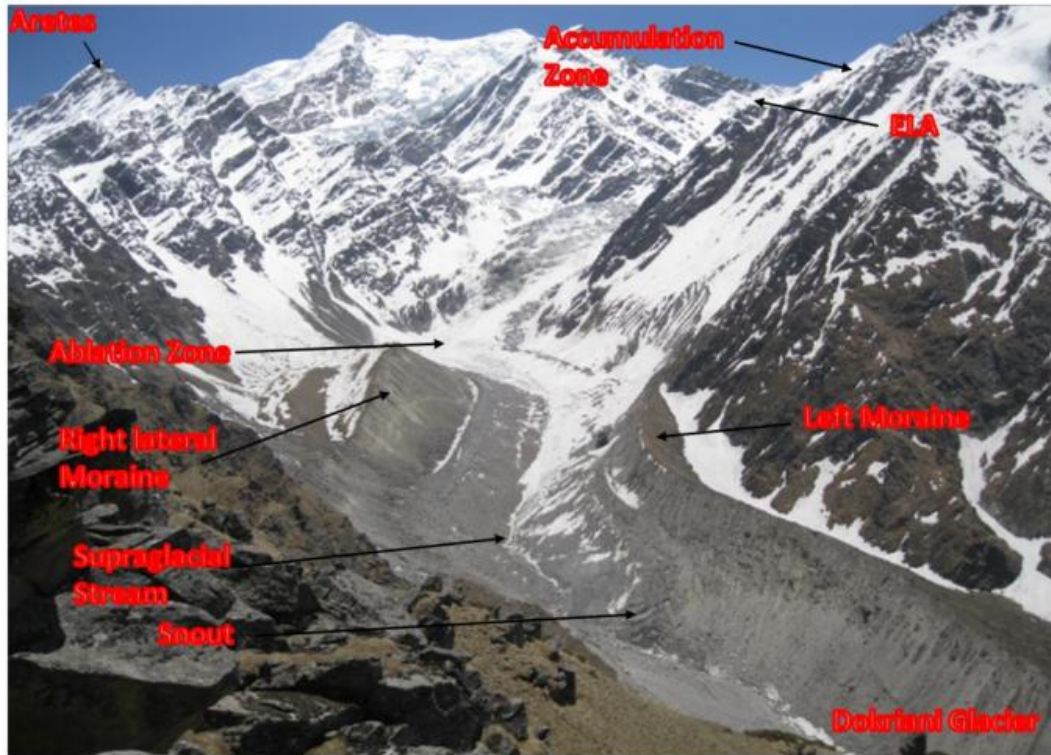
Fig.3.4: Pictorial view of Dokriani Glacier system along with its characteristics feature. Landforms presented as moraine ridges reflect the past glacial extension of the valley.

XI. Crevasses: Crevasses are tensional fractures in the ice. The pattern they form in simple situations can be deduced from the directions of the principal stresses. The shape, sizeand pattern of crevasses depend upon stress field in the glacier, flow direction and velocity, bed rock topography and slope. In Dokriani Glacier these features is mainly formed in and around the equilibrium line (4400-5300 m a.s.l.) and in the lower part of ablation zone. Between equilibrium lines (perpendicular to glacier length) transverse and radial zone are observed. Crevasses also develop where the valley is narrow and is changing its course of orientation. Few longitudinal crevasses also are developed at the margin of the glacier which run parallel to the glacier length (Fig.3.5). The development of transverse and longitudinal crevasses is indicative of extending and compressive flow of the glacier. The crevasses are clearly visible in the month of September to October when seasonal snow completely melted out before winter precipitation starts (Fig 3.5)

33

Fig. 3.5: Distribution of longitudinal, transverse and radial type crevasses at the glacial surface of the Dokriani Glacier.

XII.   Glacier Tables and Till: A massive boulder or rock placed on an ice pillar above the glacier surface. Such kind of formation is developed by the difference in melting of icemass. The boulder repel the melting of under the ice while nearby snow/ice starts to melt. Dokriani Glacier has a large number of glacier tables and till in the ablation zone (4200-4600 m a.s.l). These are the unsorted depositional feature formed by the rock fragment in the ablation period. These features are important to understand the flow of glacier (Fig3.6)

XIII.   Melt water streams: There are the several channels in glacier system which regulates the melt water system in the catchment. In ablation zone deforming and forming of channels due to the melting of snow/ice forms channels in the glaciers. The channel which erodes the ice surface and creates surface drainage is known as supraglacial stream (Fig 3.6). There is a large number of streams over the Dokriani glacier. The magnitude of flow of this stream depends on the glacier melt and slope of glacier surface. The meltwater stream is 2 km downstream from the snout (Fig 3.7). The gauging site isat 800 m downstream from the BC and 1 km upstream of the adjoining points of nallahs which joins the main stream of glacier near Bhukki village. Till now Dokriani Glacier has lost upto 22% of its volume from total storage 385×10^6 m^3 (Dobhal et al., 2004). Another small glacier with an area of 0.46 km^2 is also contribute the main catchment and just above the Gujjar hut the proglacial stream   at   3400   m   a.s.l   joins   the

34
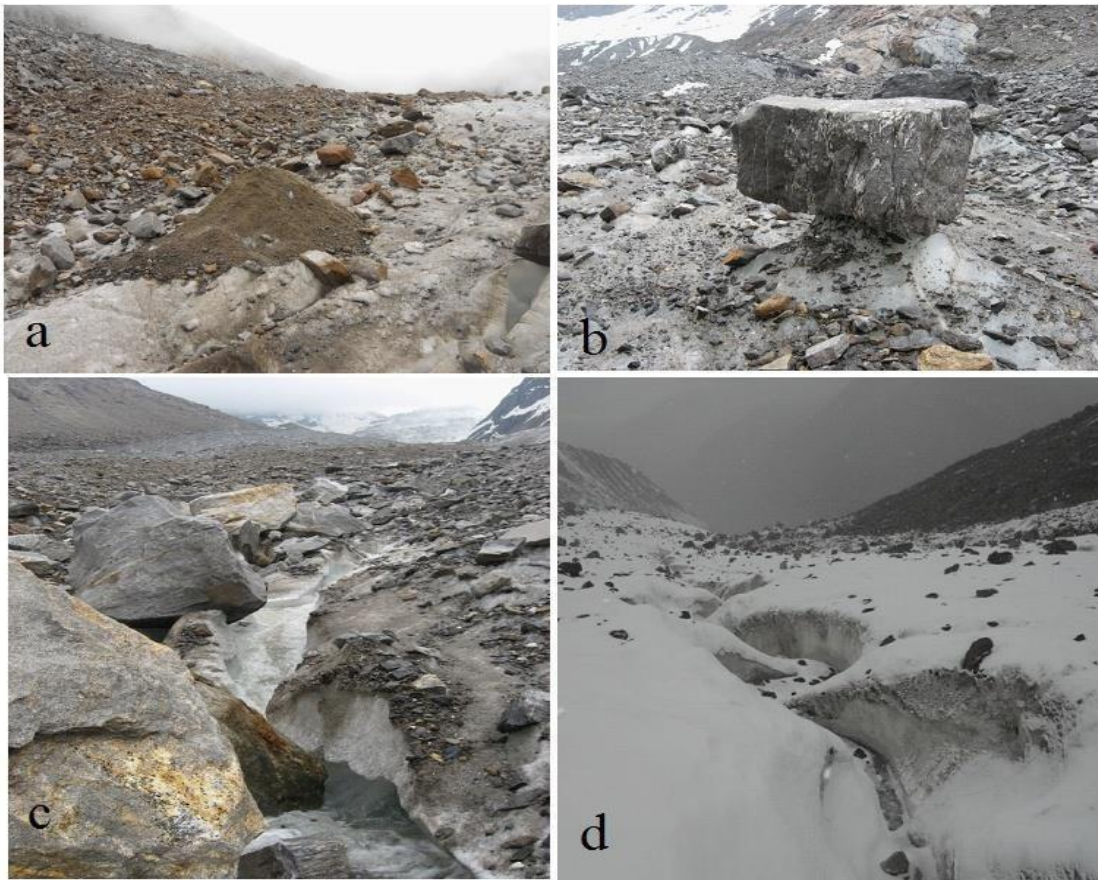
Fig. 3.6: Field photographs of the ablation zone of Dokriani Glacier. a-b. Presents the supraglacial debris cover (ranging between 1- 40 cm), c-d. Shows supraglacial meltwater streams.

Dingad catchment. The total runoff is the amount of liquid precipitation, amount of ice melt and the amount of snowmelt in the accumulation area. The discharge from the Glacierized basin consists of superimposed upon base flow. The diurnal rhythm is considered a feature of glacier fed stream. In the melting season melt runoff, an increase in the baseflow alsocanbe seenwhen continuous higher melting take place over the glacier. During winter season, the temp drop below the freezing point, so the stream is covered by snow which effect the melting. Irregularly, surface snow melts into deep crevasses and Moulin which form englacial and subglacial channels in the Dokriani glacier (Fig 3.8).
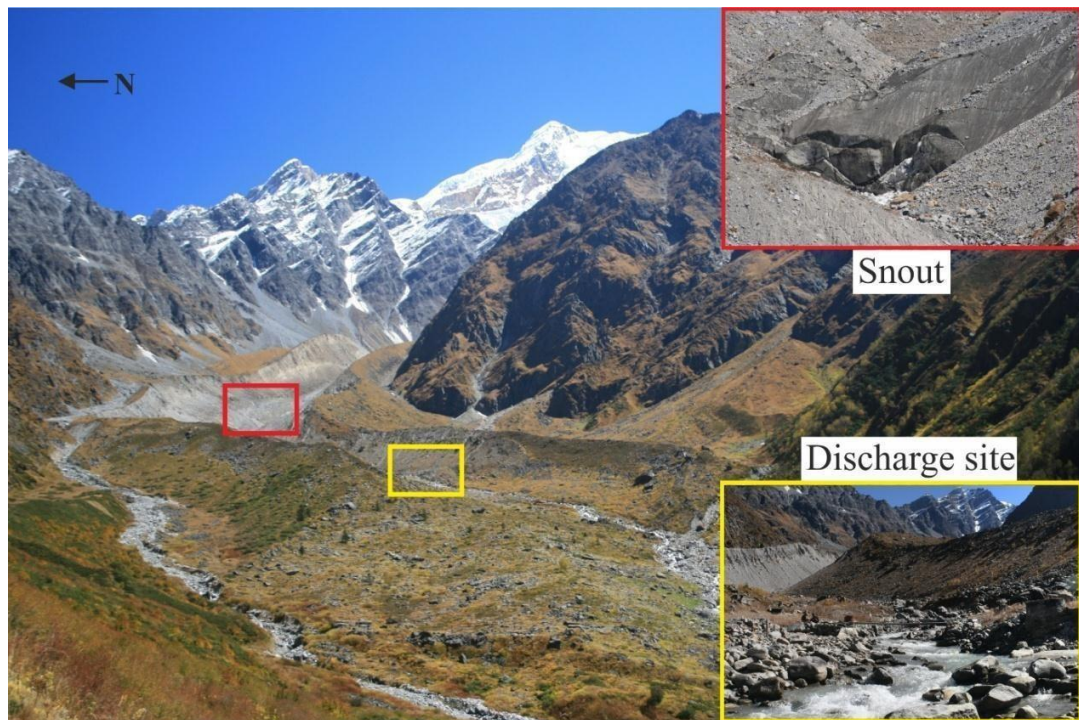
Fig. 3.7: Field photographs showing part of Dokriani catchment during ablation period. In this picture snout, discharge site, geomorphological setting can be seen.
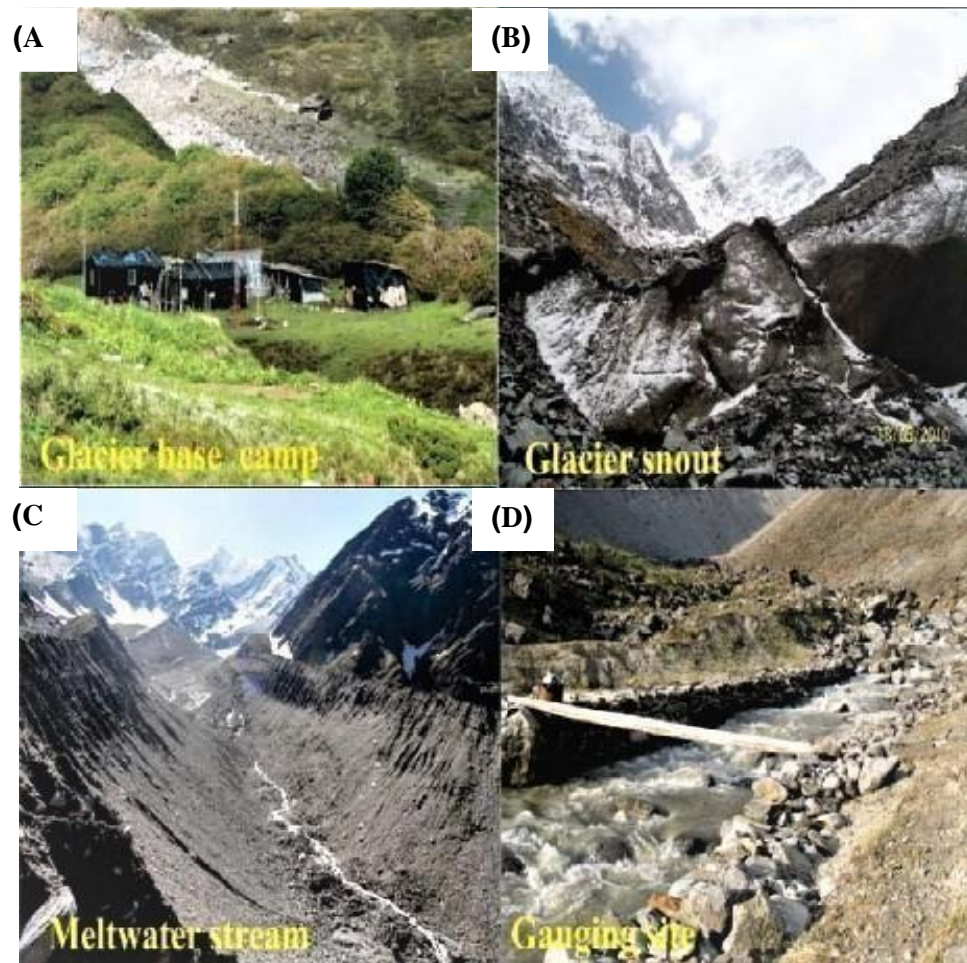
Fig.3.8: (A) Pictorial view of Dokriani Glacier basecamp (B) snout (C) meltwater stream and (D) Gauging site at Dokriani Glacier.

CHAPTER 4

METHODOLOGY AND ANALYTICALPROCEDURE

4.1   Overview of Research Methodology

The important component of hydro-geochemical research problem is to quantify the geochemical status quo of the samples. The important components of glacial hydrochemistry are broadly divided into compositional fractions of snowmelt, icemelt and direct runoff. To access and quantify the hydro-geochemical composition of meltwater draining Dokriani Glacier a total number of 207 samples were collected from different zones of Dokriani Glacier system (Fig 3.1 shown in study area) during the course field work in each ablation period between 2015 to 2018 years. Besides, this physical parameters like surface temperature, discharge, pH, EC, water temperature and geographic location measured in-situ. Following strategies were adopted to achieve our objectives:

1) Sampling of snow samples from different snow pit profiles
2) Supraglacial streams and lakes were sampled
3) Meltwater sampling from Dingad stream emerging from glacial terminus

The collected samples represent melt-water, supraglacial stream and snow-pit compositions of Dokriani Glacier. The outline of procedure was used during the work is as follow.

1) It includes the geomorphological and lithological survey of Dokriani Glacier based on field maps and collection of new data points and samples.

2) In-situ measurements of physical parameter such as pH, EC, water temperature etc.

3) Meltwater collection from different zones explained above.

4) Geochemical analysis such as major ion, alkalinity, trace elements from Ion Chromatography, Auto-Titrator & Inductively coupled plasma mass spectrometry (ICP-MS)of meltwater samples.

4.2   Field Work

The sample collection was divided into different zones of Dokriani Glacier i.e. supra, peri and proglacial zones. It represents the composition of meltwater, snowmelt from snowpit, supraglacial stream and their respective process. The samples were then brought to the laboratories of Wadia Institute of Himalayan Geology, Dehradun (WIHG) and National Institute of Hydrology, Roorkee (NIH) for further geochemical analysis i.e. cation and anion composition, trace elements composition. The sampling period chosen for sampling was divided into three seasons i.e., Pre-monsoon, Monsoon and Post-monsoon. Due to the rough terrain and climatic condition, it wasn't possible every time to collect the sample in the monsoon season, therefore the sample in the post and pre monsoon seasons of different years were preferred. During the entire sampling procedures, field work was usually carried out in the months of May-June and September-October. The sampling frequency followed to collect meltwater samples from the discharge site was sampling thrice a day i.e. 8:00, 13:00 and 17:00 hrs corresponding to Indian standard time zone. Collection of meltwater samples of supraglacial stream from the glacier surface by following the supraglacial drainage pattern of Dokriani Glacier. Furthermore, the precipitation samples (rainfall and snowfall both) were collected at the base camp site of Dokriani Glacier. The sampling of snow profile was conducted in the month of May during the year 2013, 2015 and 2017 respectively. Total numbers of 36 samples from the snow pit profile were collected from ablation zone on an elevation between 4300-4500 m a.s.l (fig 4.2). The snow pit samples taken at a 10cm interval (depending upon the availability of snow layer) and the whole sampling done under intense care

and follow the standard protocols (Dalai et al., 2002) to avoid the external contamination. All the things are taken firstly are precleaned mask and gloves (polyethylene) to avoid the contamination during the whole sampling campaign. After collection, samples were melted at room temperature by avoiding direct sunlight exposure therefore kept in black polybags. After melting at room temperature, the filtration of samples done by 0.22µm Millipore nylon membrane filter and transferred into 30ml amber narrow mouth bottles followed by acidification to pH 2 using concentrated ultra clean HCL for the trace elements analysis. Another aliquot of 120ml water filtered is kept on the precleaned HDPE bottles for major ion and trace elements analysis. In Addition, of that another aliquot of unfiltered water sample is kept in the 60 ml HDPE bottles for alkalinity measurements. All the samples were sealed with Teflon tape at site to avoid the splitting (leakage) of the sample. The samples were carried to the laboratories of Wadia Institute of Himalayan Geology (WIHG), Dehradun and National Institute of Hydrology (NIH), Roorkee for advance analysis. Detailed sample characteristics like location, elevation, Lat/Long are summarized in Table 4.1.

Table 4.1: Detailed sample collection characteristics from different zone of Dokriani Glacier.

Sample type	Lat/Long	Elevation (m a.s.l)	No. of sample	Sampling Year
Melt water	30^0 54'N/78^0 52'E	3760	145	2015 - 2018
Supraglacial	30^0 60'N/78^0 62'E	3906	25	2017
Englacial	30^0 58'N/78^0 60'E	3886	13	2015
Supraglacial lake	30^0 52'N/78^0 50'E	3926	12	2015
Rainfall	30^0 52'N/78^0 50'E	3760	8	2015, 2017
Snowfall	30^0 52'N/78^0 50'E	3760	4	2015, 2017

4.2.1. *Insitu* measurements

4.2.1.1 Geographical location and altitude

Geographical location like latitude, longitude and elevation of the sampling site were taken by Garmin Global Positioning system (GPS) with an accuracy of 12±4m (Ackerman et al., 2001). This device plays an important role especially in the remote locations where no other mode is available.

4.2.1.2 *Insitu* measurements of physical parameters

Measurements of physical parameters i.e. pH, EC, discharge and water temperature of melt-water samples were done on site at the time of sampling by using multi-parameter kit. The measurement precision of the instrument was as follows: pH ±0.01 (SD 0.01); EC ±1 µS cm^{-1}; water temperature ±0.5°C. Before analysis the pH probe is calibrated by using buffer solution of 4, 7 & 9.2 of Merck®. Before going on to the sample the electrical conductivity probe is calibrated by using a standard of 1413 µScm^{-1} and 6668 µScm^{-1}. Further, the discharge measurements were taken at the gauging site located at ~500 meters below from the present snout of the glacier. The stability of the discharge site is balanced through the big boulders on the both side of stream. In the gauging site there is a manual staff gauge installed to measure the daily water level throughout the ablation season. Surface velocity of the stream was taken through float flow method by using the methods of Kumar et al. (2014). The mean velocity, surface velocity and discharge were then calculated by the area velocity method. The calculated discharge values are presented in Table 4.2.

Table 4.2: Detailed value of mean velocity, surface velocity and discharge of melt water of Dokriani Glacier.

Year of measurement	Mean water level (cm)	Surface Velocity (m/s)	Mean Velocity (m/s)	Mean disch (m^3 sec
2015	16	1	0.9	1.4
2016	22	1	0.8	1.5
2017	25	0.9	0.7	2.3
2018	20	0.6	0.5	0.9

4.3   Laboratory measurements

4.3.1   Alkalinity measurement

Alkalinity is defined as the measure of capability of solute or any colloid which act as a base to neutralize acid. It is a sum of CO_3^{2-}, HCO_3^- and dissolved CO_2 in the solution. The amount of acid-base neutralizing volume is essential to access the "buffering" capacity of the water against pH. In solute or in a solution alkalinity formed from by the combination of bicarbonate and carbonate ions. Alkalinity is measured by titrating a known volume of the analyte against an acid (HCl, in this case) of known normality (Fig 4.2). After measuring the volume of acid consumed, alkalinity is measured using the following equation 1.

Alkalinity = (1000*0.01*61*volume of titrant consumed)/volume of analyte

(1)

The unit is expressed in $\mu E\ L^{-1}$

Fig.4.1: a) Sampling of meltwater b) *Insitu* measurements of physical parameters c) snow samples collection from snow pit profile d) closure view

of snow pit at 3500 m a.s.l at Dokriani Glacier showing the seasonal variability of snow deposition.

4.3.2 Major Ion Analysis

Major ions in snow/ice, snowpit, meltwater (Cl^-, F^-, SO_4^{-2}, NO_3^-, Na^+, K^+, Mg^{+2}, Ca^{+2}) were analyzed through Ion Chromatography (Dionex series ICS-5000) instrument. Ion Chromatography is
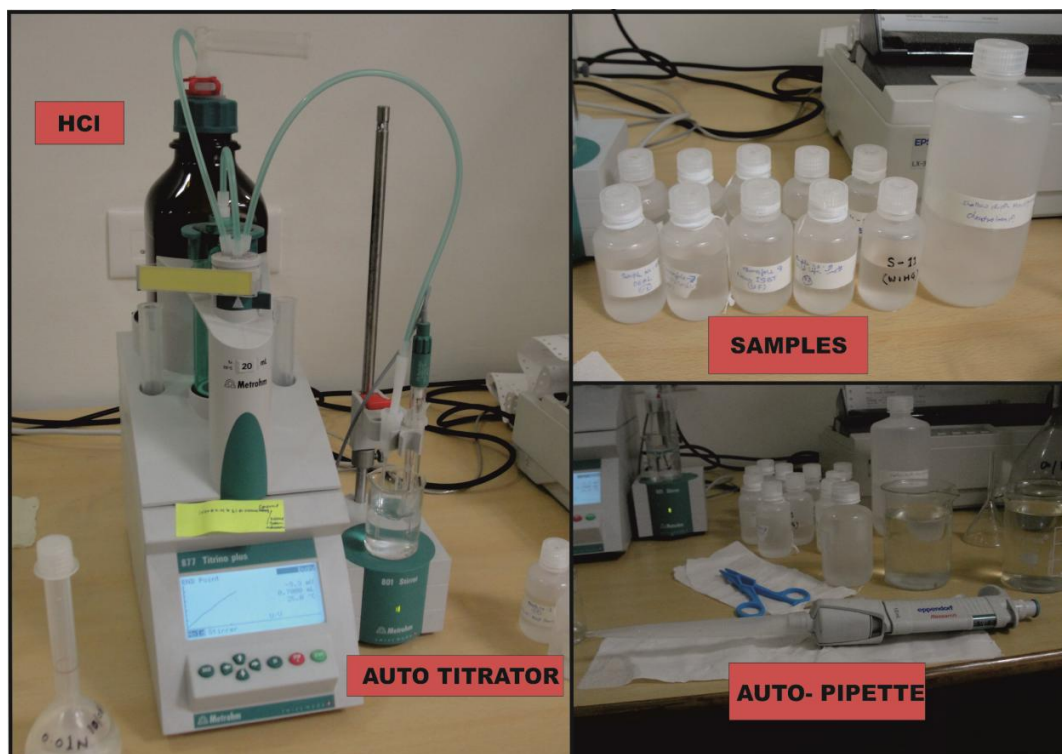
Fig.4.2: Instrumental setup of alkalinity by using pH based auto Titrator (titrino plus by Metrohm)

based on liquid chromatography method with based on ionic species which is charged whether it is from positively or negatively (Na^+, Cl^- etc.) and polar analytes can be detected. It is based on the interaction and partition of the sample ion between the mobile phase(eluent) and the stationary phase (resin column). Ion chromatography is capable to quantity the concentrations of major anions, for e.g. F^-, Cl^-, NO_3^-, NO_2^-, and SO_4^{-2}, and major cations for e.g. Na^+, Li^+, Ca^{+2}, Mg^{+2}, K^+ in the milligram per litre (mg/l) scale or even less. Organic compound concentrations also be analyzed by ion chromatography

using suitable configuration of column and eluent. Some typical applications of ion chromatography include:

1) Drinking water analysis for pollution and other constituents

2) Determination of water chemistry in aquatic ecosystems

3) Determination of sugar and salt content in foods

4) Isolation of selected proteins

Major cations (Ca^{+2}, Mg^{+2}, K^{+2} and Na^+) and anions (Cl^-, F^-, SO_4^{-2}, NO_3^-) were analyzed using on a Metrohm ion chromatograph system (Dionex series ICS-5000) (Fig 4.5.). Approximately 150 mL of undiluted sample was injected on an anion column (Metrosep A SUP 5 250/4 mm with suppressor) in 50 m M L^{-1} Na_2CO_3 and 1.0 mM L^{-1} $NaHCO_3$ eluents, and in 1.7 mM L^{-1} dipiclonic acid with 1.0 mM L^{-1} HNO_3 on a cation column (Cation Colum Metrosep C 6 250/4 mm cation column). One blank (Milli-Q water) and one standard were injected after every 5 measured samples to check the accuracy and precision. The standard result obtained from ion chromatography measurements are shown in fig 4.6. Standards from National Institute of Standard Technology (NIST) were used as primary standards (Fig 4.3 & 4.4). The concentrations of ions in the sample were calculated based on a 5-point standard calibration curve. The analytical accuracy and precision was in the range of ±5% for analytes. The total alkalinity (TA) was measured on a Metrohm potentiometric auto titrator (Model Number 888) by using 0.02 N H_2SO_4 as a titrant. The alkalinity of the solution has been classified as M alkalinity (pH indicator methyl orange, end point 4.2 to 4.5) and P alkalinity (pH indicator phenolphthalein, end point 8.2-8.3). The overall titration accuracy was within 2.0%, and precision was within 1.5%.

Elution order for the ionic species.

For anions: F^-, Cl^-, NO_3^-, SO_4^{-2}

For cations: Na^+, NH_4^+, K^+, Mg^{+2}, Ca^{+2}

No.	Time min	Peak Name	Type	Area µS*min	Height µS	Amount measured PPM	Amount reported PPM
1	2.08	F	BMB	0.112	1.436	2.0125	2.00
2	2.96	Cl	BMB	0.296	3.497	10.0664	10.00
3	3.35	NO$_2$	BMB	0.223	2.201	10.0636	10.00
4	3.94	SO$_4$	BMB	0.232	1.678	10.0567	10.00
5	5.05	Br	BMB	0.106	0.784	10.0731	10.00
6	5.38	NO$_3$	BMB	0.147	0.964	10.0772	10.00
7	7.39	PO$_4$	BMB	0.197	0.634	20.0981	20.00
		TOTAL:		1.31	11.18	72.45	72.00
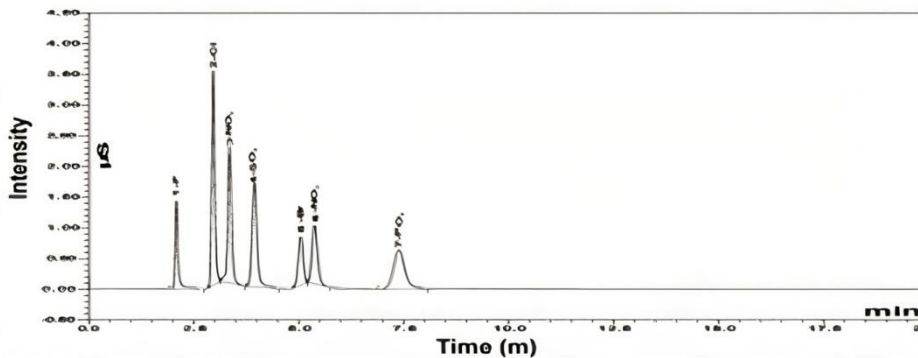
Fig.4.3: Chromatograph of anion standard, observable at National Institute of Standard

No.	Time min	Peak Name	Type	Area µS*min	Height µS	Amount measured ppm	Amount reported PPM
2	4.08	Li	BMB	0.563	3.938	1.0016	1.00
3	4.42	Na	BMB	0.507	4.040	4.0035	4.00
4	4.87	NH$_4$	BMB	0.499	3.423	4.9822	5.00
5	5.09	K	BMB	1.183	7.701	10.0421	10.00
6	12.57	Mg	BMB	1.485	2.432	5.0103	5.00
7	13.84	Ca	BMB	1.950	2.824	10.0113	10.00
		TOTAL:		6.19	24.36	35.03	35.00
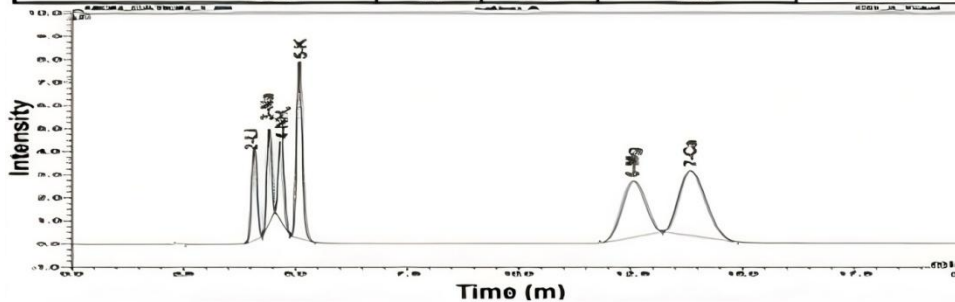
Fig. 4.4: Chromatograph of cation standard, observable at National Institute of Standard
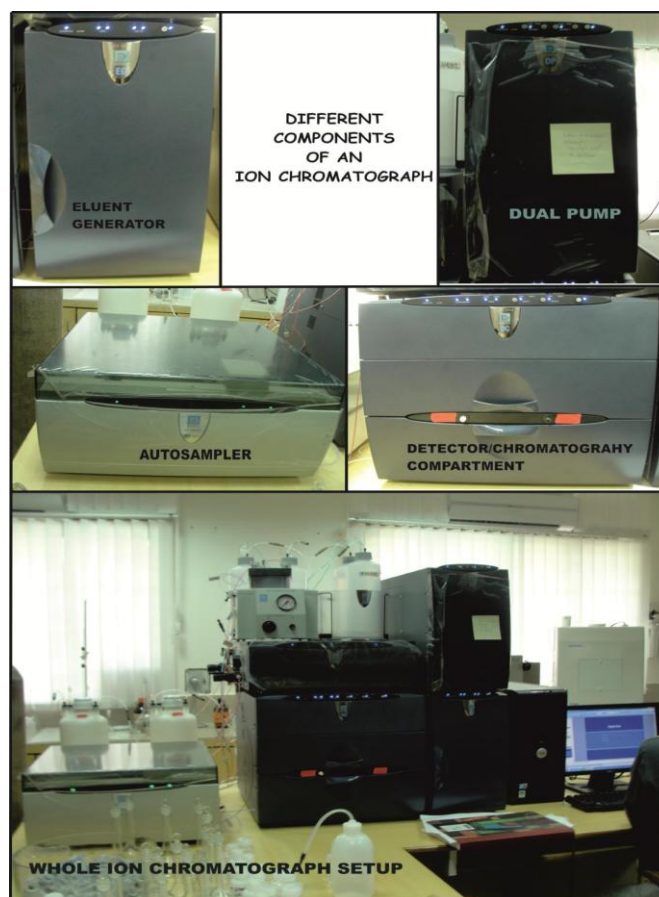
Fig.4.5: Components of Ion Chromatograph System at WIHG, Dehradun

(A)

(B)
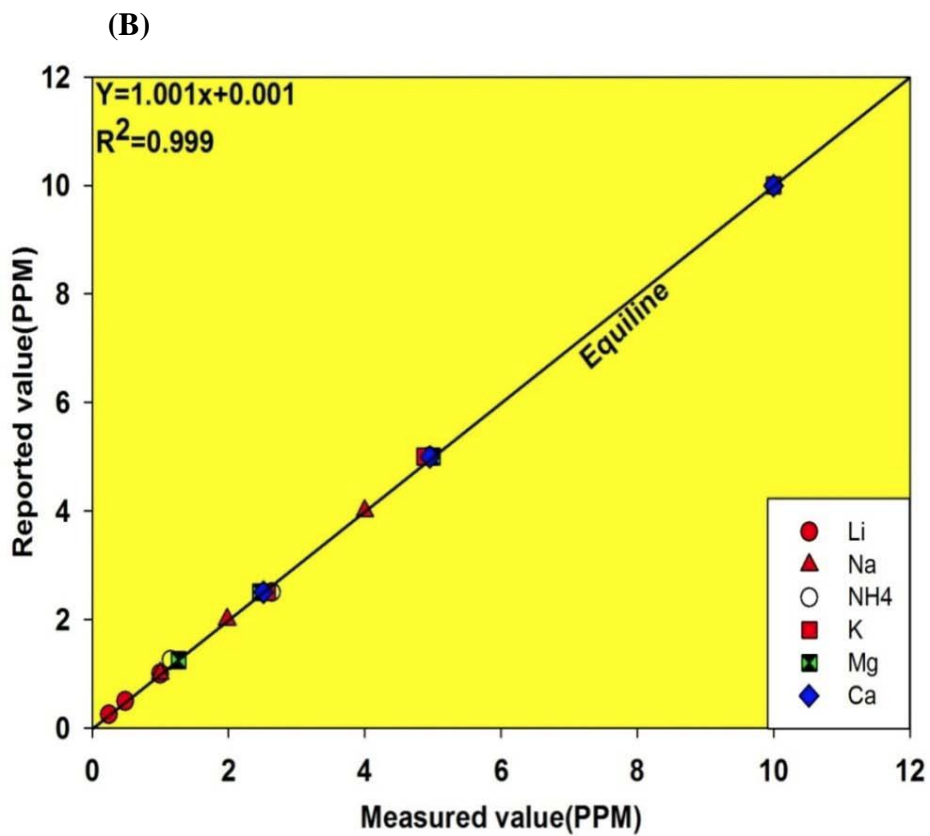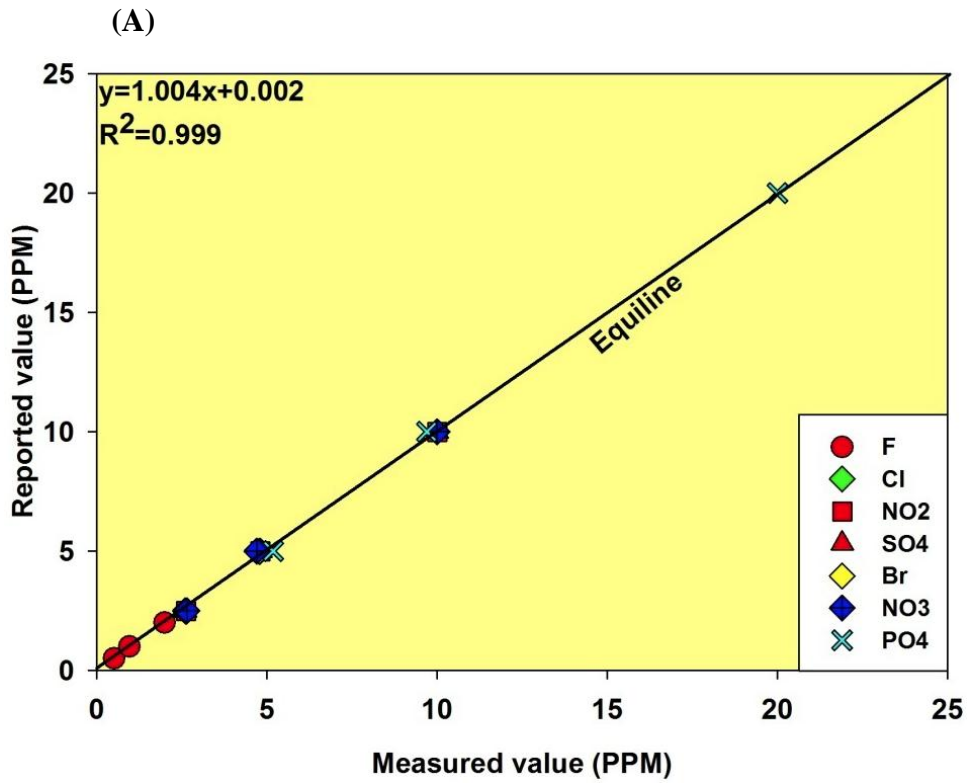
Fig.4.6: Measured vs. reported ionic concentrations with reference standard of National Institute of Standard Technology (A) for anions; (B) for cation.

4.3.2.1 Repeat Measurements

Precision of the samples is more important in analytical chemistry. To avoid the error in the data or flexibility in our data it is necessary to repeat random samples in measurements as shown in below table 4.3 & 4.4.

Table 4.3: Shows the repeat analysis of random samples of Major anions with a precision of ±5% (all concentration unit is in $\mu E\ L^{-1}$)

S.No.	Sample Name	F^-	Cl^-	SO_4^{-2}	NO_3^-
1	BG/18/5/15/9AM	0.45	0.25	25.60	0.69
	BG/18/5/15/9AM(R)	0.46	0.26	26.01	0.68
2	BB/15/5/15/1PM	0.39	0.16	43.25	0.50
	BB/15/5/15/1PM(R)	0.35	0.15	45.86	0.48

Table 4.4: Shows the repeat analysis of random samples of major cation with a precision of ±5% error (all concentration unit is in $\mu E\ L^{-1}$)

S.No.	Sample Name	Na^+	K^+	Mg^{+2}	Ca^{+2}
1	BG/18/5/15/9AM	0.98	0.86	1.25	6.15
	BG/18/5/15/9AM(R)	1.21	0.82	0.95	6.30
2	BB/15/5/15/1PM	1.03	1.27	1.09	6.05
	BB/15/5/15/1PM(R)	1.05	1.26	1.30	5.59

The samples analysis was followed by the charge balance error (CBE) which suggests the errors caused due to precipitation of dissolved species, measurement error and/or sample filtration. The charge balance error (CBE) calculation was done using equation2. Positive CBE value indicates the higher concentrations of cations than anions and if *vice-versa* for negative.CBE below 30% shows the other post processes such as evaporation etc. The CBE is functional to check the quality of data. The Eq 2 to calculate CBE is as follows

$$CBE = (\sum X^+ - \sum X^-)/(\sum X^+ - \sum X^-) * 100\% \qquad (2)$$

Where,

X represent the concentration of major ions in $\mu E L^{-1}$ in sample, 'X⁻' refers to sum of anions while 'X⁺' refers to sum of cations.

As the site is more prone to the atmospheric transportation and transports moisture from ocean, therefore it is more important to apply some corrections to major ionic concentrations. The ionic concentration corrected for atmospheric input has been denoted with '*' mark. Corrections were based on the principal quotients between major ion concentration and Cl^- from snow pit are as following: $SO_4^{-2}/Cl^- = 1.47$, $Na^+/Cl^- = 0.42$, $K^+/Cl^- = 0.019$, $Ca^{+2}/Cl^- = 2.86$, $Mg^{+2}/Cl^- = 0.27$ (Sundriyal et al., 2018). Here Cl^- was considered as a conventional ion for correction due to its atmospheric origin. The presence of Cl^- in terrestrial rocks of the catchment is not yet reported. Corrections of solute concentrations were done as follow Eq 3.

$$*X = {}^{total}X - {}^{total}Cl^- \ (X/Cl^-)_{seasalt} \tag{3}$$

Where,

$*X$ = concentration of corrected solute concentration

$^{total}X$ = total concentration of ion

$^{total}Cl^-$ = total concentration of Cl^- ion in sample

(X/Cl^-) = sea salt ratio of ion X: Cl^- in seawater

Further, the calculation of sulphate mass fraction (SMF) was done which is used to quantify the drift for dissolution and precipitation of mineral. Following Eq 4 was used to calculate SMF.

$$SMF = SO_4^{-2} / (SO_4^{-2} + HCO_3^-) \tag{4}$$

SO_4^{-2} is the value of corrected concentration by atmospheric input in $\mu E \ L^{-1}$, HCO_3^- is the concentration of bicarbonate in $\mu E \ L^{-1}$.

If SMF is equivalent to 0.5 displays the prevalence of sulphide oxidation (SO) process coupled to carbonate dissolution. When SMF<0.5, CD increases and if SMF>0.5 suggested further source SO_4^{-2} coupled with carbonate and silicate

weathering or Ca-Mg efflorescent salt dissolution (Cooper et al., 2002; Tranter et al., 2002).

4.3.3 Trace Elements Analysis

The samples from glacier were collected as above mentioned procedure. The unfiltered sample is used to analysis trace elements and silica in an inductively coupled plasma mass spectrometer at WIHG & NIH lab. Internal standard sample is used after every 3 to 4 sample s to check the instrumental drift and calculate precision. All the trace element samples were operating in a class 10 laboratory. Snow sample were not filtered, so the results show the dissolved and the colloidal species as well as acid soluble concentrations dissolved particulate matter. An Agilent Inductively coupled plasma mass spectrometry (ICP-MS) with guard electrode employed for detection of trace elements analysis.

4.3.3.1 Working Principle

ICP-MS is an important tool to detect the concentration of metal in low concentrations (ppb) and ultra-low concentration (ppt). This instrument is detecting on the basis of mass/charge ratio. The sample is introduced into the device by a needle after that plasma which contain an argon gas at a very high temperature i.e. 5726-7726 ^{o}C approximately and after that on the basis of mass /charge ratio ionization happen. For analysis a small amount of samples is indeed to quantify. Following are the parts which consist the mass spectrometer:

1)   Interface is also called sample shaft in this system free ion generated by plasma are transmitted this process done under high temperature and atmospheric pressure at a high vacuum (<0,001 Pa).

2)   Electrostatic lenses emphasis on +vely charge ions against the access on mass spectrometer

3)   The mass spectrophotometer consists of metal rod which separate ions based upon their mass by a resonance principle.

4)   The detector containing active surface, which detect the metal based on colliding ion signal which generate a measurable pulse.

5)   Electronic count the pulses and sperate the metals base upon their charge/mass ratio. This processor can be done in a millisecond, so that the whole graph acquired in less time.

The instrument is based at what wavelength atoms and ions absorb and move from ground state to excited state. The amount of energy required for the electrons to move between the different energy levels corresponds to very specific wavelength light. Every metal has a different number of wavelengths such as Al= 396.152, Cd=226.502, Cr=205.560, Cu=324.754, Fe=238.204, Mn=257.610, Ni=231.604, Pb=220.353, Zn=202.548 so on. Firstly, the sample transport to a PFA nebulizer at 1 mLmin^{-1} by using a peristaltic pump and a spray chamber (Elemental Scientific). An internal standard for ICP-MS (~100 nm) run to correct the instrumental drift or the precision. We detect elemental concentration of Sr, Zn, Mn, Cu, Fe, Ni, Co, As and Si. It is necessary to know the concentration of element with lower range, due to their high level detection capacity over other analytical technique. The accuracy of this instrument is ±5% for trace elements and silica in water sample.
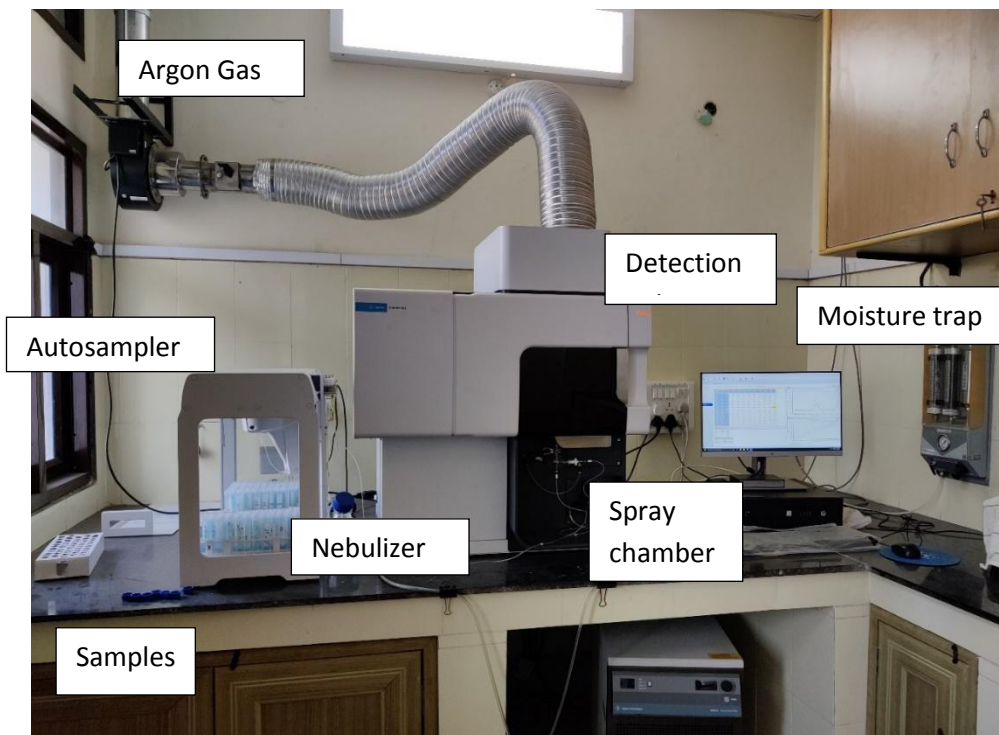
To check the accuracy of the instrument the repeat analysis is also done every after 10 samples. Results of repeat samples are as follows.

Table 4.5: Details of the repeat analysis of random samples of trace elements with a precision of ±5% error (all unit are in ppb).

Sample Id	Cd	Cr	Cu	Mn	Ni	Pb	Zn	Fe
D/MW/2018/8Pm	0.08	ND	0.14	11.87	2.17	0.7	2.8	20
D/MW/2018/8Pm(R)	0.06	ND	0.13	11.58	2.13	0.65	2.78	19.5

4.5 Calculation of solute provenance

To evaluate the effects of chemical weathering over ionic release from Dokriani glacier basin in detail a conceptual model of solute acquisition (primarily developed by Hodson et al., 2000) were used. Since the bulk melt water chemistry is composed of ions resulting from different geochemical reactions (equation 5-8) operation at the supra/ sub and englacial zone of the glacier system. Therefore, apportioning of ionic sources are were applied through this method which determines the HCO_3^- provenance for its association with aerosol hydrolysis, sulphide oxidation coupled to carbonate carbonation (SO-CD), simple hydrolysis (of carbonates), carbonate carbonation (CC), silicate dissolution and direct atmospheric drawdown. Briefly, the ionic mass balance is applied to calculate different provenance for SO_4^{-2} and HCO_3^- as they were the dominant anion in melt water. The cation has been calculated from the atmospheric corrections. Detailed methods and assumptions taken during calculations are presented below: Solute partitioning of glacial meltwater was based on methods of Sharp et al., (1998) which divides the solute release from an alpine glacier basin into atmospheric, seasalt, black carbon aerosol and solute derived from crustal source in runoff. With some basic assumptions as all Cl⁻ is of marine source, from standard sea-salt ratios to Cl⁻ is 0.58 (Holland, 1978) is used to calculate the marine constituent of the cations $^{sea}Ca^{+2}$, $^{sea}Mg^{+2}$, $^{sea}Na^+$, $^{sea}K^+$. The rest is assumed to

be derived from crustal source $^*Ca^{+2}, ^*Mg^{+2}, ^*Na^+, ^*K^+, ^*NO_3^-, ^*SO_4^{-2}, NO_3^-$ amount is assumed to be from atmospheric aerosols with a quantity of SO_4^{-2} with later can be subtract from the difference between snowpit SO_4^{-2} and $^{sea}SO_4^{-2}$ concentrations. HCO_3^- can be derived from two constituent's i.e. crustally derived (carbonate) and atmospherically derived (CO_2) components. We assumed below reactions generates total HCO_3^- ($^{tot}HCO_3^-$).

(1) Sulphuric acid dissolution by carbonate weathering, for example:

$$H^+_{(l)} + NO_3^-{}_{(l)} + CaCO_{3(s)} \leftrightarrow Ca^{+2}{}_{(l)} + HCO_3^-{}_{(l)} + NO_3^-{}_{(l)} \qquad (5)$$
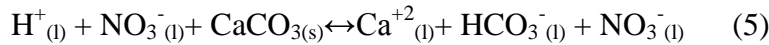
(2) Sulphide oxidation coupled with carbonate dissolution, for example:

$$4FeS_{2(s)} + 16CaCO_{3(s)} + 15O_{2(l)} + 14H_2O \leftrightarrow 16Ca^{+2}{}_{(l)} + 16HCO_3^-{}_{(l)} + 8SO_4^{-2}{}_{(l)} + 4Fe(OH)_{3(s)} (6)$$
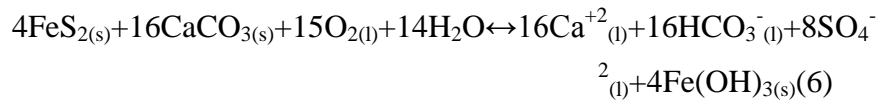
(3) Silicate dissolution with carbonic acid, divalent ion, for example:

$$CaAl_2Si_2O_{8(s)} + 2CO_{2(l)} + 2H_2O \leftrightarrow Ca^{+2}{}_{(l)} + 2HCO_3^-{}_{(l)} + H_2Al_2Si_2O_{8(s)} (7)$$
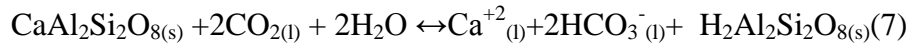
(4) Carbonation of carbonates, for example:

$$CaCO_{3(s)} + CO_{2(l)} + H_2O \leftrightarrow Ca^{+2}{}_{(l)} + 2HCO_3^-{}_{(l)} \qquad (8)$$
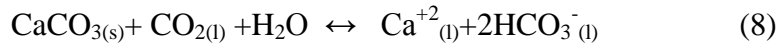
Here $^*HCO_3^-$ represent as a crustal bicarbonate contribution which produced from equations 5

Table 4.6. Detailed calculation of cation provenance in seasalt and continental crust source (modified after Hodson et al., 2000)

Solute	Component	Provenance calculation
1. Ca^{+2}, Mg^{+2}	(a) $^{seasalt}Ca^{+2}, Mg^{+2}$	$^{sea}(Ca^{+2}, Mg^{+2}/Cl^-) \times ^{total}Cl^-$
	(b) ^{crustal} or $^*Ca^{+2}, ^*Mg^{+2}$	$^{total}(Ca^{+2}, Mg^{+2}) - ^{seasalt}(Ca^{+2}, Mg^{+2})$
2. Na^+, K^+	(a) $^{seasalt}Na^+, K^+$	$^{sea}(Na^+, K^+/Cl^-) \times ^{total}Cl^-$
	(b) ^{crustal} or $^*Na+, ^*K^+$	$^{total}(Na^+, K^+) - ^{seasalt}(Na^+, K^+)$

and 2, besides half of the HCO_3^- formed by equation 4 while rest of HCO_3^- is atmospheric i.e. $^{atms}HCO_3^-$. Here, in model we assumed that the snowpack

SO_4^{-2} and the proportion of $^{atms}HCO_3^-$ derived from silicate carbonation. Estimation of snowpack SO_4^{-2} (i.e. $^{sea}SO_4^{-2}$ and $^{aerosol}SO_4^{-2}$), assumed that in snowpack ratio of $SO_4^{-2}:Cl^-$ was 0.05.

4.5.1 Simple hydrolysis of carbonates (SHC)

In SHC process i assumed that under subglacial conditions approximately ~110 μM of bicarbonate the total concentration of HCO_3^- extensivelystated for chemical weathering (Tranter et al., 2002; Wadham et al., 2010). In early phase of the melt-water when meltwater release and get in contact with subglacial bedrock/sediment plays a crucial role in chemical weathering.

4.5.2 HCO_3^- concentration linked with aerosol hydrolysis

This process involved neutralization of HNO_3^- and SO_4^{-2} in carbonate weathering occurs. In process one mole of NO_3^- releases one mole of HCO_3^- and one mole of SO_4^{-2} (atmospherically derived) produces 2 moles of HCO_3^-. Atmospheric sulphate was assumed between the variance of total sulphate and marine derived sulphate concentration.

4.5.3 Sulphide oxidation coupled with carbonate dissolution (SOCD)

The occurrence of S^{-2} (Sulphide) and CO_3^{-2} mineral basically derived from rocks even in minor quantity because of their rapid dissolution nature. Therefore SO-CD regulates from crustally derived SO_4^{-2} and CO_3^{-2} like 2 moles of HCO_3^- originates from 2 mole of SO_4^{-2}.

4.5.4 Concentration associates with monovalent cation

In this part presumed that the sodium and potassium are crustally consequent (i.e. $^*Na^+$ and $^*K^+$) through carbonation of aluminosilicate minerals. Therefore, aluminosilicate mineral concentration is 3.4 times higher than the concentration of HCO_3^-.

4.5.5 Concentration associated with carbonate for carbonation (CC) mineral

CC produces from both atmospheric and crustal derived. H^+ ion derived from nitrate and sulphate supposed to yield from crustally derivative via carbonate weathering, and rest of the concentration derived from SHC and carbonate carbonation.

4.5.6 Concentration associated with microbial oxidation of carbon

Carbonate association with microbial oxidation has a potential source of CO_2 in subglacial environments (Hodson et al., 2000; Wadham et al., 2010; Hindshaw et al., 2017). Latest studies suggest that Himalaya basin is mainly dominated with silicatic rocks that's why organic carbon is less significant (Graly et al., 2017). Furthermore, dissolved organic carbon (DIC) is less in Himalayan catchment, so here assumed that DIC produced via organic carbon is negligible.

4.5.7 Saturation indices calculation for pCO₂

The saturation indices calculation was performed to determine the partial pressure of CO_2 (pCO_2). By using PHREEQC software by MINTEQ software (Parkhurst and Appelo, 2013).

4.6 Calculation of trace elements provenance

4.6.1 Crustal enrichment factors

The enrichment factor (EF) is important to distinguish between natural vs. anthropogenic influence of the trace elements (TEs) (Tripathee et al. 2016). Therefore, we calculated EF to interpret the contribution of crustal or anthropogenic influence on TEs in the snow/rain samples collected from our sampling site. It is defined as the concentration ratio of the element to that of crustal elemental concentration (e.g., Al, Fe). To determine the relative crustal enrichment in the composition of an element, we used the major rock type present in the form of debris over the glacial belt of Higher Himalayan Crystalline (HHC) rocks as a reference material; this effort maximized the probability of quantifying the relative effects of natural crustal and anthropogenic sources in precipitation. The EF is calculated as Eq 9:

$$EF_{(x)}= (C_x/C_r)_{\text{precipitation}}/(C_x/C_r)_{\text{crust}} \qquad (9)$$

Here, Cx represents the element of interest, and Cr represents the concentration of reference material. The precipitation represents the wet deposition while crust represents the crustal material (dry/solid), respectively (Cong et al. 2010). We used Fe as a reference material due to its abundance in crustal rocks and absence of contamination affinity. Many previous studies were established on the upper continental crust (UCC) because the categories of crustal material are differ at differ sites. Consequently, this study, we took an elemental reference (UCC) to reduce uncertainty. The interpretation is based on the consideration that values between 0.1 and 10 are only slightly or not affected by the enrichment of local soil or lithology. On the contrary, the values between 10 and 100 are considered moderately enriched and indicate that the natural or anthropogenic sources are the contribution to precipitation. Moreover, the values more than 100 are categorized as highly enriched of the particular element, and the level of contamination increases with the higher values of EF (Kang et al. 2010; Huang et al. 2009; Tripathee et al. 2014).

4.6.2 Correlation matrix and principal component analysis

In order to understand the inter-relation and common source of trace metals during the non-monsoon and monsoon seasons, correlation and principal component analyses were performed. Pearson correlation matrix is a bivariate method used to compute the associated strength among 2variables where it is suggestive of the relationship between the two variables regarding positive or negative values, whether it increases/decreases with the other values, respectively. Principal component analysis (PCA) provides information about the factors controlling the dissociation of elements. PCA analyses for the non-monsoon and monsoon season were performed using XSLAT software. The PCA was the components extracted varimax rotation to provide a clear picture of variable loading in factor (Tripathee et al. 2016b; Cheng et al. 2011). Kruskal-Wallis is also known as ANOVA non-parametric test that accesses the difference between non-normally distributed data if there is a statistically significant difference between two or more variables. Here,

ANOVA is applied between those datasets which has two or more subgroups, to test the k independent values for all the subgroups as equally distributed function against the alternative hypothesis with respect to the median. All statistical analysis was performed under SPSS software version 16.0.

4.6.3 Backward trajectory analysis

Globally to know the source of circulation pattern of wind and transportation of ion was assessed from HYSPLIT (Hybrid Single-particle lagrangian Integrated Trajectory) model from NOAA (National Oceanic and atmospheric Administration) Air Resources Laboratory (Draxler et al., 2010) it is created on the assimilation of the position of air regarding time. Meanwhile, air parcel is moved with the wind, when particle is in primary position P(t) s inert transport would be estimated by estimating 3-D mean of speed vector and approximate position P'(t+dt). Speed vector is plotted against both space and time. The calculation used in HYPSLIT are as follows Eq 10,11.

$$P(t+dt) = P(t)+V(P.t)dt \qquad (10)$$

So assume last point of air parcel

$$P(t+dt) = P(t)+0.5[V(P,t)+V(P', t+dt)]dt \qquad (11)$$

The backward trajectories were calculated for everyday analyzed (at morning, at noon, at evening, at midnight in accord with local time) available at 3 differ heights i.e. 1500m, 1000m, 500m. it is suggested that heights chosen with pressure interval of 950-10mb because the pressure less than 950 mb results the air mass in ground(Smith et al., 2005). With HYSPLIT model the pattern of air parcel was deliberated, the map is used from NOAA site.

CHAPTER 5

RESULTS & DISCUSSION

This study presents a combination of time series and dimensional analysis of the chemical weathering mechanism operating at a monsoon dominated glacier system of central Himalaya. The primary assessment of meltwater chemistry from basin has been done using surface layer of snow and snowpit in the accumulation zone and secondary from the meltwater discharge from snout of the glacier. The resultant of weathering fluxes typically represents the characteristics of a glacier system including its geometry, geomorphology, source of ionic inputs, mineral dissolution process is governed by physical disintegration of reactive grain surfaces and kinetic reactions. The properties of ionic ratio and total ionic concentration of meltwater were used to trace the various reactions controlling the ions in the meltwater. Major ions including cations (calcium, magnesium, sodium, and potassium), anions (bicarbonate, chloride, nitrate, fluoride andsulphate) and trace elements (arsenic, manganese, copper, cesium, lead, zinc, cadmium and iron) were used to trace the source of mineral dissolution in mixing solution through mass balance of ion stoichiometry. To better understand the trends of ions releasing through chemical weathering at Dokriani Glacier system, this study has examined different input of ions in melt waters i.e. through precipitation, snowfall, supraglacial lakes and supraglacial streams. This allowed us to differentiate the atmospheric, supraglacial and englacial ionic chemistry influencing the overall chemical budget of Dokriani Glacier system.

5.1 Chemical characterization of precipitation and supraglacial waters

The mechanism which controls the both regional ionic transport along with atmospheric circulation pattern would reflect in suspended dust particle and chemical ions present in snow (Eichler et al., 2001; Li et al., 2007; Ming et al., 2009). Therefore to build a better understanding of water chemistry at Dokriani Glacier, dry and wet deposition sources was examined. Firstly the dry deposition (snowfall) was accessed using snow samples collected through snowpit profiling. During the study period (2013-2015), the surface snow samples from two snow pit profiles at an altitude of 4350 and 4364 m a.s.l. were collected. The snowpit was recorded twice during pre-monsoon season (April- May) only. Post monsoon period sampling couldn't be done due to accessibility issues. A total number of 34 representative samples have been collected from ablation zone of Dokriani Glacier (Table 5.1). The average concentration of major anions HCO_3^-, Cl^-, SO_4^{2-}, NO_3^- and F^- fluctuated between 0-50, 0-20, 8-18, 0-19 and1-18µE L^{-1} respectively for the years 2013 to2015. Similarly, the concentration of major cations Na^+, K^+, Mg^{+2}, and Ca^{+2} fluctuated between 2-19, 1-17, 1-10, 2-36 µE L^{-1} respectively for the year 2013 to 2015. Details of the ions are presented in (Table 5.1). The results of major ions in snow pit suggests that in anion HCO_3^-, SO_4^{2-} and in cation Na^+, Ca^{+2} were dominant for the year 2013 whereas the SO_4^{-2}, NO_3^- were major anion; Ca^{+2} was dominant anion for the year 2015 (Figure 5.1). Similarly, the average concentration of major anions HCO_3^-, Cl^-, SO_4^{-2}, NO_3^- and F^- were fluctuated between 0-9.34, 1.95-13.6, 1.51-124.70, 1.07-19.28 and 0.69-18.48 µE L^{-1} respectively. Correspondingly, the concentration of major cations Na^+, K^+, Mg^{+2}, and Ca^{+2} fluctuated in between 2.03-9.01, 0.65-16.86, 1.82-9.83, 1.82-30.39 µE L^{-1} respectively for the year 2015. Details of the ions are presented in (Table 5.1). The observed K^+/Na^+ (0.42), Mg^{+2}/Na^+ (0.27), and Ca^{+2}/Na^+ (3.66) ratios in the snowpit samples are significantly higher than sea salts ratios K^+/Na^+ (0.02), Mg^{+2}/Na^+ (0.11), and Ca^{+2}/Na^+ (0.02) suggests that the ionic contribution from terrestrial sources are higher than atmospheric deposition. Higher concentrations of these major ions also originated through combustion of vegetation/wood, unburnt fossil fuel burning and industrial emission (Lyons et al. 1981).

Concentration of SO_4^{-2} was similar to Ca^{+2} that could be correlated with dissolution of carbonate dust in supraglacial melt waters during melting (Tranter et al., 2002; Stanchik et al., 2016). Earlier observations also support the fact that contribution of K^+, Ca^{+2} and Mg^{+2}, is principally controlled by various other factor like weathering, industrial or biological missions (Nijampurkar et al., 1993). Furthermore, it was also observed that the ratio between the different ions like Cl^-/Na^+, K^+/Na^+, Mg^{+2}/Na^+, and Ca^{+2}/Na^+ are elevated in the snow pit compared with those in surface snow. It was suppose that this much likely accused due to the elution effect of snow melting during the peak ablation season. Generally, most of the ions are concentrated on the surface and easily are most of the salts concentrate on the snow surface and easily eluted by percolating melt water.

Secondly, we accessed the ionic variability in wet deposition (rainfall) through ionic concentration. Examined order of variability for ions follows following trend: $HCO_3^->SO_4^{-2}>NO_3^->Cl^->F^-$ for anion and $Ca^{+2}>Na^+>Mg^{+2}>K^+$ for cation during the period of May 2013, for May 2015 the ionic trend shows the order are as follows: $SO_4^{-2}>NO_3^->HCO_3^->F^->Cl^-$ for anion and $Ca^{+2}>Mg^{+2}>K^+$ for cation. The snowpit datasets are represented in Table 5.1. The percentage contribution of anion is HCO_3^- contribution was~28% of the total sum of the ions, while in case of cation Ca^{+2} was the most abundant ion contributing ~18% with respect to the total ions. Simultaneously, Ca^{+2} and HCO_3^- derived from crustal supply contributed ~ 66% of the total ion concentration that will be caused by the dissolution of carbonate dirt. The ionic composition in precipitation and aerosol over the central Himalayan region correlate well with different studies (Tripathee et al., 2014, 2016, 2017).

The concentration of Ca^{+2} showed the good peak throughout each the seasons successively recommend the only management of precipitation driven through region aerosol deposition.

Table 5.1: Ionic equivalent ratios of snowpit at Dokriani Glacier

Variables	Pre-monsoon 2013				Pre-monsoon 2015			
	Min.	Max.	Mean	Stdev	Min.	Max.	Mean	Stdev
pH	5.10	7.09	6.25	0.00	6.32	7.32	6.57	0.52
EC	6.28	9.08	7.10	1.00	19.08	25.00	19.53	3.35
Na^+	2.09	20.00	8.59	5.58	0.00	9.01	5.02	2.57
K^+	1.00	11.00	3.41	2.62	0.00	16.86	5.14	4.11
Mg^{+2}	1.00	4.00	1.79	0.77	0.00	9.83	5.42	2.71
Ca^{+2}	17.00	59.90	25.70	10.54	0.00	30.39	15.13	9.29
HCO_3^-	10.00	50.00	21.88	12.05	0.00	9.34	0.62	2.41
F^-	1.00	4.00	1.85	0.90	0.69	18.48	7.49	7.42
Cl^-	4.00	20.00	8.65	5.02	1.95	13.60	7.53	3.65
SO_4^{-2}	8.00	21.00	12.94	4.37	1.51	124.70	15.56	31.49
NO_3^-	3.00	16.00	8.00	3.66	1.07	19.28	7.01	5.13

Further, the assessment of major anions sources suggests the origin of Cl^- and NO_3^- within the glacial atmosphere, in the main controlled through the dissolution of oceansalt and aerosols (Souchez and Lemmens, 1987). The concentration of major ion within the snow pit indicates affinity towards the marine and terrestrial sources as most of the anions like Cl^- and SO_4^{-2} are in the main originated from region circulation of ocean salt and combustion of fossil fuel that might be transported to the upper Himalaya region and at the glacial atmosphere (Tripathee et al., 2014, 2017). The correlation of Na^+ and Cl^- within the snow pit showed good associations among one another (r^2=0.85) suggesting that these ions largely originated from the sea-salt from the Indian Ocean (Table 5.2). Moreover, in thepresent study, the quantitative relationof Na^+/Cl^- has been used as a relation to infer the supply of Cl^- within the winter precipitation, which is wealthy in oceansalt (Sequeira and Kelkar, 1978). However, the quantitative relation of Ca^{+2}/Na^+ within the snowpit shows the affinity towards terrestrial

sources that has been supported by the previous studies from the Himalayan region (Sequeira and Kumar 1978; Nijampurkar et al. 1986).

Table 5.2: Correlation coefficients of major ions in snow pit at Dokriani Glacier in the month of May for the years 2013 and 2015

2013	HCO_3^-	F^-	Cl^-	SO_4^{-2}	NO_3^-	Na^+	K^+	Mg^{+2}	Ca^{+2}
HCO_3^-	1								
F^-	0.34	1							
Cl^-	0.31	0.31	1						
SO_4^{-2}	-0.19	-0.10	0.24	1					
NO_3^-	-0.07	0.16	0.04	0.72	1				
Na^+	0.51	0.55	0.83	0.06	-0.08	1			
K^+	0.53	0.40	0.88	0.09	0.06	0.79	1		
Mg^{+2}	0.69	0.47	0.02	-0.15	0.15	0.13	0.16	1	
Ca^{+2}	0.63	0.13	0.33	0.28	0.06	0.50	0.27	0.38	1

2015	HCO_3^-	F^-	Cl^-	SO_4^{-2}	NO_3^-	Na^+	K^+	Mg^{+2}	Ca^{+2}
HCO_3^-	1								
F^-	-0.13	1							
Cl^-	-0.42	-0.17	1						
SO_4^{-2}	0.96	-0.05	-0.39	1					
NO_3^-	0.30	-0.35	-0.06	0.28	1				
Na^+	-0.08	-0.06	-0.47	0.01	-0.18	1			
K^+	-0.25	0.14	0.13	-0.24	-0.69	0.41	1		
Mg^{+2}	0.23	0.14	-0.25	0.27	-0.49	0.28	0.63	1	
Ca^{+2}	0.13	0.52	0.07	0.12	-0.49	-0.07	0.61	0.38	1

To establish correlation among ionic concentrations, factor analysis, principal component analysishas been computed (Table 5.3). It is based on the fact that the number of principal components is less or equal to the original

variables and reduces the larger value into alittle style of illustration. The observations suggests that in 2013, the primary issue F1 accounts for thirty 32.46. Total variance in major ions represents higher loadings for Na^+ and Cl^- and K^+ that additionally supports the previous facts that the ocean salt, mineral, and therefore the continental dust is that the major supply of this particle deposition over glacier surface. On the contrary, the second issue F2 accounts for 20.9% variance which show the second highest loadings for SO_4^{-2} in 2013 whereas issue shows 19.7% variance and shows the upper concentration of Cl^- within the year 2015 database (Table 5.3). This loading of major ions signifies that the most input is sourcing from each the atmosphere and native valley dust. The upper loadings of SO_4^{-2} and NO_3^- are originated from the two sources biogenic and phylogeny activity, that transport through an extended varies of atmospheric state. These ions are the secondary supply of the aerosol, which directly emitted into the atmosphere or produced within the atmosphere together with numerous reactions like reaction, radical and carbonate pervasion reactions (Jacobson et al., 2002).

Table 5.3: Principal component analysis of Dokriani Glacier throughout the study period May 2013 and 2015.

	Snow pit-2013-May				Snow pit-2015-May		
Variables	**F1**	**F2**	**F3**	**Variables**	**F1**	**F2**	**F3**
pH	-0.56	-0.13	0.16	**pH**	ND	ND	ND
EC	-0.6	-0.16	0.34	**EC**	ND	ND	ND
Na^+	0.82	-0.38	-0.1	**HCO_3^-**	0	0	0
NH_4^+	0.26	0.7	0.5	**Cl^-**	-0.11	0.86	0.04
K^+	0.84	-0.14	-0.11	**SO_4^{-2}**	-0.07	-0.68	-0.47
Mg^{+2}	0.21	-0.3	0.81	**NO_3^-**	-0.81	-0.26	-0.13
Ca^{+2}	0.6	-0.26	0.19	**Na^+**	0.35	-0.52	0.65
HCO_3^-	0.58	-0.49	0.49	**NH_4^+**	0.18	-0.2	-0.22
Cl^-	0.87	-0.03	-0.24	**K^+**	0.88	0.17	0.32
SO_4^{-2}	0.33	0.73	0.09	**Mg^{+2}**	0.75	-0.36	0.01

NO$_3^-$	0.29	0.84	0.34	Ca^{+2}	0.74	0.19	-0.46
Variability				Variability			
(%)	32.46	20.91	14.38	(%)	32.63	19.74	14.67

ND refers to not determined

5.1.1 Determination the long range transport of ion source by prevailing air masses

Further the HYPSLIT (section 4.6.3 methods) model was applied to constrain the long-range dust deposition sources (Figure 5.1) (Draxler et al., 2010; Carrico et al., 2003; Yalcinet al., 2006b). Results from backward trajectory analysis generally shows the during winter months (November-February), the dominated sources of moisture and dust were coming from North-Western Himalaya, i.e. dominated with Western Disturbances. Western Disturbance sources the elements through marine and terrestrial waters carries the marine elements (Na$^+$, K$^+$, Mg^{+2}, Ca^{+2} and Cl$^-$) derived from the sea salt proportion and terrestrial elements (K$^+$, Ca^{+2}) derived from the biological emission. However,we observed for rest of the year (Fig 5.3) the precipitation sources were sourcing from South-western part of Asia, i.e. the Thar Desert. This could be suggested that the dust proportions were much probably source from arid and semi-arid region of Asia (Luo and Yanai, 1983; Murakami, 1987; Wake et al., 1992, 1994; Williams et al., 1992) and promotes the higher concentration of aerosols during pre-monsoon season characterised as long range transport mechanism. The dust remained within the atmosphere for a time and it scavenged through a precipitation.
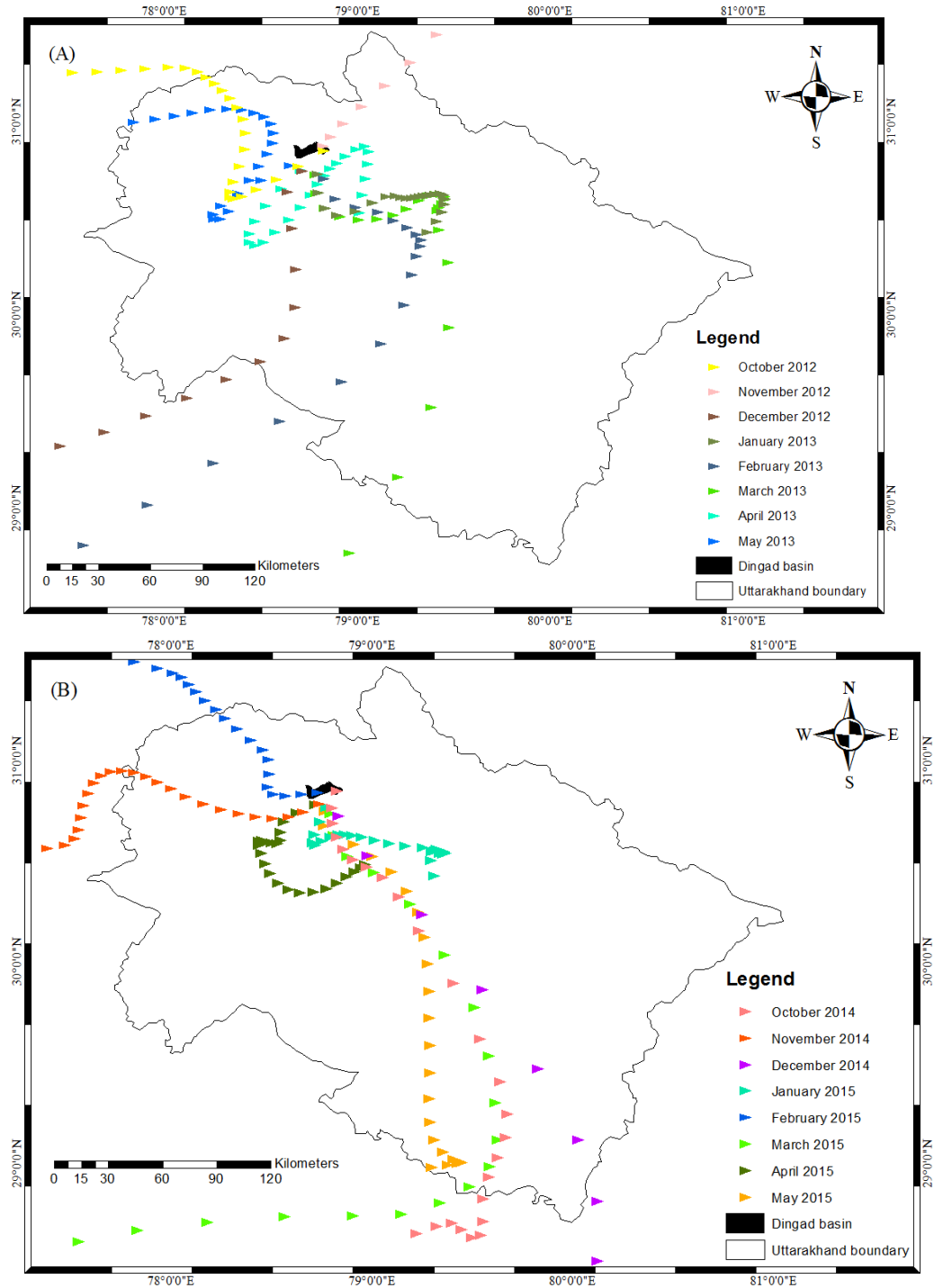
Fig.5.1: Air mass backward trajectories by HYSPLIT model ending at 0400 GMT at Dingad catchment is the sampling site throughout winter months A) represents the sampling period from October 2012 to May 2013 B) represents the sampling period from October 2014 to May 2015.

5.2 Chemical characterization and seasonal meltwater chemistry

Given the chemistry of dry and wet deposition over glacier, this study has further evaluated the meltwater chemistry of Dingad meltwater stream coming out from the terminus of Dokriani Glacier. The physical parameters i.e. pH, water temperature, EC data were measured *insitu* and major ion and trace element of the glacial melt water stream were analyzed in laboratory. Details of analysis are presented in chapter 4 section.

To better understand the seasonal variation and quantify the prominent change in the meltwater chemistry at the Dokriani Glacier, the whole ablation period was divided into 3 different seasons i.e. early ablation (May-mid to June), peak ablation (mid-June to August) and Late ablation (September-October). The general observation on physical parameter and major ions concentrations of theses melt water were as follows:

5.2.1 Early Ablation Season

To evaluate the early ablation season chemistry the sample collection was done for the year 2015 and 2017 during the month of May and mid-June. The physical parameters recorded from hydrological site ranges as follows: pH 6.35 to 7.44, EC from 43.80 to 131 μScm^{-1}, whereas the major cations Na^+ and Cl^- shows the range 4.81 to 54.70 $\mu E\ L^{-1}$ and 3.81 to 13.21 $\mu E\ L^{-1}$ respectively, SO_4^{-2} shows the highest concentration among anions i.e. from 257.79 to 433.69 $\mu E\ L^{-1}$. Examined order of variability for ions follows the following trend: $SO_4^{-2} > NO_3^-$ $> HCO_3^- > F^- > Cl^-$ for anion and $Ca^{+2} > Mg^{+2} > Na^+ > K^+$ for cation for the early ablation season. The pH value (<7) of early ablation period suggests slight acidic nature of the meltwater stream; however, in range of other central and western Himalayan glaciers (Hasnain et al., 1999; Singh and Ramanathan, 2015). Average concentration and standard deviation of the datasets are presented in Table5.5. Among the major anions, SO_4^{-2} constitutes up to 80% of TZ^- (total anions) concentration and Ca^{+2} as major anion adding up to 76% of TZ^+ (total cations)

concentration. At the starting of June, the concentrations of ions decreased slightly much likely due to the dilution effect caused by heavy rainfall events. While as the year progressed change (drop) in concentrations for all ionswas observed throughout the ablation season. This might be linked with dilution effect of discharge, however due to unavailability of daily discharge data it cannot be linked with change in chemical weathering patterns.

5.2.2 Peak Ablation Season

In the peak ablation season, sample collection was done in June 2016 & 2018 only due to sampling restrictions. In the late period of June, which characteristically represents the period coincided with heavy monsoonal precipitation and thereby high runoff. Examined order of variability for ions follows early similar trend as early ablation period: $SO_4^{-2} > NO_3^- > HCO_3^- > Cl^- > F^-$ for anion and $Ca^{+2} > Mg^{+2} > Na^+ > K^+$ for cation for the early ablation season. Due to sampling limitations the peak ablation season data were not recorded therefore major conclusions cannot be drawn from present data. However, it is much likely that the increase and decrease of these changes in ions is much likely caused due to the leaching of ions from snowmelt. A marked decrease in the ionic concentration was observed during this period that could be correlated with the dilution effect due to excessive rainfall during peak rainfall. The average concentration value of Na^+ (12.45 µE L^{-1}), Cl^- (5.66 µE L^{-1}), Mg^{+2} (20.04 µE L^{-1}) and SO_4^{-2} (156.75 µE L^{-1}) is fallen between whereas Ca^{+2} and HCO_3^- concentration ranging from 209.6 µE L^{-1} to 9.18 µE L^{-1} in 2016 whereas average concentration value of Na^+ (30.75 µE L^{-1}), Cl^- (7.32 µE L^{-1}), Mg^{+2} (20.04 µE L^{-1}) and SO_4^{-2} (172.66 µE L^{-1}) is fallen between whereas Ca^{+2} and HCO_3^- concentration ranging from 317.01 µE L^{-1} to 14.64 µE L^{-1} in 2018.

5.2.3 Late Ablation Season

The melt water samples for late ablation season were collected for the year October 2015 during September and October month. The late ablation melting

rate decrease compared to peak ablation period. Subsequently the ionic concentration has increased particularly for crustally derived elements except the NO_3^- and Cl^- which is assumed to be derived from the atmosphere (Hodson et al., 2000). The increase in the concentration of SO_4^{-2} and Ca^{+2} further prominent from 300 μE L^{-1} to 550 μE L^{-1}. The contribution of SO_4^{-2} in comparison with total anion reached 40% which exceeding rest of the ablation season (Fig 5.2). The Mg^{+2} and Cl^- shows the same consistency from the early ablation season, and the concentration of Na^+, K^+, F^-, Cl^- remain 150 μE L^{-1} similar in early and peak flow season. To access the overall seasonal hydrogeochemistry and dominance of weathering reactions releasing major ions in meltwater biplots of dominant cations were used. Fig 5.3 shows strong correlation of Ca^{+2}, Mg^{+2} ions against total cationic release both for silicate and carbonate weathering. However, the Ca^{+2}, Mg^{+2} release from carbonate minerals lies near the equiline suggests its dominance in meltwater compared to silicate mineral weathering. Overlooking the fig 5.2 suggests the trends of ions release from Dokriani glacier basin has not changes much in recent years. However, with bulk chemistry only speculation could be made regarding the dominance of chemical weathering type.

Table 5.4: Statistical analysis of water chemistry in different period at the Dokriani Glacier.

Year		pH	EC	HCO_3^-	F^-	Cl^-	SO_4^{-2}	NO_3^-	Na^+	NH_4^+	K^+	Mg^{+2}	Ca^{+2}
	Mean	6.54	114.57	35.74	8.67	5.77	304.39	38.79	33.47	3.09	28.72	41.07	404.24
	Max	7.30	131.00	42.62	13.27	7.44	364.49	79.50	45.66	25.64	35.58	51.63	509.86
	Min	6.35	96.30	31.15	6.32	3.81	257.79	24.19	4.81	0.00	4.79	6.82	12.88
	Stev	0.23	3.41	3.41	2.23	1.11	30.71	12.85	10.50	7.51	7.27	10.34	119.84
Early Ablation	Mean	7.06	73.87	34.63	5.94	6.59	366.63	26.76	28.52	4.86	34.78	37.50	406.63
	Max	7.44	116.40	42.62	11.02	13.21	433.69	49.56	54.70	10.09	43.93	47.12	497.95
	Min	6.66	43.80	29.51	3.93	3.90	311.50	2.25	22.33	2.61	30.64	30.95	312.96
	Stdev	0.18	20.06	3.36	1.64	1.90	33.74	12.39	6.22	1.65	2.78	4.37	47.91
	Mean	6.67	43.00	9.18	4.69	5.66	156.75	20.65	12.45	2.26	22.12	20.04	209.60
	Max	6.86	59.70	15.08	6.85	10.10	228.56	31.43	22.90	7.90	34.83	31.98	273.52
	Min	4.88	16.31	2.05	0.78	0.71	11.83	0.16	2.58	1.17	1.54	101.64	140.75
	Stdev	0.11	6.24	2.98	1.75	2.27	38.12	7.15	4.61	2.21	5.91	7.05	49.44
Peak Ablation	Mean	6.10	40.09	18.43	5.90	7.27	177.09	7.81	31.46	9.75	38.37	222.79	315.97
	Max	6.40	72.40	43.45	229.28	123.17	379.96	84.87	194.60	230.22	148.23	396.72	572.65
	Min	5.98	37.00	10.70	0.78	0.71	11.83	0.15	2.58	1.17	1.54	101.64	140.75
	Stdev	0.25	14.79	6.6	29.3	15.3	94.8	15.3	27.5	33.3	20.2	49.4	105.3
	Mean	7.08	62.85	28.06	3.71	3.43	342.62	3.29	28.85	4.86	34.74	45.48	411.81
	Max	7.13	81.60	36.07	5.57	5.99	427.44	8.83	38.60	10.29	42.47	59.31	508.90
Late ablation	Min	6.66	43.80	29.51	3.93	3.90	311.50	2.25	22.33	2.61	30.64	30.95	312.96
	Stdev	0.05	10.06	4.37	0.67	1.38	61.52	1.87	6.62	1.88	5.12	13.59	83.88

Here all major ions are in µE L^{-1}, EC in µS cm^{-1}
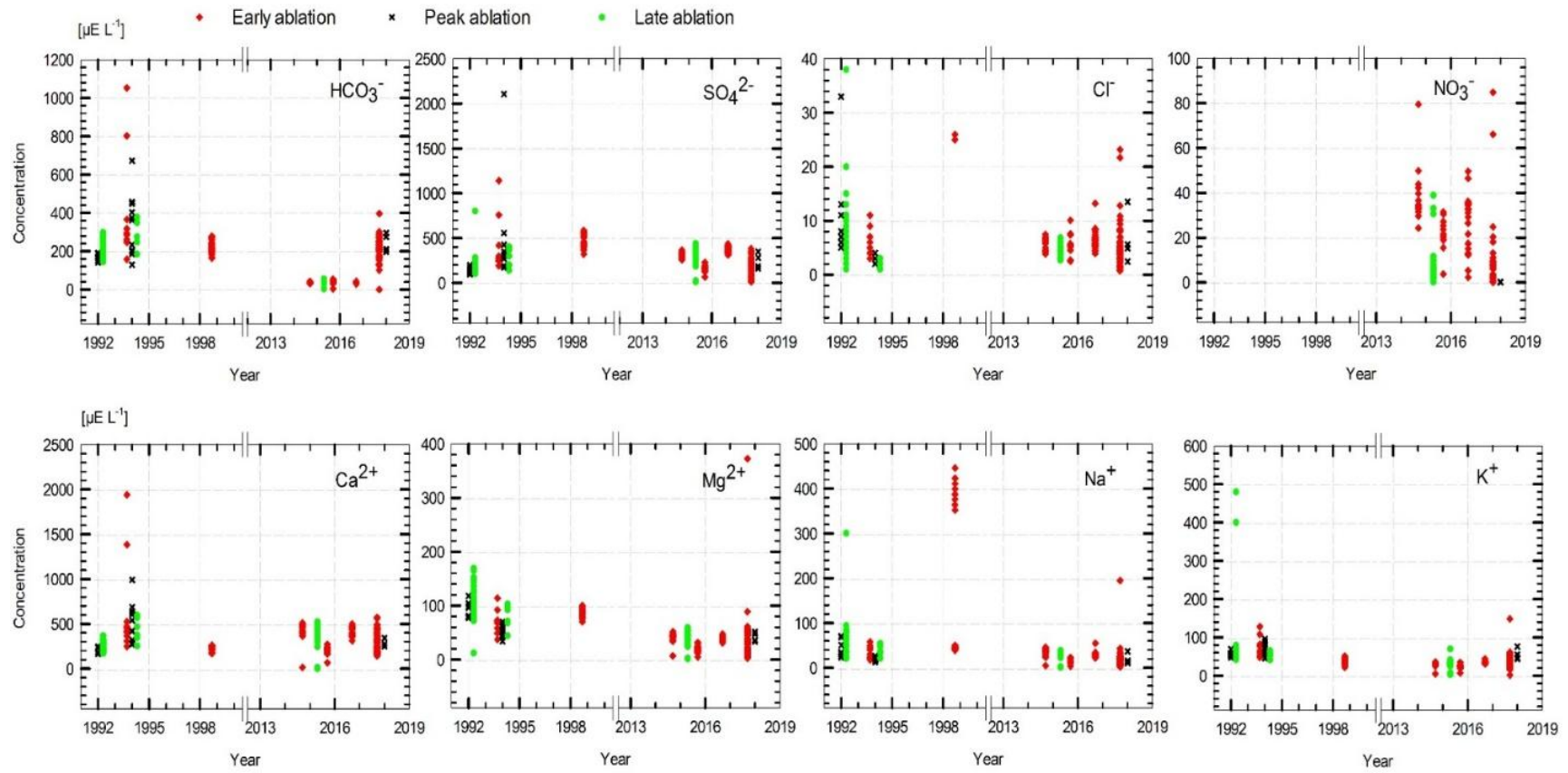
Fig.5.2: Average concentration of water chemistry in different period of the ablation season at the Dokriani Glacier.
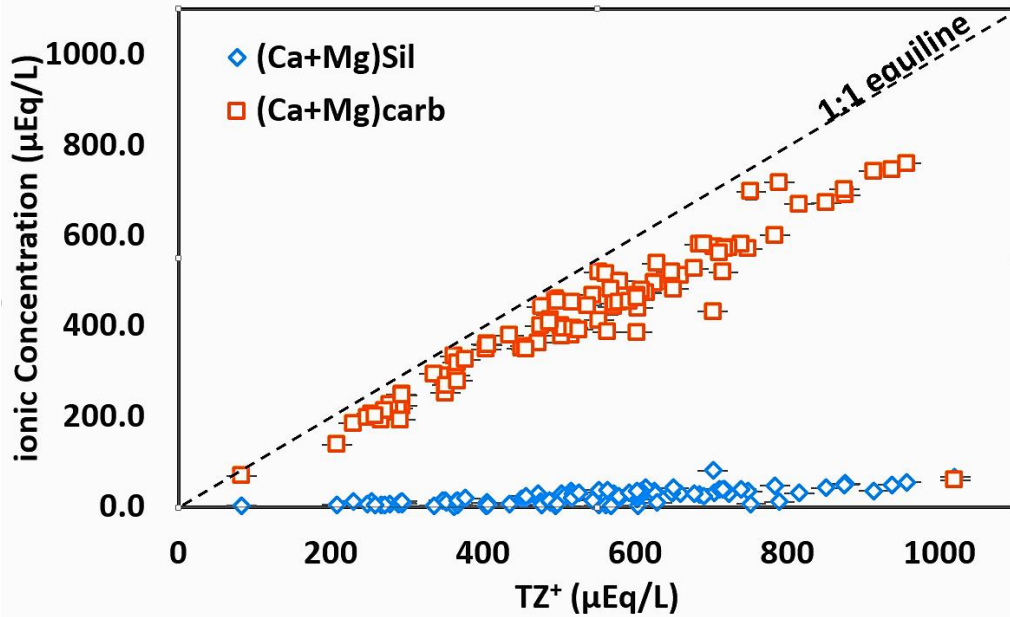
Fig.5.3: Scatter plot between ionic concentration vs TZ^+ in the late ablation

season.

5.3   Concentration-discharge relationships

During the whole ablation season, ionic concentration has been changed significantly (Fig. 5.2). During early to peak ablation period an increase in the average discharge was observed from 2.5 m^3s^{-1} to 5 m^3s^{-1} was observed due to increased rainfall and its attendant runoff. It has decreased gradually during late ablation season starting from early September fig 5.4 suggests some order control over ionic release. Although, overall relationship between ionic concentration and discharge is week (>0.2) for all ions, yet they decrease initially with increase of discharge suggesting dilution effect, but for higher discharge we have observed variable results especially for Ca^{+2} ion. The order of magnitude of the dissolute consecutive over the whole entire season is as follows $^*Ca^{+2}>^*SO_4^{-2}>^*Mg^{+2}>*HCO_3^->^*Na^+>^*K^+$. The entire ablation shows the solute yield was estimated to be 80.6× 10^6 m^3, 49.8×10^6 m^3 and 14.1× 10^6 m^3 respectively. The solute corrected from the atmospheric concentration reached only 8 $mEm^{-2}yr^{-1}$. Here we assume that the denudation rate in glacial environment was equal to atmospheric deposition because the solute yield delivered by wet precipitation is

71

negligible. To access the concentration-discharge relationships of major ions release from Dokriani glacier basin, all the datasets collected in present study and from published estimates from Dokriani glacier basin has been combined (Fig 5.4). The concentration–discharge relationships have been used widely to trace hydrochemical processes that control runoff chemistry (Godsey et al., 2009). These are linear logarithmic plots representing power-law relationship between concentration and discharge where the slope has physical relationship. A slope of zero would represent the glacier are behaving chemostatically, while the negative slope are indication of discharge dilution effects i.e. ionic fluxesgets diluted as discharge increase. The observed variability for precipitation corrected cations and anions in concentration-discharge relationships are presented in Fig 5.4. A clear trend of negative slopes was observed for all the ions during peak monsoon periods suggesting dilution effect in ionic concentrations for increase in discharge.
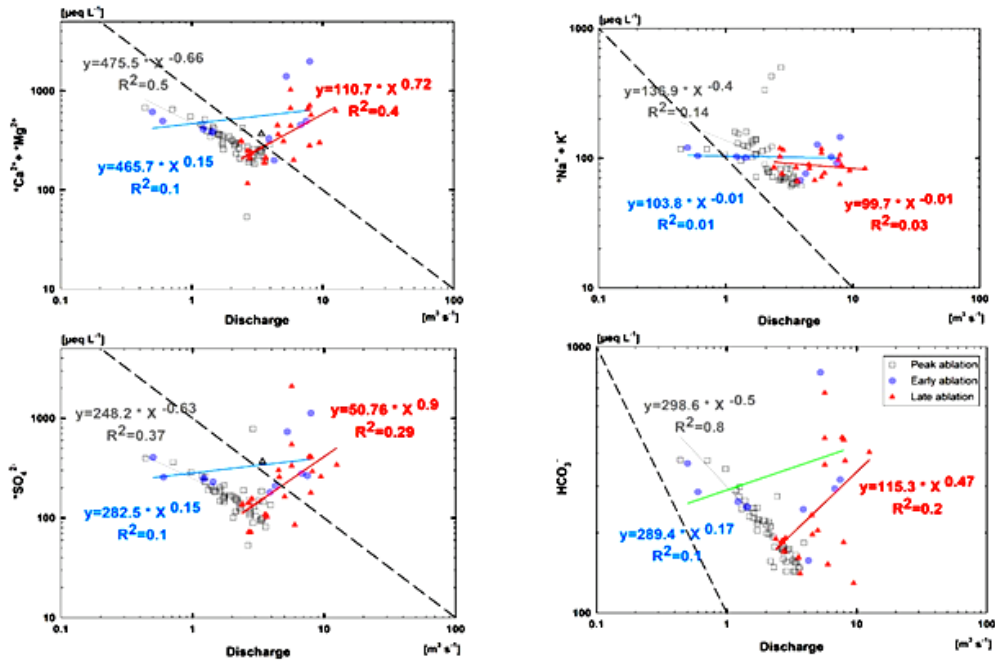
Fig. 5.4: Concentration of consecutive ions againstdischarge patterns during the ablation season for the years 1994-2018 at the Dokriani Glacier.

However, in near zero slopes ions were behaving chemostatically, so the discharge was not the sole factor controlling the ionic release from glacial basins in early ablation periods. This observation was opposite compared to late monsoon discharge, when discharge is usually low and controls the ionic variation. These observations are important to explain the weathering process which controls the ionic release for the basin in different ablation seasons.

5.4   Co-variation of silicate and carbonate weathering and its attendant CO_2 release

5.4.1   Seasonal variability at Dokriani Glacier

Chemical weathering in glacial basin were characterized by the availability of H^+ ion that interact with rock/mineral surface and results into several reactions. These reactions (eq 1-7) include simple hydrolysis, carbonation, sulfide oxidation, organic carbon oxidation, sulphide oxidation reaction coupled with carbonate/feldspar dissolution and carbonation of carbonate (Eq. 1-2). The reactions mentioned above affect the ionic release and results in the change in ionic ratios. The results generated through linear regressions and scatter plot among ions evidenced the above mentioned facts for reactions i.e., silicate, carbonate, sulphide oxidation possible in subglacial weathering regimes (Fig 5.5). In our results, it is assumed that if the weathering occurred only due to the silicate minerals, then the slope of data shows that the sulphide oxidation coupled with carbonate dissolution (SOCD) might play an important role in the whole ablation season. SOCD reaction has slope coefficients of 2.0 to 1.0 for ion associations with total cations (TZ^+) vs SO_4^{-2} and TZ^+ vs HCO_3^- respectively (Eq 3,4) (Tranter et al., 2002; Wadham et al., 2010a). It could be observed that the reaction i.e. sulphide dissolution coupled with carbonate carbonation is not occurring in concurrence with silicate weathering as all the data lies between organic matter oxidation and SDC in 1:1 equiline in whole ablation season (Eq 5). Sulphide oxidation coupled with silicate dissolution (SOSD) causes increase of SO_4^{-2} concentrations leading to increase the slope of TZ^+ vs SO_4^{-2} and decrease the slope

73

of TZ^+ vs HCO_3^-. Tranter et al. (2002) suggested that these intercept suggests the initial stage of weathering when water comes in contact with rock for the very first time in early ablations seasons and release one Ca^{+2} and HCO_3^- ion in meltwater through simple hydrolysis weathering process (Eq 6). However, the higher intercept indicate the production of supplementary H^+ ion formed by other reaction such as oxidation of organic carbon present in glacial substrate soils (Eq 7). In case of simple hydrolysis weathering silicate minerals, pH increase but intercept didn't change (Eq 9). Further, the second assumption is that if Ca^{+2} and Mg^{+2} is derived mainly from the carbonate weathering then the proportions of SO_4^{-2} and HCO_3^- (Fig 5.3) release in melt water indicates that processes that release sulphate in melt water are dominating. The good slope of intercept between TZ^+ vs SO_4^{-2} and TZ^+ vs HCO_3^- ($r^2= 0.75$ and $r^2= 0.31$) suggests the processes of sulphuric acid mediated reaction might also be possible in subglacial environments. To test the fact bivariate plots of TZ^+ vs SO_4^{-2} and HCO_3^- has been prepared (Fig 5.5). Here the plots of total cations (Ca+Mg+Na+K) at y axis were plotted against most domination anions of SO_4^{-2} and HCO_3^- as they represent the products of carbonate, silicate and sulphuric mineral dissolution process. Concentrations have been corrected for precipitation inputs and theoretical slopes (dashed lines) describing idealized reactions which can generate the anions in meltwater. Here in the top two figure 5.5 depict idealized silicate weathering reactions assuming all the cations are from silicates. The slopes of 1:1 lines presents the SOSD and silicate dissolution through carbonic acid respectively which suggests one mole of respective cation will release for one mole of SO_4^- ^{2} and HCO_3^-. Results show that the cation release in meltwater is weakly correlated with the SOSD and silicate dissolution through carbonic acid process. So the SOSD and SDC mineral weathering effect in ionic release is very less likely. Further in bottom two figures suggests the total cationic release from carbonate weathering reactions and accessed the effect of SOCD and carbonate mineral dissolution process. 2:1 line (short dash) in each figure represents the slope if only SOCD weathering reaction is occurring in the dominance of SOCD

method and carbonate mineral weathering process at glacierized basins of the Himalayas.

It is been observed that the sulphuric acid mediated weathering are producing majority of the cation and anions through carbonate weathering, however, SOCD which indicate that in carbonate weathering SOCD is mainly regulate the reactions. In nutshell, the results show that out of above reactions two reactions are mainly dominated i.e. SOCD and carbonation reactions. The sulphide oxidation could be a key reaction in subglacial environment. The high ratio of silicate weathering is due the active layer present on the top of the layer which consist of loose mineral surface, the majority shows that the carbonate phases leached out after that only silicate mineral remain to weather. In distinction high rate of chemical erosion occur within the glaciated catchment exposing silicate weathering. The nature of weathering reactions in the glaciated indicated that the sulphide oxidation pays an important role in glaciated environments.
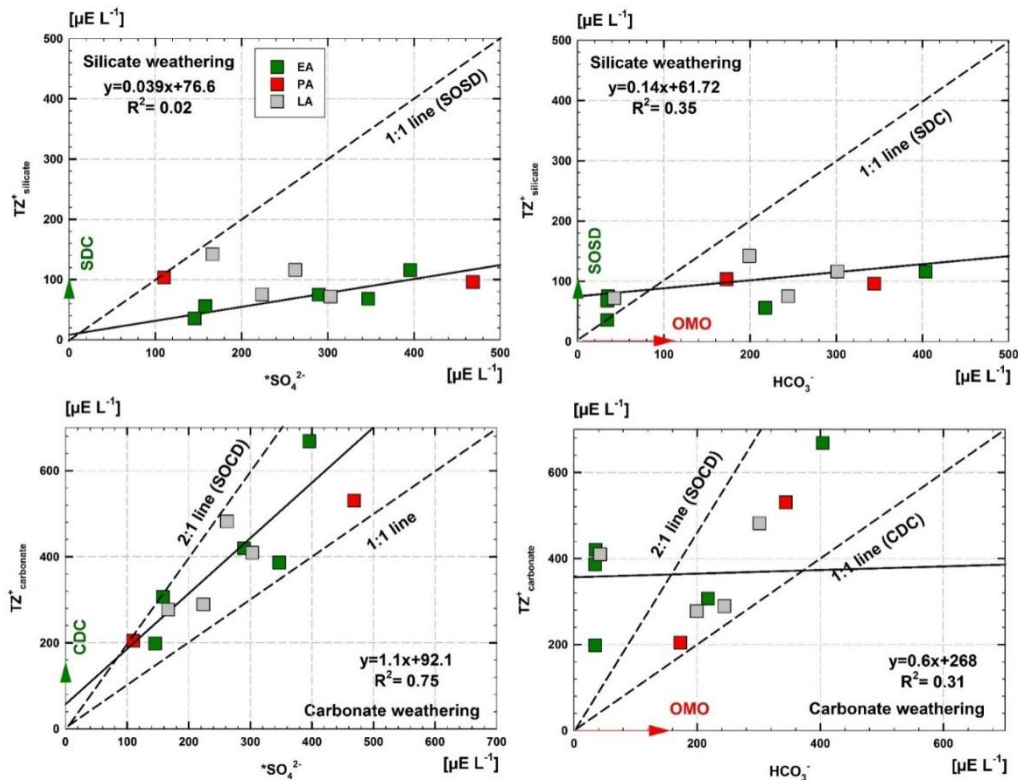
Fig.5.5: Plots of total cations TZ^+ versus sulphate and bicarbonate ion concentrations. Here "*" symbol symbolize the ions corrected for precipitation inputs. The solid line represent orthogonal regression lines for each ablation season with the theoretical slopes (dashed and red arrows). These lines were based on ideal reactions shown in equation 1-7.

1. Sulfide oxidation coupled to carbonate dissolution (SOCD)

$$4FeS_2+16Ca(Mg)CO_3+15O_2+14H_2O \rightarrow 16Ca^{+2}+16Mg^{+2}+16HCO_3+8SO_4^2+4Fe(OH)_3 \tag{1}$$
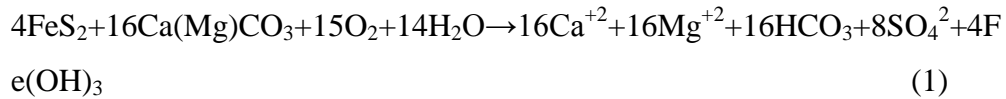
2. Sulfide oxidation coupled to silicate weathering (SOSW)

$$4FeS_2+16NaKAlSi_3O_8+15O_2+86H_2O \rightarrow 16Na^++16K^++8SO_4^{2-}$$
$$+4Al_4Si_4O_{10}(OH)_8+32H_4SiO_4+4Fe(OH)_3 \tag{2}$$

3. Carbonation of carbonate

$$Ca(Mg)CO_3+CO_2+H_2O \rightarrow Ca^{+2}+Mg^{+2}+2HCO_3^- \tag{3}$$
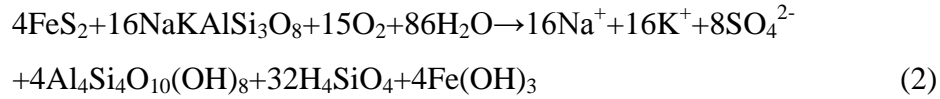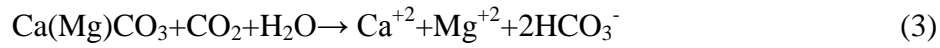
4. Carbonation of feldspar surfaces (albite/microcline-orthoclase)

$$2(Na,K)AlSi_2O_8+2CO_2+9H_2O \rightarrow 2(Na,K)+2HCO_3^-+Al_2Si_2O_5+4H_4SiO_4 \tag{4}$$
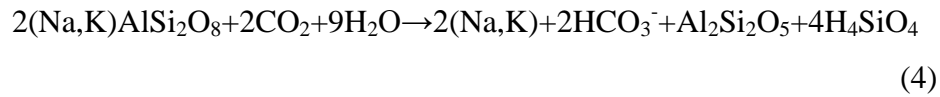
5. Dissolution of gypsum (an example of efflorescent salts)

$$CaSO_4.2H_2O \rightarrow Ca^{+2}+SO_4^{-2}+2H_2O \tag{5}$$

6. Simple hydrolysis of carbonate

$$Ca(Mg)CO_3+H_2O \rightarrow Ca^{+2}+H_2O \rightarrow H^++HCO_3^- \tag{6}$$

7. Oxidation of organic carbon

$$C_{org}+O_2+H_2O \rightarrow CO_2+H_2O \rightarrow H^++HCO_3^- \tag{7}$$
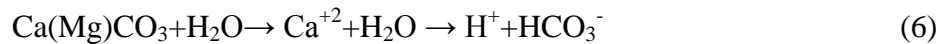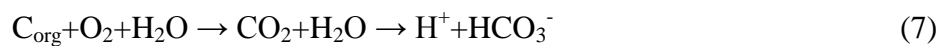
The primary sign in weathering reaction could be observed by seeing the identical elemental ratios later the reaction of silicate and carbonate with either carbonic and sulfuric acids can provide same ratio of cations vs. SO_4^{-2} and HCO_3^- (Fairchild et al., 1994; Hodson et al., 2000; Singh et al., 2015; Shukla et al., 2018). Reactions with the equivalent slope of intercept are presented above fig 5.3. In silicate mineral feldspar are the primary mineral found in the Dokriani glacier (feldspar compositional of feldspar between $CaAl_2Si_2O_8$, $NaAlSi_3O_8$, $KAlSi_3O_8$), do not affect the ratio of product composition in cations and either in anions (Eqs. 3,4,5,6). Corresponding equations for cation bearing silicate phase: Quartz, Gypsum, Illite, chlorite etc. In the glaciated catchment the slope between TZ^+ vs SO_4^{-2} is 1.04±0.036 which is similar to as expected by SOSD Eqs. 1 and 2. However the intercept is not zero which suggest that the silicate weathering is also governed by some other reactions. In slope of intercept between TZ^+ and HCO_3^- the slope is less than 1 which suggests that the weathering through carbonic acid is not dominant in the catchment. This might be suggested that quantifying the importance of whole reaction the data from Dokriani glacier is reliable with sulphide oxidation coupled with carbonate dissolution process and organic matter oxidation.

5.4.2 Glacier-weathering-carbon feedbacks at the Himalayan glacial basins

This ionic concentration presents the mixture of ions originated from different chemical weathering reactions operating at glacial/subglacial environment. To unmix the ionic concentration solute apportioning model (discussed in chapter 4, section 4.5) was used. Results suggest some contrasting results. It has been observed that total sulphate concentrationin melt water was composed of ~90% released from terrestrial weathering reactions, i.e., crustal sulphide oxidation, ~9% from the sulphates formed via aerosols and just 1% via sea salts (Table 5.6). For atmospheric corrections datasets of dry deposition was used (Section 4.3.2.1, chapter 4). Further, the sulphide oxidation, dissolution of evaporates may conjointly give rise thesupply of Ca^{2+} and SO_4^{-2}, however while

not the simultaneous increase in CO_2 unleash. However, it is advised that the carbonate dissolution presumably controls the Ca^{+2} concentrations in water as the meltwater of Himalayan glacial streams are under saturated with reference to calcite (Fig 5.5). Also, evaporite dissolution is observed very littlein previous studies from glacierized basin of the Himalaya (e.g., Sharma et al., 2013; Singh et al., 2015). The provenance of HCO_3^-calculated suggests a complex nature of ionic release. The mass balance calculations presented in section 4.5 show the theoretical values that could produce the HCO_3^- in melt water. The results for proportions of HCO_3^- in total HCO_3^- concentrations in melt water suggests following results: aerosol hydrolysis contributes ~2%, carbonate carbonation contributes ~9.4%, SOCD contributes ~21%, silicate dissolution contributes ~21.4%, simple hydrolysis contributes 20%, and, direct atmospheric exchange contributes ~26.1% (Table 5.5). These values are not in agreement with the results of Blum et al. (1998) much likely due totheir work were focussed on downstream where calcite oversaturation happens more frequently than higher altitudes. It has been observed that rivers of the Himalayan system are usually oversaturated for calcite, and result as loss of Ca^{+2}in the solid phase (Bickle et al., 2015). To check thepossibility of calcite saturation the PHREEQC geochemical model were used (Fig 5.5)which suggests under saturated nature of melt water streams for carbonate minerals (calcite and dolomite saturation indices < 0), halite and gypsum, but oversaturated for quartz. This might be suggested that the process of carbonate precipitation is very nnunlikely for the present system and reactions will switch towards dissolution than precipitation.

5.4.3 Regional perspective of chemical weathering from Himalayan glacial basins

It has been observed in previous studies that the glacial catchments representshigh chemical denudation rates (1.2 to 4 times greater than the global means) due to increased meltwater fluxes and suspended sediment loads (Anderson et al., 1997; Tranter and Wadham, 2013). It could be surmise

thatintense physical weathering and, as in our case, a favourable monsoonal climate results the higher chemical denudation rates at Himalayas. The Himalayan glaciers are directed by robust seasonal discharge (Tipper et al., 2006b; Bookhagen and Burbank, 2010) and speedy retreat (Bolch et al., 2012), causative to a rise in solute yields and its attendant CO_2 consumption.Given that theHimalayanglaciers receive nearly ~80% of their precipitation from the Southwest monsoon system (Bookhagen and Burbank, 2010), any possible modification in global climate patterns, i.e.,the global monsoon circulationweakening, reductionin the forest cover, a rise in atmospheric aerosol concentration due to long range transport, and surface energy budget, couldconsiderably affect the precipitation intensityand moisture convenience (Gaffen and Ross, 1999; Duan and Yao, 2003; Ramanathan et al., 2001, 2005). These processes could ultimately affect the weathering pattern of the region alongsidephysical weathering controlled through temperature and precipitation (Gabet et al., 2010). Globally the chemical weathering, specifically the silicate weathering process if know to consume atmospheric CO_2(Gaillardet et al., 1999) and related to the tectonic uplift induced increased ionic release and drawdown of CO_2 at the Himalaya (Sharp et al., 1995).However, the tectonic uplift induced rise in chemical weathering are notmirroredwithin the long-term (>1 Ma) drawdown of CO_2 budgets, asthe calculated CO_2 consumption rate has been increased by a factor of~ 2 (Jacobson and Blum, 2003). This study presents some important insights in terms of atmospheric deposition contribution of aerosols and aeolian dust is found to be highercompared to previous studies (Wake and Mayewski, 1993). The high SO_4^{-2}/Cl^-magnitude ratio in snow deposition attributes to high altitude favouring of aerosol deposition process giving rise to an rise in SO_4^{-2} (Polesello et al., 2007), through atmospheric circulation, domestic biomass burning (Shrestha et al., 2000) or associated inflow of $CaSO_4$ (Mayewski et al., 1983). The sulphate release from aerosols couldbe already oxidized and mightoverestimate the total SO_4^{-2} concentration.Similarly, good distinction between the cation/Cl^- ratios liquid *vs.*solid precipitationin rainfall, snow and ice

may also contribute cations (Shrestha et al., 2000, 1997). Apart from dissolution of aged sea salts $CaSO_4$ aerosol delivers additional SO_4^{-2} (Geng et al., 2010; Evans et al., 2002). However, throughout the monsoon, aerosols remains depleted, whereas throughout the winter and also the pre-monsoon period, the aerosol concentration will increase (Shrestha et al., 2000, 2010).

Further, previous studies from Himalayan suggest cold and warm springs release high concentrations of Cl^- deposits with relation to halite (Evans et al., 2002). However, the results from present study suggest low Cl^- concentration in melt water and undersaturation for halite (Fig 5.5). This study suggests even though the Himalayan springs source high Cl^- in the surface water, their contribution to dissolved solids yields could be very low. Apart from atmospheric deposition, terrestrial process also contributes the ionic to melt water. Previous studies suggested, contrary to previous understanding, the silicate weathering reaction and notably plagioclase weathering is the most rapid within the Himalayas (West et al., 2002). Notably the Dokriani and Lirung Glaciers at central Himalayas liberates high fluxes of silicate and carbonates and release a proportionately low silicate flux compared to the Bore and Chinnya catchments of the Middle Hills Nepalese Himalaya (West et al., 2002). Current trends of ions do not support the carbonate precipitation (Fig 5.5), in contrast to previously reported travertine deposits from carbonate precipitation at the Himalayan glacierized basins (Tipper et al., 2006a). This study highlights the chemical weathering processes at the Himalayas are operating with higher intensity than anticipated. Examined variability at Himalayan basins has underlined the fact that melt water chemistries of several glaciers i.e., Gangotri, Chhota Shigri, Bagni, Kafni, Dokriani and Patsio Glaciers exist at neutral pH scale capable to promote carbonate weathering and sulphide oxidation as a dominating process(Fig 5.6). A marked change in the sea salt, aerosol and crustal proportions were observed at the years 2006 and 2007 compared to 2003, 2004, 2005, 2008 and 2009.

Table 5.5: Calculated fluxes of solute sourced through atmospheric, aerosol, marine and crustal provenance categories.

Glacier Name	Year of Study	Cl⁻		SO₄²⁻		NO₃⁻		HCO₃⁻			
		All Cl-marine	Seasalt	Aerosol	Crustal	Aerosol	Aerosol Hydrolysis	SO-CD	Silicate derived	Carbonate Carbonation	Atmospheric
Gangotri		20.4	1	7.9	223	2.8	18.7	446.1	190.4	216.6	298.7
	2008	13.4	0.7	5.2	190.1	0	10.4	380.2	242.8	217.5	351.5
		12.2	0.6	4.8	217.6	6.2	15.7	435.3	302.3	245.6	425.1
Dokriani	2009	10	0.5	3.9	213.7	3.7	11.5	427.4	528.7	352.4	704.9
	2015	2.9	0	0	160.9	2.6	2.7	321.8	210.4	253.4	337.1
	2016	6.8	0.3	0.3	11.8	38.8	39.4	23.6	57.2	52.9	83.6
	2017	6.6	0.3	0.3	164.9	26.8	27.4	329.9	172.1	247.3	295.7
	2018	5.3	0.4	0.4	29.5	24.6	25.4	59	105.1	85.7	148
Chota Shigri	2003	11.4	0.6	4.4	66.5	6.8	15.7	133	124.4	47.1	148
	2004	10.5	0.5	4.1	90.4	6.3	14.4	180.8	165.2	75.7	203.1
	2005	11.2	0.6	4.4	288.1	9.4	18.1	576.1	171.7	47.5	195.4
	2006	13.9	0.7	5.4	235.4	4.6	15.4	470.8	227.8	3.5	229.5
	2007	12.5	0.6	4.9	265	5	14.8	530	217.3	19	226.8
	2008	15	0.8	5.8	107.4	39	50.7	214.8	421.6	148	495.6
Bara Shigri	2009	23	1.2	9	153.9	37	54.9	307.8	489.6	255.6	617.4
	2012	37	1.9	14.4	123.7	56	84.8	247.4	442	126.1	505.1
	2013	17	0.9	6.6	28	18	31.2	56	227.8	5.5	225.1
Patsio	2010	23	1.2	9	38.9	13	30.9	77.8	153	5.3	155.7
	2011	10.6	0.5	4.1	75.3	1.3	9.6	150.7	303.6	101.4	354.3
	2012	3.3	0.2	1.3	50.6	1.5	4.1	101.1	207.7	47	231.2
Chaturangi	2008	12.8	0.7	5	412.9	2.9	12.8	825.7	561.7	556.1	839.7
Satopanth	1989	36.7	1.9	14.3	0.6	0	28.5	1.3	50	94.1	97
	1991	0	0	0	44.5	0	0	88.9	400.4	151.3	476.1
	Average	14.9	0.8	5.8	149.7	10.7	22.2	299.5	286.9	143.1	358.2

Values are in µmol L⁻¹.
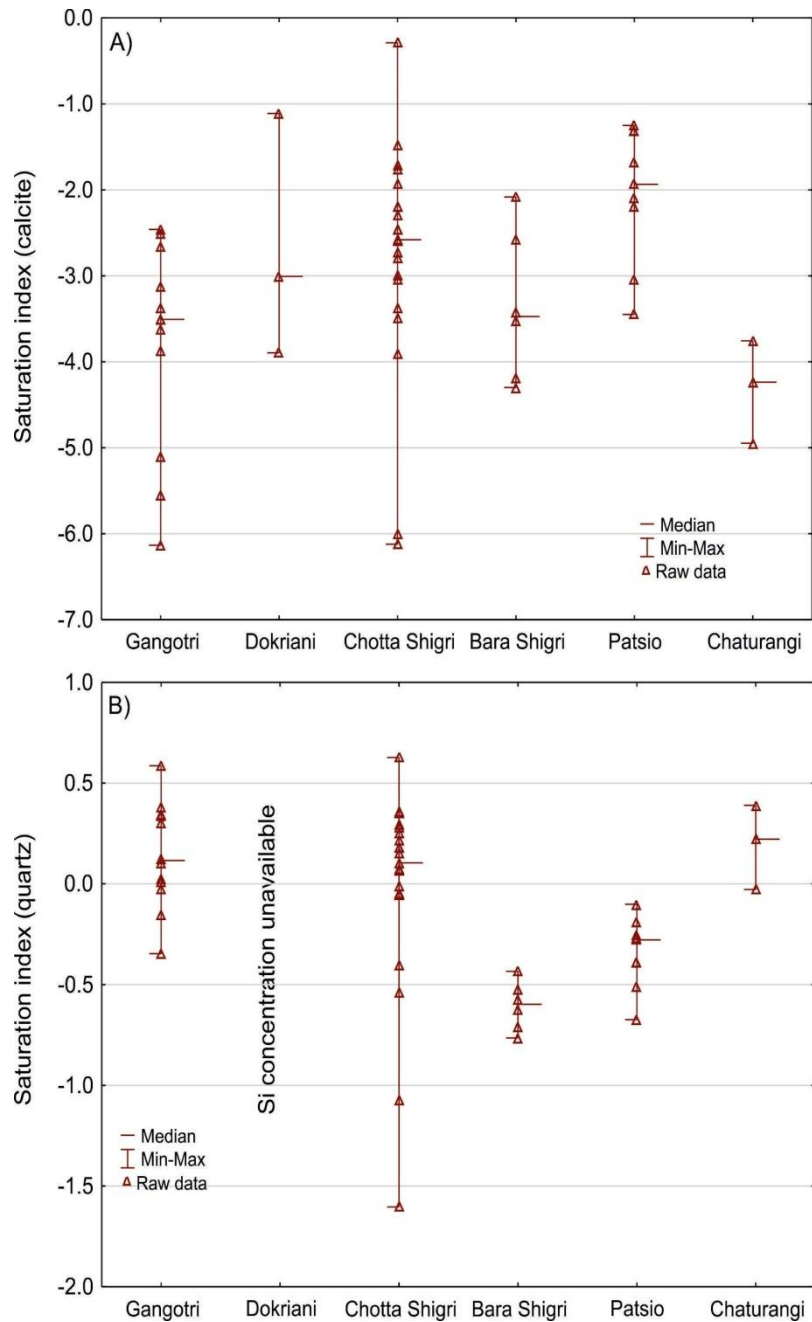
Fig.5.6: The trend of saturation indices for calcite (A) and quartz (B)plotted againstrange of parameters.

This could be correlated to variable flow regimes of glacierized basins, however, immature to say due to data scarcity. The observed variability for HCO_3^- fluxes suggests domination of silicate weathering and simple hydrolysis processes at Chhota Shigri, Bada Shigri and Patsio Glaciers (majorly from western Himalayan Glaciers)compared to the Gangotri, Dokriani and Satopanth Glaciers of central Himalaya (Fig 5.6). The SOCD

processes were dominant for HCO_3^- fluxes at the central Himalaya. Combining all it could be suggested that carbonate carbonation and SO-CD are the dominant process releasing HCO_3^- fluxes than the silicate-derived fluxes.

5.5   Sulphide oxidation and silicate weathering

Observed variability at the Chhota Shigri, Patsio, Dokriani, and Lirung Glaciers clearly highlight that the oxidation of sulphide minerals releasing sulphate in the melt water (Fig. 5.6), similar to the observations of previous researchers (West et al., 2002; Sharma et al., 2013; Singh et al., 2015). Carbonate and silicate weathering derived through sulphuric acid could release CO_2 in the melt water without its drawdown from the atmosphere. The coupling of SOSW under a subglacial system suggests an extended residence time for the water (Wadham et al., 2010).The high saturation indices with regard to quartz recommend each dissolution and precipitation happens within the glacierized basins (Fig 5.5). This agrees with alternative studies from the Yukon stating that each precipitation and dissolution reactions control silicate fluxes from subglacial conditions (Crompton et al., 2015). The SO-CD is so known as a crucial process that releases CO_2 into the hydrological system, thereby compensatory the drawdown of atmospheric CO_2 by carbonation. The SO-CD reaction is therefore identified as a transient source of CO_2 to the atmosphere (Torres et al., 2014, 2017). Nearer observation of bicarbonate and sulphate solute fluxes indicates a negative correlation (r=-0.42) between crustally derived SO_4^{-2} and hydrolysis derived HCO_3^- and between SO-CD and silicate-derived HCO_3^- (r= -0.63) for all of the studied glaciers. Figure 5.6 shows that because the HCO_3^- produced from SO-CD become low, more silicate carbonation occurs consuming the CO_2 produced via the SO-CD reactions (equations 1 and 2) within the subglacial environment. This means an excess of CO_2 release from SO-CD being balanced with CO_2 consumption via carbonation during the silicate weathering process. However, out there meltwater chemistry provenance models (e.g., Sharp et al., 1995; Hodson et al., 2000) that we have employed in our study seem to not embody that source of CO_2 in glacierized basins. We tend to propose that additional works on

solute provenance in glacierized catchments ought to embody CO_2 release associated with SO-CD. Scrutiny the current study to those from totally different components of the world (e.g., the Mackenzie River in Canada by Calmela et al., 2007; Liwa River in Taiwan by Das et al., 2012) conjointly links silicate weathering and sulphide oxidation to the CO_2 release.
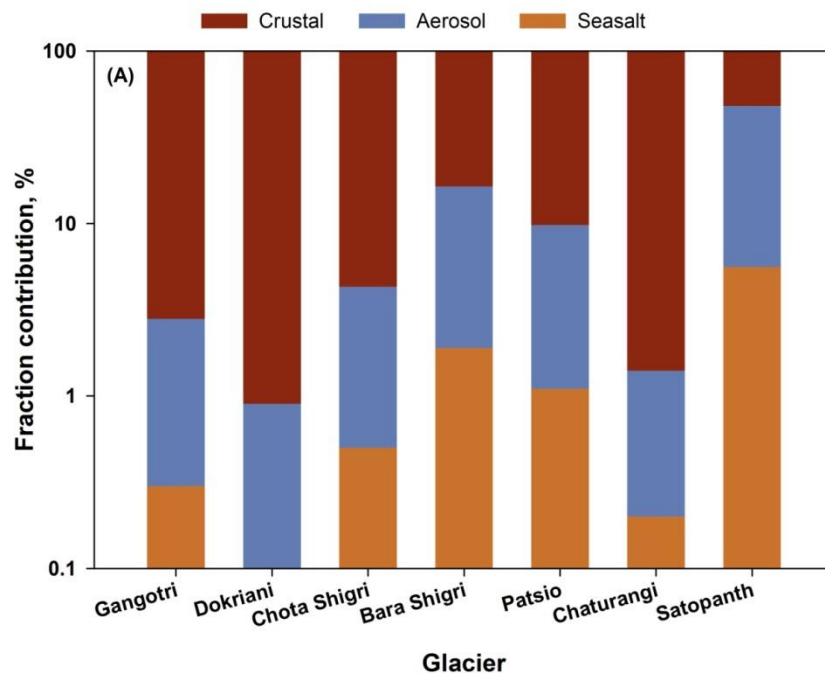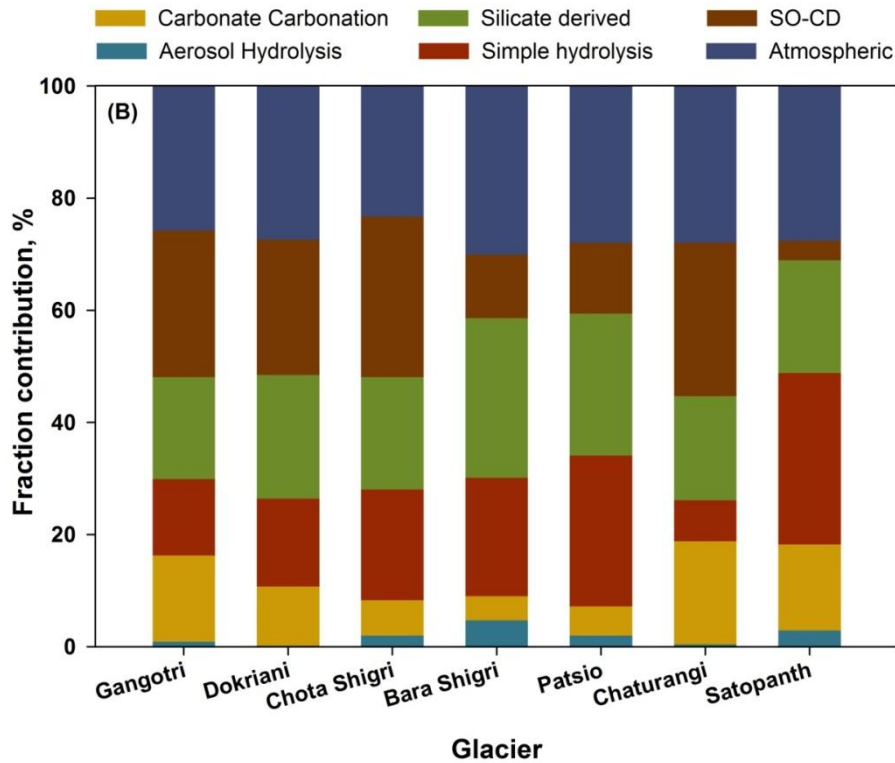
Fig.5.7: Calculated solute fluxes of selected central Himalayan glacierized catchments showing relationship of partitioned atmospheric and crustal components. Provenance categories represent here the fraction contribution (%) of respective solute flux. A) Shows the solute provenance of sulphate B) shows the bicarbonate solute provenance respectively.

Similarly, the Mackenzie River weathering study estimates 62% of the carbonate weathering is via sulphuric acid (Calmela et al., 2007). The high sulphide oxidation rates at the Liwa River (Das et al., 2012) and the importance of sulphide oxidation coupled with carbonate carbonation reaction (Stachnik et al., 2016 a,b) conjointly indicate the likely importance of sulphides for simulating CO_2 release.

5.5.1 Weathering induced Carbon dioxide consumption in the Himalayan region

Geographical and geological topographies of a catchment have a pronounced impact on weathering in glacial environments (Hodson et al., 2000; Tranter and Wadham, 2013). A comparison of global CO_2consumption

rates attributed only to Ca-Mg of silicate weathering is ~9.0 × 10^4 mole (km^2yr^{-1}) (Gaillardet et al., 1999) and in the New Zealand Southern Alps 6.9 × 10^4 mole (km^2yr^{-1}) on the eastern side and 14 × 10^4 mole (km^2yr^{-1}) on the western side (Jacobson and Blum, 2003). This is often like the current study of CO_2consumption within the Himalaya calculable from different concentrations. This contribution of silicate weathering to CO_2 consumption within the Himalaya is ~2 times but the typical global CO_2 consumption through silicate weathering. This could be possible because short water residence times under subglacial conditions may limit rates of silicate weathering (Wadham et al., 2010; Stachnik et al., 2016b). Considering the study of the Indian Himalayan Rivers (Krishnaswami and Singh, 2005) within the Ganga River catchment, the entire consumption of atmospheric $CO_2$from the weathering of silicate rocks was found to be $4 × 10^5$ mole $(km^2.yr^{-1})$, nearly 10 times higher than the values of this study. This is often as a result of the majority chemistry of the large rivers reflects their silicate lithology and thus underestimates the importance of carbonate weathering. However, in our first-order catchments, we have a tendency to don't seem to be considering the production/burial or respiration/oxidation of organic matter and associated CO_2 released into the atmosphere within the watershed likewise because the secondary mineral precipitation that's prevailing within the larger Himalayan river systems.

5.6 Anthropogenic vs Natural influence on trace element concentrations in wet or dry deposition

Present study shown that TEs concentration present in the snowpit profile and precipitation for the samples collected during the year 2017. The average concentration of TEs for the whole season at a different elevation is listed in Table 5.7. The snow-pit stratigraphy data presented here infers to the possibly transported and deposited sources of trace metals for monsoon and non-monsoon seasons, respectively. Based on a seasonal concentration of snow pit profiles, the trace element data set could be divided into 3 principal groups; first comprises the elements having a concentration higher than 10 µg L^{-1}, *i.e.*, Zn in non-monsoon period. The second group lies in between 1 to 10 µg L^{-1},

i.e., Fe. Finally, the remaining elements in the third section, which belongs to a concentration level lower than 1, *i.e.,* Mn, Sr, Cu, Al, Si, Cr, Co, and Ni. During monsoon season, the concentration of Zn, Cu, Mn, and Fe was above 10 μg L^{-1}, whereas the Sr, Al, Si, and Co concentrations were in the range of 1 to 10 μgL^{-1}, and the rest of the trace metals concentration (Cr and Ni) was below 1 μgL^{-1}. Present study resultsare compared with the concentration of TEs in drinking waters standards from the world health organization (Table 5.6; WHO, 2006). The concentration of Zn exceeded the WHO permissible limit, which is the most dominant element found in both monsoon and non-monsoon seasons, suggesting, Zn could pose a significant impact on the mountain ecosystem over the region. Meanwhile, the concentration of all the measured TEs showed clear seasonality inferring higher values in the monsoon as compared to the non-monsoon season (Table 5.7). Since the TEs concentration for monsoon months are higher than snow precipitation in the region, this might be possible as the old snow survives through the ongoing melting and refreezing cycles of snow and go through different process after deposition such as (i) photo-reduction (ii) percolation within the snowpack and (iii) settling of aerosols etc. These processes reduce the concentration of TEs after deposition. In most cases, the concentration of metals in snow pit samples are always lower than the fresh precipitation samples as the old snow goes through the various post-depositional process after deposition. Therefore, the post-depositional modifications in the TEs concentrations are possible and the concentration of metals from the snowpit samples (winter samples) is in most cases lower than the concentration of monsoon precipitation samples.

Table 5.6: The average trace elements (TEs) concentration (ppb) of snowpit (non-monsoon) and rainfall (monsoon)at Dokriani Glacier. The WHO data here represents average drinking water values according to the standards set by the World Health Organization (WHO, 2006).

Metal	Non-monsoon	Monsoon	NM/M ratio	WHO
Zn	104.61	845.03	0.12	3000

Mn	0.91	18.93	0.05	400
Sr	0.42	5.1	0.08	-
Cu	0.13	29.53	0	2000
Al	0.29	3.33	0.09	9
Si	0.78	1.9	0.41	-
Fe	3.44	15.15	0.23	20
Cr	0.02	0.68	0.03	50
Co	0.05	1.08	0.05	-
Ni	0.82	0.4	2.04	70

Here NM= Non monsoon period while M= Monsoon Period, WHO= World Health Organization

5.3.1 Enrichment factor of trace elements

The enrichment factor (EF) was calculated to identify the potential sources of TEs (Dong et al., 2017). The EF values for the non-monsoon and monsoon seasons for Dokriani Glacier is presented in Figure 5.8. We divided the value of EF into two parts: the first set of data consists of least concentrations of elements, *i.e.,* Al, Si, and Fe, while the remaining elements were of higher concentration, including Zn, Cu, Co, Ni, Mn, Sr, and Cr, both in monsoon as well as non-monsoon seasons. Further, I calculated the ratio of $EF_{non-monsoon/monsoon}$ of snow pit sample to compare the ratio of EFs values with the previously published records from other regions of the Himalayas. The elemental concentration of snow-pit profile for the non-monsoon represents that the EFs for Zn, Mn, Sr, Cu, Co have high enriched value i.e. greater than 1000, suggesting the influence of anthropogenic sources of these elements in the deposition. Similarly, during the monsoon period Zn, Mn, Sr, Cu, Cr, Co and Ni show significant enrichment, with Zn and Cu being highest >10,000, attributing that anthropogenic pollutant transport and deposition during this period from industrialized areas of South Asia to the Dokriani Glacier (Tripathee et al., 2014). The concentration of Zn and Cu showed noticeable regional anthropogenic deposition in the region. The larger EFs value in the snow-pit profile indicates that the westerly air masses brought and deposited the pollutants during the non-monsoon period (Bookhagen and Burbank, 2010;

Shukla et al., 2018). However, the EFs in precipitation samples suggest enhanced elemental deposition through SW monsoon. In addition, some other south Asian valleys also play a key role in increasing the concentration of pollutants. These air masses transport a large amount of anthropogenic pollutants from low-altitude urban areas. The ratios ranged from 0 (Ni) to 267 (Cu), indicating the differences in the seasonal concentrations. The average concentration of all trace metals except Al and Si is much higher during monsoon as compared to the non-monsoon season which is subjected to post depositional changes. In the non-monsoon period, a layer of black-dust is visible on the snow layer to a depth of 100cm in the snow stratigraphy. The higher enrichment ratio of TEs in the monsoon season suggests that the trace element is majorly transported from the South Asian region in the monsoon season. A low enrichment ratio of elements in the non-monsoon season suggests post-depositional changes in the snow stratigraphy through melting and refreezing resulting as the washout of elements from the strata.Enrichment factors calculated in the present study evaluated the enrichment of element in snow and rainfall comparative to crustal material and provided the anthropogenic influence/natural sources of TEs. Two major sources were observed for TEs in the region, i.e., human activities (anthropogenic) and the natural occurrences (crustal). The anthropogenic derived elements were As, Cd, Pb, Zn, and Cu, whereas, elements such as Cr, Mn, Ti, Ni and V were derived from natural sources. The highly enriched element was Cu, while Ni had lower enrichment. According to Tripathee et al (2014, 2016b) have instructed that elements like Cd, Pb, and Zn are derived from the anthropogenic sources. According to Nriagu, 1996 the primarily source of copper in environment is traffic emissions, fossil fuel burning, industrial combustion and fuel combustion. Meanwhile, Cr is derived from incomplete combustion of fossil fuels, and waste dumping (Wise et al., 2009) and Zn is emitted, transported and distributed from the natural phenomenon like dust storms, volcanic eruptions, forest fires, and sea sprays. However, manganese (Mn) could be derived from both the anthropogenic as well as natural processes. The natural form of Mn is ubiquitous, and the main source is the crustal rock. Besides, ocean spray, forest fires, vegetation, and volcanic

activities can also emit Mn in the atmosphere (Schroeder et al., 1987). Anthropogenic mining and mineral processing (particularly Ni) the emissions from alloy, steel, and iron production, combustion of fossil fuels, combustion of fuel gives rise to Ni. The EFs values determined in the present study with comparison to the other Tibetan Glaciers suggested that most of TEs had high enrichment values in the Dokriani Glacier (Fig 5.8). This suggests that in the Dokriani Glacierwas highly affected by south Asian pollutants transport and deposition through seasonal winds. Furthermore, our results agree well with the previous studies in the central Himalayan region where, it was suggested that southern slope are more prone to pollutants deposit than in the Tibetan Plateau (Tripathee et al., 2014, 2019).The major source of TEs over the Himalayan-Tibetan region is also derived from dust traveling through Western Asian countries (i.e. Pakistan, Afghanistan,etc.), which emits and enrich TEs pollution regionally (Kang et al., 2010; Huang et al., 2012a, 2013a). Whereas in Himalayas southernslope, the pollutants transported from the heavily polluted Indo-Gangetic plain (IGP) with various anthropogenic activities could not be ignored (Ansari et al., 2000; Tripathee et al., 2017).

5.3.2 Associations among the elements: correlation analysis

To understand the association and sources of trace metals between the non-monsoon and monsoon seasons, statistical analyses such as correlation matrix and PCA was performed (Table 5.7).
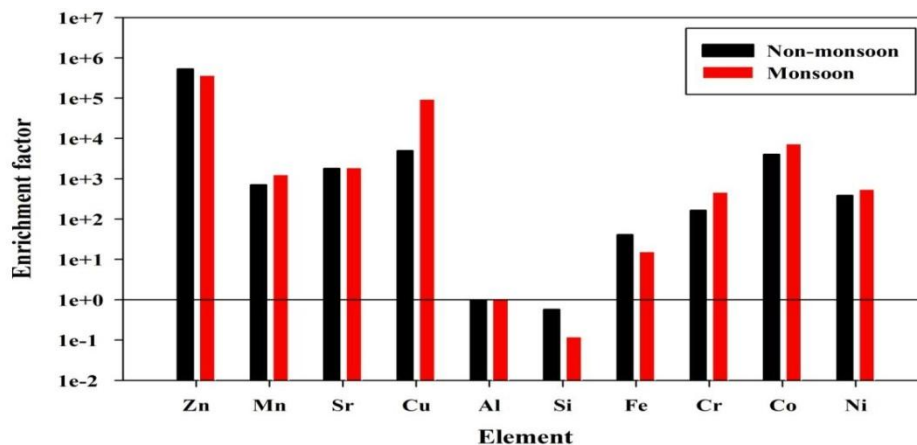
Fig 5.8. Average enrichment factor of trace elements at Dokriani Glacier.

Three PCs were extracted in this study, which involved in the factor loading dependent on the eigenvalue. It normalizes the principal component that can be extracted and provides a reliable result. In non-monsoon snow deposition, Sr was strongly associatedamong Si (r^2=0.99), Cr (r^2=0.96) and Fe (r^2=0.85), while remaining elements are strongly correlated with Cr (r^2= 0.91).Further, Si showed a good correlation with Cr (r^2=0.92) and Fe (r^2=0.82) (Table 5.7 A, B). The great affinity of Co towards Sr (r^2=1), Cu (r^2=0.85), Fe (r^2=0.92), Cr (r^2=0.88) was observed. Similarly, Zn showed strong correlation with Mn (r^2=0.94), Si (r^2=0.99) and Fe (r^2=0.95), while Mn showed strong correlation with Si (r^2=0.95). The Sr showed a strong correlation with Fe (r^2=0.94), Cu (r^2=0.83), and Cr (r^2=0.86), while Cu and Cr showed the highest correlation (r^2=1). Interestingly, during the monsoonal precipitation, Co showed a positive correlation with the variables such as Zn, Mn, Sr, Cu, Fe, Si, Fe, and Cr. Moreover, Ni showed perfect association with Sr, Cu, and Cr, indicating those elements were derived from similar anthropogenic sources (Table 5.7 C, D).Furthermore, rotated component matrix PCA results obtained in the non-monsoon and monsoon seasons are shown in Table 5.7C. In the non-monsoon season, the first factor was loadedwith Zn and Cu with a percentage variance of 94.66%, suggesting their anthropogenic origin. Zinc is an anomalously enriched element (AEEs), and aplausible source of anthropogenic input in the atmosphere is from volcanic eruptions, forest fires, fuel combustion, metal smelting, traffic emission, and sea salt sprays (Al-momani et al., 2003). The second factor was loaded with Strontium (Sr), Silica (Si), Iron (Fe), and Chromium (Cr) with variance percentage of 4.59%, attributing their origin from crustal sources. Finally, factor 3 indicates the sources of Mn and Si, which might suggest their mixed sources from both natural and anthropogenic emissions. For the monsoon season, the PCs showed significant loadings of Co, Zn, Mn, Sr, Cu, Si, Fe, Cr, in the same factor with percentage variance of 66.80% (Table 5.7D), suggesting that these elements might have deposited at the same time (Tripathee et al., 2017). Meanwhile, the second factor was loaded with Zn, Mn, and Si with a percentage variance of 28.57%, which are mostly derived from anthropogenic sources. The third PC showed the loading of Cu, which must have derived from traffic-related sources, smelting, and

fossil fuels combustions (Al- Momani et al., 2003; Pachynaetal., 1984; Chueintaet al., 2000).

5.3.2 Global comparison of elemental abundance

The mean concentrations in all snow samples compared to other parts of the Himalayan sites are listed in (Table 5.8). Predominantly, Zn showed higher concentration while others Cr, Co, Ni, Cu, Sr, and Fe showed similar concentrations, with the Al shows exceptionally lower concentration. The concentration of Zn is 5 times higher in Dokriani glacier as compare with Zhadang, Urumqi, Mt. Everest, Mt Cho Oyo, Namco station.

Table 5.7:Statistical analysis of Dokriani Glacier snow pit. Pearson Correlation Matrix for (A) Non- monsoonal season; (B) Monsoonal season; (C) Pearson Correlation Analysis in Non-monsoon; and (D) PCA in monsoon season.

(A)

Non Monsoon variable	Zn	Mn	Sr	Cu	Si	Fe	Cr
Zn	1						
Mn	-0.4	1					
Sr	-0.26	**0.44**	1				
Cu	**0.55**	-0.22	-0.09	1			
Si	0	0.19	**0.99**	0.09	1		
Fe	-0.03	0.21	**0.85**	-0.2	0.83	1	
Cr	-0.32	0.31	**0.96**	-0.5	0.92	0.91	1

(B)

Monsoon Variables	Co	Zn	Mn	Sr	Cu	Al	Si	Fe	Cr	Ni
Co	1									
Zn	**0.73**	1								
Mn	**0.6**	**0.94**	1							
Sr	**1**	**0.72**	0.6	1						
Cu	0.85	0.49	0.21	0.83	1					
Al	0.42	0.3	0.47	0.42	**0.62**	1				
Si	**0.79**	**0.99**	0.95	**0.79**	**0.5**	0.23	1			
Fe	**0.92**	0.61	0.59	**0.94**	0.62	0.39	**0.71**	1		
Cr	**0.88**	0.49	0.23	**0.86**	**1**	0.65	0.51	0.67	1	

Ni	**0.6**	0.95	**1**	**0.61**	0.23	0.46	**0.96**	**0.6**	0.24	1

(C)				(D)			
Non Monsoon	**PC1**	**PC2**	**PC3**	**Non Monsoon**	**PC1**	**PC2**	**PC3**
Zn	1	0	0	**Co**	0.96	-0.26	-0.06
Mn	-0.39	0.22	0.64	**Zn**	0.89	0.42	0.2
Sr	-0.21	0.86	0.39	**Mn**	0.78	0.62	-0.06
Cu	0.36	-0.16	0.11	**Sr**	0.96	-0.25	-0.12
Al	0	0	0	**Cu**	0.75	-0.57	0.33
Si	0	0.81	0.42	**Al**	-0.16	0.97	0.16
Fe	-0.04	0.99	-0.1	**Si**	0.92	0.38	0.06
Cr	-0.08	0.72	0.23	**Fe**	0.87	-0.19	-0.45
As	0	0	0	**Cr**	0.77	-0.58	0.25
Co	ND	ND	ND	**Ni**	0.79	0.61	-0.05
%variance	94.66	4.59	0.4	**%variance**	66.8	28.57	4.63

ND refers to not determine

Such data shows that this might be possible due to the high convection precipitation brought more dust particles (Tripathee et al., 2014). May be regional dust activity is one of the causes of high concentration of anthropogenic elements specially; however, non-identical sources in precipitation further need to be explored. Whereas a homogenous trend is observed in Cr, Mn, Ni, Cu, Fe, Sr. As compared with other remaining glaciers the higher concentration of Al in Zhadang Glacier is due to the long-range atmospheric transport of pollutant in the Tibetan plateau.

A higher concentration of anthropogenic elements like Mn, Co, Ni in Zhadang Glacier wasdue to strong Asian dust particlestransported and affected the glacier as well as the concentration of chemical constituent (Dong et al., 2016). Thus, the results counsel that a high concentration of trace metals in Zhadang Glacier is additional contaminated, demonstrating that the region is usually suffering by anthropogenic emissions. While in our study region except for Zn, rest of metal shows the neutral values. It seems that the higher concentration of Zn is due to substantial anthropogenic activitiesinfluence on the Dokriani Glacier.

5.3.3 Climate change and its impact on human health

The perspective of the presence of TEs for human health could be valid after its division into two major parts, i.e., major and minor. The minor TEs are those that are required in less amount; the accumulation of the excessive amount of TE may cause severe health issues, whereas the major amount of these arerequired of our body (Prashanth et al., 2017; Plum et al., 2010; Durubie et al., 2007; Goldhaber et al., 2003). Climate change will have a notable effect on the food web and food security, which directly affects human health. According to the World Health Organization (WHO), there are permissible and desirable limits of each element in the environment. Regional as well as the global difference of these elements such as Zn, Cr, Pb, Co and Cu in the human diet impacts health, and later this impact also affects the food security regionally (Lake et al., 2012; Oliver 1997).

Table5.8: Comparison of concentration trace elements in snowpit at Dokriani glacier with other remote areas of high Asia. All the data sets are reported in $\mu g\ L^{-1}$

Trace elements	Zhadang Glacier [a]	Urumqi Glacier No 1 [b]	Mt. Everest [c]	Mt. Cho Oyu [d]	Dokriani Glacier [e]
	Snowpit	Snowpit	Snowpit	Snowpit	Snowpit
Al	1064.1	612.5	121	-	0.29
Cr	1.98	-	0.1	0.13	0.02
Mn	42.66	-	1.3	1.38	0.91
Co	0.7	-	0.04	0.02	0.05
Ni	2.74	-	0.09	0.06	0.82
Cu	5.27	-	0.08	0.09	0.13
Zn	18.7	24.6	0.48	0.72	104.61
Fe	-	-	-	-	3.44
Sr	-	-	-	-	0.42

a)   Huang et al. (2013)

b)   Li et al.(2007a)

c)   Lee et al. (2008)

d)   Liu et al.(2011b)

The present study underlines the presence of a high concentration of Zn, Cu, Mn, Ni, Fe, Sr, etc. in atmospheric pollutants transported to the high-altitude Himalayan region, which in our view should be a primary concern for the receding population in Uttrakhand. The long exposure of humans to these toxic elements can have carcinogenic, as well as the peripheral nervous system and circulatory effects (Dwivedi et al., 2018). According to a survey of the hilly regions of north India, it was reported that a total 32.6% cases of skin and subcutaneous tissue-damaging are reported, out of which 19.8% is from a skin disorder, while 18.8% is from dermatitis and eczema (Dimri et al., 2016). This might probably because of drinking water supply contaminated with Zn and Cd, which is potentially known for skin-related issues. The high concentration of Zn in this region causes epidermis, dermis, and skin cancer problems, whereas, deficiency of zinc telogen effluvium, abnormal hair keratinization, necrolytic migratory erythema, pellagra, and biotin deficiency (Ogawa et al., 2018). High concentrations of other elements also can cause severe health issues. Therefore, ignoring this toxicity associated with trace metals may have serious health issues, especially in children who get affectedeasily because of low immunity to such diseases. Furthermore, the impact of these diseases isexpected to be furthersevere in the regions where the suffering is from an imbalanced diet. During the last few decades, a sudden increase in the number of chemical fertilizers, mechanization and irrigation (Matson et al., 1997) has resulted in spiraling of adverse effects worldwide (Foley et al., 2005, Dong et al., 2017). In order to secure food supply and prevent further negative impact from the harmful infectious diseases and the imbalance in the natural cycle, it is necessary to reduce or minimize the use of these potentially toxic elements and their production. The overall result reflects that the problem related to TEs is potentially high, and further long-term research is needed to identify to understand these problems in details. Ultimately, more robust data are required to design and implement policies on TEs pollution reduction for the pristine Himalayan regions.

CHAPTER 6

CONCLUSION AND FUTURE OUTLOOK

The Himalayan glaciers contribute to the river flow of the Ganga, the Brahmaputra and the Indus, three of the major river systems of South Asia. The contribution is of special importance during winter periods andyears of low precipitation. The cryosphere water in any basin forms a reservoir of fresh water which accumulates in some part of the year and releases it to the river system in another part of the year. The main consequences of changes in the cryosphere can hence expected to be changes in the seasonality of the river discharge from the Glaciers. The annual glacier ice melt water contributions vary across the Himalayan river basins depending upon the precipitation; monsoon and significant ice melt contribution. Himalayan glaciers are enhancing weathering reactions rates comparable to the other regions of the globe. The mechanism of water and rock interaction is very sensitive towards the glacier not only the glacier wastage is mainly attributed to the current phase of accelerated climate change. The chemical balance in High altitudesare able to comprehend the controls and significance of weathering fluxes either it is silicate and carbonate in the region. Globally, the total fluxof Himalayan weathering is recorded. Sulphide oxidation plays an important process in generating the acidity by different mechanism. The dominate ions in glacierized catchment is SO_4^{-2} and HCO_3^-. The Dokriani Glacier experiences a both silicate as well as carbonate weathering system: silicate and carbonate weathering by carbonic and sulphuric acid. It is venturing that high chemical weathering rate continuously expose from carbonate mineral.The high ablation record in the glacierized catchment shows that in early and peak ablation season re-dissolution of calcite driven by atmospheric CO_2,

causing a higher concentration of Ca^{+2} and HCO_3^- in the meltwater draining out from snout of Glacier. The thesis can be divided into two parts, first part gave knowledge of processes to understand plausible source of weathering process and reactions. This could help out in finding the question of most heated topic nowadays on the global CO_2 drawdown and chemical weathering enhance the climate change and their impact. The sources and transport of these ions in the glacier melt water and the processes linking with the weathering reaction are discussed. Elucidation of the data of the Dokriani Glacier shows that the difference in proglacial melt-water controls the rich subglacial component. The investigation of geochemical data of Dokriani glacier suggests that the meltwater emerging out is alkaline in nature. There is a continuous increase in the concentration of calcium, bicarbonate, and magnesium in major cation while in case of major anion, there is an increasing trend in the concentration of sulphate and nitrate ions, which clearly indicates the highly dominated chemical weathering. The high concentration of Ca^{+2} + Mg^{+2} and $Na^+ + K^+$ shows the carbonate and silicate weathering regulates the melt water chemistry of Dokriani glacier. Present study determines the process that regulates the chemistry of meltwater in glacier system. The dominated sulphate anion and calcium cation indicates that in the Dokriani glacier proglacial meltwater stream was mainly dominated by the sulphuric acid mediated reactions. Sulphide oxidation which regulates the many chemical reaction like couple reaction and carbonation reaction is the major source of the proton dissolution sources of ion in this region. Unlike Cl^-, NH_4^+ and NO_3^- are contributing from the anthropogenic and little less from sea salt deposition process. The statistical results show that the meltwater was mainly controlled by the alumina sulphide oxidation, mineral dissolution, weathering process and anthropogenic activities. The data shows increasing trend in cations rather than anions which indicate that cations contribute higher concentration in meltwater chemistry in two decades. This is due related to the higher exposed of rock which promote the weathering reactions. Also precipitation and atmospheric deposition act as supported agent in weathering

96

process in the glacial terrain. Increases the precipitation will result the dilution effect and loss of base cations explained by the primary silicate weathering. We also suggest the hydrological modelling will better deal in Glacio hydro chemistry in diverse climatic system to predict the water availability at goodassurance level. The first whole ablation records suggests that during early ablation and late ablation seasons, ions in relation with discharge shows the chemostatically relation while in Peak ablation season it shows the dilution effect. In early and late ablation season re-dissolution of pyrite dissolution driven by atmospheric CO_2 causing higher concentration of Ca^{+2} and HCO_3^- and low concentration in peal flow. This also illustrate that the organic matter oxidation doesn't play a major role in carbonate dissolution of proglacial stream. During, the melting period constant leaching of pyrite in the proglacial zone cause a drip in slope coefficients of ion associations $[HCO_3^-$ vs $TZ^+]$ and $[SO_4^{-2}$ vs $TZ^+]$ from between 1.0 to 2.0 values typical for SDC. Hence, sulfide oxidation is a goodconstraint for analyzed in the drainage pattern. Hence, sulphide dissolution coupled with carbonate carbonation is not occurring in silicate weathering as all data lies between organic matter oxidation and SDC in whole ablation season. In contrast, sulphuric acid mediated weathering are producing majority of the cation and anions through carbonate weathering, however, SOCD which indicate that in carbonate weathering SOCD is mainly regulate the reactions.

Another part of the thesis is the study of snow stratigraphy, the results shows that in dominant major anion SO_4^{-2}, NO_3^- were major cation Ca^{+2} whereas, major anion SO_4^{-2} and HCO_3^- and Ca^{+2} and Mg^{+2} dominant cations in the respective year. The results show that the main source of ion in snow pit is sea salt aerosol contribution which scavenging through atmospheric deposition. The crustal and marine source also made a significant contribution in ions. The trajectory plots indicate the local and terrestrial dust from arid regions like Nepal, southwest Tibetan plateau (TP) carried by winter precipitation. Here, our last component i.e. Trace elements this study presents the first dataset on TEs in precipitation and the snow-pit deposition at a monsoon dominated Himalayan

glacier. This study also suggests the first dataset on TEs in precipitation and the snowpit deposition in the monsoon and non-monsoon period. The results highlighted the presence of high concentration of Zn, Al, Si and Fe in the non-monsoon season whereas Zn, Cu, Al and Fe during the monsoon season. This prominent increase in concentration However, we contend that non-monsoonal snow deposition is modified by several post depositional changes i.e. (i) percolation within the snowpack (ii) settling of aerosols and (iii) photo reductionetc., which has modified the TEs concentration. The enriched TEs is due to anthropogenic emission, transport and deposition of trace metals over the glaciers mostly originated from the combustion of fossil fuel, metal production, and industrial processes from south Asian regions.

6.1 Contribution of present research work

Quantifying the ionic stoichiometry are key parameters to predict the chemical weathering rate in a glacierized system. The Dokriani Glaciers is the benchmark glacier and studied in nearly all aspects of glaciological research for a period more than a decade. I have this opportunity to interpret the present weathering reactions in more realistic ways. The present thesis has evaluated the data set and contributes to ongoing hydrochemical studies at local to regional scale through following outputs.

6.1.1 Deposition of atmospheric pollutant in Snowpit

The uncertainty in assessing the various part atmospheric pollutants transported *via* wind from arid and semi-arid regions is affects the glacial ecosystem. In this study I show the famed seasonal difference detected between major ions (Ca^{+2}, Mg^{2+}, SO_4^{-2}, and NO_3^-). There's a necessity for understanding the ions cycling as a completed and additionally the directivity of the feedback loops within the system. Consequently, I offer associated degree evaluation of current assumption for seasonal differences in major ion concentration from snow profile samples for two corresponding years (2013 and 2015) at Dokriani Glacier.

98

The scientific view of chemical compositions within the shallow snow profile from Dokriani Glacier was carried duringearly ablation season to understand the cycle of major ions from atmosphere to solute acquisition process. By intimating mathematical models and statistical approach I am able to determine the temporal behavior and ion cycling in snow. Between major ions, the SO_4^{-2} shows the highest concentration amongstanions on an average considered as 14.21% in 2013 and 29.46% in 2015. In case of cation Ca^{+2} is that the dominant ion contributing 28.22% in 2013 and 15.3% in 2015 on the average. The common quantitative ratio in between Na^+/Cl^- was greater in 2013 while lower in 2015. The backward trajectory analysis suggests the attainable source of inorganic ions transported via from Central Asia through the Western Disturbance (WD) as a distinguished of winter accumulation within the CH. Ionic concentration of Ca^{+2} in cations was extraordinarily dominated whereas in anion SO_4^{-2} contend the foremost role. Correlational matrix and Factor analysis proposed that, the precipitation chemistry is usually influenced by anthropogenic, crustal, and ocean salt sources over the studied region. The elemental cycling through ocean, atmosphere and biosphere opens up new ways in which to grasp the geochemical processes operational at the glacierized catchments of the Himalaya.

6.1.2 Natural vs Anthropogenic influence of trace elements concentration in wet precipitation

Atmospheric pollutant transport and deposition at the Himalaya affects the climate, cryosphere, and monsoon patterns and impose an adverse impact over the Himalayan ecosystem. At present, the data on trace elements (TEs) concentrations and dynamics over the high-altitude Himalayan region are scarce and has received less attention. Therefore, within the present study, we have a tendency to investigate the TEs concentration and depositional pattern at Dokriani Glacier, central Himalaya to grasp their levels, dynamics, and potential effects. A total of 39 samples were collected from two snowpit stratigraphy's, deposited throughout non-monsoon period and monsoonal precipitation between 4530 to 4630 m a.s.l.

altitude in the year 2017. The results of analyzed trace metals (Al, Cr, Mn, Fe, Sr, Co, Ni, Cu, Zn, Cd, As, and Pb) showed high enrichment values for Zn, Cr, Co, Ni and Mn compared to different elements of the Himalayan region, suggesting the influence of anthropogenic emissions (e.g., fossil fuel, metal production, and industrial processes) from urbanized areas of South Asia. Our results additionally unconcealed the potential health effects associated with the enrichment of Zn and Cd, which may be responsible for skin-related diseases in Uttrakhand region. We have a tendency to attribute increasing anthropogenic activities in the environment to have a significant impact on the ecosystem health of the central Himalayan region. This study provides the baseline information on TEs concentration and sources within the Himalayas that desires wide dissemination to scientific community as well as policymakers. Therefore, efficient observations, management, and preparing action plan to overcome the health effects from TEs pollution are urgently needed over the remote, pristine Himalayan region.

6.1.3   Decadal changes in Melt water chemistry

The study aims to understand the hydrogeochemical changes in proglacial meltwater stream emerging from the snout of Dokriani Glacier, CH, India. The major ion concentration of melt water between the years 1994/2015 has been reviewed to infer the glacial/subglacial weathering produced ionic release from Dokriani glacier system. The results collected from meltwater during late ablation period (October 2015) shows that dominance of Ca^{+2} cation followed by Mg^{+2}, K^+, Na^+ and in case of anion SO_4^{-2} is most dominant followed by HCO_3^- and Cl^-. The graphical interpretation like scatter plot between $Ca^{+2}+ Mg^{+2}$ vs TZ^+ shows the general dominance of carbonate weathering whereas Na^++K^+ vs TZ^+ show high positive relation suggesting domination of both carbonate and silicate weathering. In contrast, the ionic concentration for the year 2015 recommends a substantial rise since 1994; however, the discharge weighted concentrations would afford more comprehensive estimations. An increasing trend in major cations viz. calcium (Ca^{+2}) and magnesium (Mg^{+2}) while the bicarbonate

(HCO_3^-), sulphate (SO_4^{-2}) and nitrogen (NO_3^-) has been observed as major anion. Further, the supply of Cl^-, NH_4^+, and NO_3^- in the meltwater stream is especially derived from the atmospherically, anthropogenic, and weathering process. The process of carbonate weathering and dissolution of rock is determined as the one that regulates the melt water chemistry.

6.1.4 Weathering process in glacial environments and its relation to CO_2 (atm) in the Himalaya

The results of this study offers a new insights into C cycling associated with CO_2 consumption via weathering. I have unquestionable consumption and release of CO_2coupled to SO is typically responsible for regulating CO_2 cycling. Geochemical modelling suggests that the water is typicallyunder saturated with reference to carbonate minerals (calcite and dolomite), halite and gypsum however is oversaturated in terms of quartz. High saturation indices with relevance to quartz counsel each dissolution and precipitation so rigorous carbonation of silicates via CO_2 (atm). SO produces robust acid that will be related to silicate weathering resulting in attainabledecrease within the significance of long-term CO_2 consumption via atmospheric CO_2 via carbonation of silicates. Against this, the saturation indices for carbonates recommend dissolution instead of precipitation generating high solute Ca^{+2} and SO_4^{-2} fluxes shows the importance of SO coupled with carbonate weathering for glacial environments. However, results suggests that silicate weathering within the Himalaya and Southern Alps and also the SO-CD reaction are substituting CO_2 and counsel that additional thought of CO_2 unleash from the SO-CD process might give an improved way to understanding of global CO_2 consumption by weathering. Previous makes an attempt have centered on semi-permanent consumption (~millions of years) of CO_2 via silicate carbonation, however these display very minute effect is probably going in perspective of future scenario attributable to low significance as a weathering mechanism. Still, chemical weathering of carbonates additionally causes CO_2 consumption, however this process is short-

term (~thousands of years), creating it additional applicable to incorporate in climatic models. I strongly believed that in present day solute acquisition process in higher altitude of Himalayas have potential of SO weathering reaction findings for creating the semi-permanent C cycle of the Earth is stable.

6.2   Future Implication of present work

Present study it is now evident that glaciers are sensitive towards chemical weathering processes. They play a vital role in mass exchange between earth and life nourishing surface. They provide a nutrient to ecosystems and also regulate the long term carbon cycle and global climate systems. The glacier of central Himalaya are more sensitive towards the weathering process and lithology due to their location in monsoon dominated and monsoon deficient region they signify the different response to climate system. The closely line up studies in the central Himalayan region will extend our knowledge for chemical weathering and it response to climatic conditions. Water flows from the glacier employ an important control on ice mass dynamics and, also effected the quality and quantity of water in downstream area. The mass depends upon how much amount of snow is accumulate and melt till the end of mass balance year. Year by Year climatic conditions and lithology more enhance the positive feedback mechanism in glacial weathering system. This not only affects the solute acquisition process but also affected the atmospheric circulation patterns. The present day monitoring of glacier examines the glacial climate coupling will allows understanding the weathering pattern in glaciated regions in more effective ways. The oblique suggestions from the present study leave a broader scope to reconstruct the framework of long glacial cycles, controlled by forcing mechanism and could be further explained by modelled. To elucidate the glaciations irregularity in climate system more robust detailed are required. Another future viewpoint is the spatial analysis of the aerosol radiative forcing and snow-ice models over the glacier was to be tested. This makes glacial water more suitable for the water resource management. The aerosol radiative forcing and snow-ice model would be useful

to calculate the spatially distributed hydro-chemical balance models in future studies. Further, these models is helpful to predict the melting of glacier and future supply of water from glacierized catchment by using different climatic models as well as to differentiate the effect of atmospheric pollution on the cryospheric water resources of the Himalaya. To expand the thesis work, there are significant scopes for the future works. Finally, more work would be aimed to investigate the extrapolation of the other factors which regulates the melt rate and models for the Himalayan region. In future, the advanced solute modelling and atmospheric pollution will be verified with the other Himalayan Glacier for defining the solute chemistry change. Therefore, modelling the solute chemistry and its spatio-temporal variability across the glaciers, would helpful in investigating the spatial variability of chemical weathering during the ablation season are the important issues that can be convey in the future studies. This is the important issues which have to implement in the future studies.

Published Publication

1. **Shipika Sundriyal**, Tanuj Shukla, S.K. Tiwari, Lekhandra Tripathee, D.P.Dobhal, Uday Bhan (2018): "Deposition of atmospheric pollutant and their chemical characterization in snow pit profile at Dokriani Glacier, Central Himalaya" published in **Journal of Mountain Science**, 15 (10), 2236-2246.

2. **Shipika Sundriyal**, Tanuj Shukla, Lakhendra Tripathee, D P Dobhal (2019): "Natural versus anthropogenic influence on trace elemental concentrations in precipitation at Dokriani Glacier, Central Himalaya, India" published in **Environmental Science and Pollution Research**, 27 (3), 3462-3472.

3. **Shipika Sundriyal**, Rajesh Singh, S.Selvakumar, D.P.Dobhal, Uday Bhan (2021): "A review on hydrochemical changes in proglacial meltwater stream emerging from Dokriani Glacier, West central Himalaya, India" published in **Journal of Geological society of India**, 97(3), 308-314.

Published as Co-author

4. Tanuj Shukla, Jairam Yadav, **Shipika Sundriyal** (2014). "Field training at Glaciology: A way to touch feel and understand" news article published at **Current Science**, Vol. 107 Number 11.

5. Sameer K Tiwari, Amit Kumar, A k Gupta, AkshayVerma, **Shipika Sundriyal**, Jai Ram Yadav, and Rakesh Bhambri (2018): "Evolution of hydro-geochemical processes and solute sources study of Dokriani (Bamak) Glacier melt-waters, Uttarakhand Himalaya, India" Published in **Himalayan Geology**, 39(1),121-133.

6. Amit Kumar, AkshayaVerma, Anupam Anand Gokhale, Rakesh Bhambri, Anshuman Misra, **Shipika Sundriyal**, Dwarika Prasad Dobhal, Naval Kishore (2018)"Hydrometeorological assessments and suspended sediment delivery from a central Himalayan glacier in the upper Ganga basin" published in **Journal of Sediment Research,** 33(2018) 493-509.

7. Tanuj Shukla, **Shipika Sundriyal**, LuckasStanchik, Manish Mehta (2020): "Carbonate and Silicate weathering in glacial environments and its relation to atmospheric CO2 cycling in the Himalayas" Published in **Annals of Glaciology**, 59 (77), 159-170.

8. Tanuj Shukla, **Shipika Sundriyal**Indra S Sen(2020) "Contemporary inorganic carbon fluxes from rapidly changing glacierized watersheds of the Himalaya" published in **Journal of Hydrology**, 587,124972.

CHAPTER 7

REFERENCES

1) Ackerman, T., Erickson, T., & Williams, M. W. (2001). Combining GIS and GPS to improve our understanding of the spatial distribution of snow water equivalence (SWE). Proceedings of ESRI USERS Conference.

2) Ahmad, S., & Hasnain, S. I. (2000). Meltwater characteristics of Garhwal Himalayan glaciers. JOURNAL-GEOLOGICAL SOCIETY OF. INDIA, 56(4), 431–440.

3) Anderson, S., Drever, P., J., I., & Humphrey, N. F. (1997). Chemical weathering in glacial environments. Geology, 25(5), 399–402.

4) Appelo, C. A. J., & Postma, D. (2005). Geochemistry. Groundwater and pollution, 536.

5) Azam, M. F., Wagnon, P., Vincent, C., Ramanathan, A. L., Favier, V., Mandal, A., & Pottakkal, J. G. (2014). Processes governing the mass balance of Chhota Shigri Glacier (western Himalaya, India) assessed by point-scale surface energy balance measurements. The Cryosphere, 8(6), 2195-2217.

6) Azam, M. F., & Srivastava, S. (2020). Mass balance and runoff modelling of partially debris-covered Dokriani Glacier in monsoon-dominated Himalaya using ERA5 data since 1979. Journal of Hydrology, 590, 125432.

7) Bakliwal, P. C., & Das, A. K. (1971). Geology of parts of Kameng district, NEFA. Geol. Surv. India Unpubld. Progress Report for FS-1970-71.

8) Bhattacharjee, S., & Nandy, S. (2017). Petrology and geochemistry of the Himalayan granites from Western Arunachal Pradesh, India. Indian J Geosci, 71(2), 439–448.

9) Bickle, M. J., Chapman, H. J., Tipper, E., Galy, A., Christina, L., & Ahmad, T. (2018). Chemical weathering outputs from the flood plain of the Ganga. Geochimica et Cosmochimica Acta, 225, 146–175.

10) Bisht, H., Arya, P. C., & Kumar, K. (2018). Hydro-chemical analysis and ionic flux of meltwater runoff from Khangri Glacier, West Kameng, Arunachal Himalaya, India. Environmental Earth Sciences, 77(16), 1–16.

11) Blum, J. D., & Erel, Y. (1997). RbSr isotope systematics of a granitic soil chronosequence: The importance of biotite weathering. Geochimica et Cosmochimica Acta, 61(15), 3193–3204.

12) Blum, J. D., Gazis, C. A., Jacobson, A. D., & Page Chamberlain, C. (1998). Carbonate versus silicate weathering in the Raikhot watershed within the High Himalayan Crystalline Series. Geology, 26(5), 411–414.

13) Bolch, T., Kulkarni, A., Kääb, A., Huggel, C., Paul, F., Cogley, J. G., & Stoffel, M. (2012). The state and fate of Himalayan glaciers. Science, 336(6079), 310–314.

14) Bookhagen, B., & Burbank, D. W. (2010). Toward a complete Himalayan hydrological budget: Spatiotemporal distribution of snowmelt and rainfall and their impact on river discharge. Journal of Geophysical Research: Earth Surface, 115(3).

15) Burbank, D. W., Bookhagen, B., Gabet, E. J., & Putkonen, J. (2012). Modern climate and erosion in the Himalaya. Comptes Rendus Geoscience, 344(11–12), 610–626.

16) Calmels, D., Gaillardet, J., Brenot, A., & France-Lanord, C. (2007). Sustained sulfide oxidation by physical erosion processes in the Mackenzie River basin: Climatic perspectives. Geology, 35(11), 1003–1006.

17) Carrico, C. M., Bergin, M. H., Shrestha, A. B., Dibb, J. E., Gomes, L., & Harris, J. M. (2003). The importance of carbon and mineral dust to seasonal aerosol properties in the Nepal Himalaya. Atmospheric Environment, 37(20), 2811–2824.

18) Chauhan, D. S., & Hasnain, S. I. (1993). Chemical characteristics, solute and suspended sediment loads in the meltwaters draining Satopanth and Bhagirath Kharak glaciers, Ganga Basin, India. In IAHS Publications-Publications of the International Association of Hydrological Sciences (Vol. 218, p. 403).

19) Cheng, Q., Bonham-Carter, G., Wang, W., Zhang, S., Li, W., & Qinglin, X. (2011). A spatially weighted principal component analysis for multi-element geochemical data for mapping

locations of felsic intrusions in the Gejiu mineral district of Yunnan, China. Computers &Geosciences, 37(5), 662–669.

20) Cong, Z., Kang, S., Zhang, Y., & Li, X. (2010). Atmospheric wet deposition of trace elements to central Tibetan Plateau. Applied Geochemistry, 25(9), 1415–1421.

21) Cooper, R. J., Wadham, J. L., Tranter, M., Hodgkins, R., & Peters, N. E. (2002). Groundwater hydrochemistry in the active layer of the proglacial zone, Finsterwalderbreen, Svalbard. Journal of Hydrology, 269(3–4), 208–223.

22) Crompton, J. W., Flowers, G. E., Kirste, D., Hagedorn, B., & Sharp, M. J. (2015). Clay mineral precipitation and low silica in glacier meltwaters explored through reaction-path modelling. Journal of Glaciology, 61(230), 1061–1078.

23) Dalai, T. K., Krishnaswami, S., & Sarin, M. M. (2002). Major ion chemistry in the headwaters of the Yamuna river system: Chemical weathering, its temperature dependence and CO2 consumption in the Himalaya. Geochimica et Cosmochimica Acta, 66(19), 3397–3416.

24) Das, A., Chung, C. H., & You, C. F. (2012). Disproportionately high rates of sulfide oxidation from mountainous river basins of Taiwan orogeny: Sulfur isotope evidence. Geophysical Research Letters, 39(12).

25) Dobhal, D. P., Gergan, J. T., & Thayyen, R. J. (2008a). Mass balance studies of the Dokriani Glacier from to, Garhwal Himalaya, India. Bulletin of Glaciological Research, 25, 9–17.

26) Dobhal, D. P., & Mehta, M. (2010). Surface morphology, elevation changes and terminus retreat of Dokriani Glacier, Garhwal Himalaya: implication for climate change. Himalayan Geology, 31(1), 71–78.

27) Draxler, R. R., &Rolph, G. D. (2010). HYSPLIT (HYbrid Single-Particle Lagrangian Integrated Trajectory) model access via NOAA ARL READY website (http://ready.arl.noaa.gov/HYSPLIT.php), NOAA Air Resources Laboratory.

28) Duan, K., & Yao, T. (2003). Monsoon variability in the Himalayas under the condition of global warming. Journal of the Meteorological Society of Japan. Ser. II, 81(2), 251–257.

29) Eichler, A., Schwikowski, M., & Gäggeler, H. W. (2001). Meltwater-induced relocation of chemical species in Alpine firn. Tellus B:Chemical and Physical Meteorology, 53(2), 192–203.

30) Evans, M. J., & Derry, L. A. (2013). Hydrothermal Alkalinity in Central Nepal Rivers. In AGU Fall Meeting Abstracts (pp. 21–0823). Vol.

31) France-Lanord, C., & Derry, L. A. (1997). Organic carbon burial forcing of the carbon cycle from Himalayan erosion. Nature, 390(6655), 65–67.

32) Frey, H., Machguth, H., Huss, M., Huggel, C., Bajracharya, S., Bolch, T., & Stoffel, M. (2014). Estimating the volume of glaciers in the Himalayan–Karakoram region using different methods. The Cryosphere, 8(6), 2313–2333.

33) Gabet, E. J., Wolff-Boenisch, D., Langner, H., Burbank, D. W., & Putkonen, J. (2010). Geomorphic and climatic controls on chemical weathering in the High Himalayas of Nepal. Geomorphology, 122(1–2), 205–210.

34) Gaffen, D. J., & Ross, R. J. (1999). Climatology and trends of US surface humidity and temperature. Journal of Climate, 12(3), 811–828.

35) Garrels, R. M., & MACKENZIE, F. T. (1971). Gregor's denudation of the continents. Nature, 231(5302), 382–383.

36) Geng, H., Kang, S., Jung, H. J., Choël, M., Kim, H., & Ro, C. U. (2010). Characterization of individual submicrometer aerosol particles collected in Incheon, Korea, by quantitative transmission electron microscopy energy dispersive Xray spectrometry. Journal of Geophysical Research: Atmospheres, 115(15).

37) Gergan, J. T., Dobhal, D. P., & Kaushik, R. (1999). Ground penetrating radar ice thickness measurements of Dokriani bamak (glacier), Garhwal Himalaya. Current Science, 169–173.

38) Gislason, S. R., Arnorsson, S., & Armannsson, H. (1996). Chemical weathering of basalt in Southwest Iceland; effects of runoff, age of rocks and vegetative/glacial cover. American Journal of Science, 296(8), 837–907.

39) Godsey, S. E., Kirchner, J. W., & Clow, D. W. (2009). Concentration–discharge relationships reflect chemostatic characteristics of US catchments. Hydrological Processes: An. International Journal, 23(13), 1844–1864.

40) Gorham, E. (1961). Factors influencing supply of major ions to inland waters, with special reference to the atmosphere. Geological Society of America Bulletin, 72(6), 795–840.

41) Graly, J. A., Drever, J. I., & Humphrey, N. F. (2017). Calculating the balance between atmospheric CO_2 drawdown and organic carbon oxidation in subglacial hydrochemical systems. Global Biogeochemical Cycles, 31(4), 709–727.

42) Haritashya, U. K., Singh, P., Kumar, N., & Gupta, R. P. (2006). Suspended sediment from the Gangotri Glacier: Quantification, variability and associations with discharge and air temperature. Journal of Hydrology, 321(1–4), 116–130.

43) Hasnain, S. I., & Thayyen, R. J. (1994). Hydrograph separation of bulk melt-waters of Dokriani Bamak glacier basin, based on electrical conductivity. Current Science, 189–193.

44) Hasnain, S. I., & Thayyen, R. J. (1999a). Controls on the major-ion chemistry of the Dokriani glacier meltwaters, Ganga basin, Garhwal Himalaya, India. Journal of Glaciology, 45(149), 87–92.

45) Hilton, R. G., & West, A. J. (2020). Mountains, erosion and the carbon cycle. Nature Reviews Earth & Environment, 1(6), 284–299.

46) Hindshaw, R. S., Lindsay, M. R., & Boyd, E. S. (2017). Diversity and abundance of microbial eukaryotes in stream sediments from Svalbard. Polar Biology, 40(9), 1835–1843.

47) Hindshaw, R. S., Tipper, E. T., Reynolds, B. C., Lemarchand, E., Wiederhold, J. G., Magnusson, J., & Bourdon, B. (2011). Hydrological control of stream water chemistry in a glacial catchment (Damma Glacier, Switzerland). Chemical Geology, 285(1–4), 215–230.

48) Hodson, A., Tranter, M., & Vatne, G. (2000a). Contemporary rates of chemical denudation and atmospheric CO_2 sequestration in glacier basins: an Arctic perspective. Earth Surface Processes and Landforms, 25(13), 1447–1471.

49) Holland, H. D. (1978). The chemistry of atmospheres and oceans (p. 351). Wiley Interscience.

50) Hren, M. T., Chamberlain, C. P., Hilley, G. E., Blisniuk, P. M., & Bookhagen, B. (2007). Major ion chemistry of the Yarlung Tsangpo–Brahmaputra river: chemical weathering, erosion, and CO_2 consumption in the southern Tibetan plateau and eastern syntaxis of the Himalaya. Geochimica et Cosmochimica Acta, 71(12), 2907–2935.

51) Immerzeel, W. W., Van Beek, L. P., & Bierkens, M. F. (2010). Climate change will affect the Asian water towers. Science, 328(5984), 1382–1385.

52) IrvineFynn, T. D., Hodson, A. J., Moorman, B. J., Vatne, G., & Hubbard, A. L. (2011). Polythermal glacier hydrology: a review. Reviews of Geophysics, 49(4).

53) Jacobson, A. D., Blum, J. D., Chamberlain, C. P., Craw, D., &Koons, P. O. (2003). Climatic and tectonic controls on chemical weathering in the New Zealand Southern Alps. Geochimica et Cosmochimica Acta, 67(1), 29–46.

54) Jacobson, R. L., & Langmuir, D. (1970). The Chemical History of Some Spring Waters in Carbonate Rocks a. Groundwater, 8(3), 5–9.

55) Jeelani, G. H., Bhat, N. A., Shivanna, K., & Bhatt, M. Y. (2011). Geochemical characterization of surface water and spring water in. Journal of Earth System Science, 120(5), 921–932.

56) Kesarwani, K., Pratap, B., Bhambri, R., Mehta, M., Kumar, A., Karakoti, I., & Dobhal, D. P. (2012). Meteorological observations at Chorabari and Dokriani glaciers, Garhwal Himalaya, India. J. Ind. Geol. Cong, 4(1), 125–128.

57) Khadka, U. R., &Ramanathan, A. L. (2013). Major ion composition and seasonal variation in the Lesser Himalayan lake: case of Begnas Lake of the Pokhara. Valley, Nepal. Arabian Journal of Geosciences, 6(11), 4191–4206.

58) Krishnaswami, S., & Singh, S. K. (2005). Chemical weathering in the river basins of the Himalaya, India. Current Science, 841–849.

59) Kristiansen, S. M., Yde, J. C., Bárcena, T. G., Jakobsen, B. H., Olsen, J., & Knudsen, N. T. (2013). Geochemistry of groundwater in front of a warm based glacier in Southeast Greenland. GeografiskaAnnaler: Series A, Physical Geography, 95(2), 97–108.

60) Kumar, A., Verma, A., Dobhal, D. P., Mehta, M., & Kesarwani, K. (2014a). Climatic control on extreme sediment transfer from Dokriani Glacier during monsoon, Garhwal Himalaya (India). Journal of Earth System Science, 123(1), 109–120.

61) Kumar, N., Ramanathan, A. L., Tranter, M., Sharma, P., Pandey, M., Ranjan, P., & Raju, N. J. (2019). Switch in chemical weathering caused by the mass balance variability in a Himalayan glacierized basin: a case of Chhota Shigri Glacier. Hydrological Sciences Journal, 64(2), 179–189.

62) Li, Z., He, Y., Pang, H., Yang, X., Jia, W., HE, X., & ZHANG, N. (2007). Source of major anions and cations of snowpacks in the typical monsoonal temperate glacial region of China. ACTA GEOGRAPHICA SINICA-CHINESE EDITION-, 62(9), 992.

63) Luo, H., & Yanai, M. (1983). The large-scale circulation and heat sources over the Tibetan Plateau and surrounding areas during the early summer of 1979. Part I: Precipitation and kinematic analyses. Monthly Weather Review, 111(5), 922–944.

64) Lutz, A. F., Immerzeel, W. W., Shrestha, A. B., & Bierkens, M. F. P. (2014). Consistent increase in High Asia's runoff due to increasing glacier melt and precipitation. Nature Climate Change, 4(7), 587–592.

65) Mayewski, P. A., Lyons, W. B., Spencer, M. J., Twickler, M., Dansgaard, W., Koci, B., & Honrath, R. E. (1986). Sulfate and nitrate concentrations from a south Greenland ice core. Science, 232(4753), 975–977.

66) Mehta, M., Majeed, Z., Dobhal, D. P., & Srivastava, P. (2012). Geomorphological evidences of post-LGM glacial advancements in the Himalaya: a study from Chorabari Glacier, Garhwal Himalaya, India. Journal of Earth System Science, 121(1), 149–163.

67) Ming, J., Xiao, C., Cachier, H., Qin, D., Qin, X., Li, Z., & Pu, J. (2009). Black Carbon (BC) in the snow of glaciers in west China and its potential effects on albedos. Atmospheric Research, 92(1), 114–123.

68) Mitchell, A. C., & Brown, G. H. (2008). Modeling geochemical and biogeochemical reactions in subglacial environments. Arctic, Antarctic, and Alpine Research, 40(3), 531–547.

69) Nijampurkar, V. N., Bhandari, N., Ramesh, R., & Bhattacharya, K. (1986). Climatic significance of D/H ratios of a temperate glacier in Sikkim. Current Science, 55(18), 910–912.

70) Nijampurkar, V. N., Sarin, M. M., & Rao, D. K. (1993). Chemical composition of snow and ice from Chhota Shigri glacier, Central Himalaya. Journal of Hydrology, 151(1), 19–34.

71) Nijampurkar, V., Rao, K., Sarin, M., & Gergan, J. (2002). Isotopic study on Dokriani Bamak glacier, central Himalaya: implications for climatic changes and ice dynamics. Journal of Glaciology, 48(160), 81–86.

72) Owen, L. A., Finkel, R. C., & Caffee, M. W. (2002). A note on the extent of glaciation throughout the Himalaya during the global Last Glacial Maximum. Quaternary Science Reviews, 21(1–3), 147–157.

73) Pandey, S. K., Singh, A. K., & Hasnain, S. I. (1999). Weathering and geochemical processes controlling solute acquisition in Ganga headwater–Bhagirathi river, Garhwal Himalaya, India. Aquatic Geochemistry, 5(4), 357–379.

74) Parkhurst, D. L., & Appelo, C. A. J. (2013). Description of input and examples for PHREEQC version 3: a computer program for speciation, batch-reaction, one-dimensional transport, and inverse geochemical calculations (No. 6-A43). US Geological Survey.

75) Polesello, S., Comi, M., Guzzella, L., Marinoni, A., Pecci, M., Roscioli, C., & Vuillermoz, E. (2007a). 28 Chemical composition of fresh snow in the Himalaya and Karakoram. In Developments in Earth Surface Processes (Vol. 10, pp. 251–262).

76) Pratap, B., Dobhal, D. P., Bhambri, R., Mehta, M., & Tewari, V. C. (2016). Four decades of glacier mass balance observations in the Indian Himalaya. Regional Environmental Change, 16(3), 643–658.

77) Prestrud Anderson, S., Drever, J. I., & Humphrey, N. F. (1997). Chemical weathering in glacial environments. Geology, 25(5), 399–402.

78) Raghavan, K. (1973). Break-monsoon over India. Monthly Weather Review, 101(1), 33–43.

79) Rai, S. P., Thayyen, R. J., Purushothaman, P., & Kumar, B. (2016). Isotopic characteristics of cryospheric waters in parts of Western Himalayas, India. Environmental Earth Sciences, 75(7), 600.

80) Raina, V. K., & Srivastava, D. (2014). Glacier atlas of India. GSI Publications, 7(1).

81) Raiswell, R. (1984). Chemical models of solute acquisition in glacial melt waters. Journal of Glaciology, 30(104), 49–57.

82) Ramanathan, V. C. P. J., Crutzen, P. J., Kiehl, J. T., & Rosenfeld, D. (2001). Aerosols, climate, and the hydrological cycle. Science, 294(5549), 2119–2124.

83) Ramanathan, V., Chung, C., Kim, D., Bettge, T., Buja, L., Kiehl, J. T., & Wild, M. (2005). Atmospheric brown clouds: Impacts on South Asian climate and hydrological cycle. Proceedings of the National Academy of Sciences, 102(15), 5326–5333.

84) Raymo, M. E., & Ruddiman, W. F. (1992). Tectonic forcing of late Cenozoic climate. Nature, 359(6391), 117–122.

85) Reynolds Jr, R. C., & Johnson, N. M. (1972). Chemical weathering in the temperate glacial environment of the Northern Cascade Mountains. Geochimica et Cosmochimica Acta, 36(5), 537-554.

86) Sharma, M. K., Thayyen, R. J., Jain, C. K., Arora, M., & Lal, S. (2019). Assessment of system characteristics of Gangotri glacier headwater stream. Science of The Total Environment, 662, 842–851.

87) Sharma, P., Ramanathan, A. L., & Pottakkal, J. (2013a). Study of solute sources and evolution of hydrogeochemical processes of the Chhota Shigri Glacier meltwaters, Himachal Himalaya, India. Hydrological Sciences Journal, 58(5), 1128–1143.

88) Brown, G. H. (2002). Glacier meltwater hydrochemistry. Applied Geochemistry, 17(7), 855-883.

89) Sharp, M., Tranter, M., Brown, G. H., & Skidmore, M. (1995). Rates of chemical denudation and CO_2 drawdown in a glacier-covered alpine catchment. Geology, 23(1), 61–64.

90) Shekhar, M. S., Chand, H., Kumar, S., Srinivasan, K., & Ganju, A. (2010). Climate-change studies in the western Himalaya. Annals of Glaciology, 51(54), 105-112.

91) Shrestha, A. B., & Devkota, L. P. (2010). Climate change in the Eastern Himalayas: observed trends and model projections. International Centre for Integrated Mountain Development (ICIMOD).

92) Shrestha, A. B., Giriraj, A., & Kumar, R. (2009). Meeting Report: Snow and glacier melt runoff modelling in the Himalayas. Current Science, 97(7), 985–985.

93) Shrestha, A. B., Wake, C. P., & Dibb, J. E. (1997a). Chemical composition of aerosol and snow in the high Himalaya during the summer monsoon season. Atmospheric Environment, 31(17), 2815–2826.

94) Shrestha, A. B., Wake, C. P., Dibb, J. E., & Mayewski, P. A. (2000). Precipitation fluctuations in the Nepal Himalaya and its vicinity and relationship with some large scale climatological parameters. International Journal of Climatology: A Journal of the Royal Meteorological Society, 20(3), 317–327.

95) Shukla, T., Mehta, M., Jaiswal, M. K., Srivastava, P., Dobhal, D. P., Nainwal, H. C., & Singh, A. K. (2018). Late Quaternary glaciation history of monsoon-dominated Dingad basin, central Himalaya, India. Quaternary Science Reviews, 181, 43–64.

96) Shukla, T., Sundriyal, S., & Sen, I. S. (2020). Contemporary inorganic carbon fluxes from rapidly changing glacierized watersheds of the Himalaya. Journal of Hydrology, 587, 124972.

97) Shukla, T., Sundriyal, S., Stachnik, L., & Mehta, M. (2018a). Carbonate and silicate weathering in glacial environments and its relation to atmospheric CO 2 cycling in the Himalaya. Annals of Glaciology, 59(77), 159–170.

98) Singh, P., & Bengtsson, L. (2004). Hydrological sensitivity of a large Himalayan basin to climate change. Hydrological Processes, 18(13), 2363-2385.

99) Singh, A. K. (1998). Dissolved and sediment load characteristics of Kafni glacier meltwater, Pindar valley, Kumaon Himalaya. Journal of Geological Society of India, 52(3), 905–912.

100) Singh, A. K., & Hasnain, S. I. (2002). Aspects of weathering and solute acquisition processes controlling chemistry of sub- Alpine proglacial streams of Garhwal Himalaya, India. Hydrological Processes, 16(4), 835–849.

101) Singh, P. (2001). Snow and glacier hydrology (Vol. 37). Springer Science & Business Media.

102) Singh, P., Haritashya, U. K., & Kumar, N. (2007a). Meteorological study for Gangotri Glacier and its comparison with other high altitude meteorological stations in central Himalayan region. Hydrology Research, 38(1), 59–77.

103) Singh, V. B., Keshari, A. K., & Ramanathan, A. L. (2020). Major ion chemistry and atmospheric CO_2 consumption deduced from the Batal glacier, Lahaul–Spiti valley, Western Himalaya, India. Environment, Development and Sustainability, 22(7), 6585–6603.

104) Singh, V. B., & Ramanathan, A. L. (2017a). Characterization of hydrogeochemical processes controlling major ion chemistry of the Batal glacier meltwater, Chandra basin, Himachal Pradesh, India. Proceedings of the National Academy of Sciences, India Section A: Physical Sciences, 87(1), 145–153.

105) Singh, V. B., & Ramanathan, A. L. (2017b). Hydrogeochemistry of the Chhota Shigri glacier meltwater, Chandra basin, Himachal Pradesh, India: solute acquisition processes, dissolved load and chemical weathering rates. Environmental Earth Sciences, 76(5), 223.

106) Singh, V. B., Ramanathan, A. L., & Kuriakose, T. (2015). Hydrogeochemical assessment of meltwater quality using major ion chemistry: a case study of Bara Shigri Glacier, western Himalaya, India. National Academy Science Letters, 38(2), 147–151.

107) Singh, V. B., Ramanathan, A. L., Mandal, A., & Angchuk, T. (2015). Transportation of suspended sediment from meltwater of the Patsio Glacier, Western Himalaya, India. Proceedings of the National Academy of Sciences, India Section A: Physical Sciences, 85(1), 169–175.

108) Singh, V. B., Ramanathan, A. L., & Pottakkal, J. G. (2016). Glacial runoff and transport of suspended sediment from the Chhota Shigri glacier, Western Himalaya, India. Environmental Earth Sciences, 75(8), 695.

109) Singh, V. B., Ramanathan, A. L., Pottakkal, J. G., & Kumar, M. (2014). Seasonal variation of the solute and suspended sediment load in Gangotri glacier meltwater, central Himalaya, India. Journal of Asian Earth Sciences, 79, 224–234.

110) Singh, V. B., Ramanathan, A. L., Pottakkal, J. G., & Kumar, M. (2015). Hydrogeochemistry of meltwater of the Chaturangi glacier, Garhwal Himalaya, India. Proceedings of the National Academy of Sciences, India Section A: Physical Sciences, 85(1), 187–195.

111) Singh, V. B., Ramanathan, A. L., Pottakkal, J. G., Linda, A., & Sharma, P. (2013). Temporal variation in the major ion chemistry of Chhota Shigri glacier meltwater, Lahaul–Spiti valley, Himachal Pradesh, India. National Academy Science Letters, 36(3), 335–342.

112) Singh, V. B., Ramanathan, A. L., & Sharma, P. (2015). Major ion chemistry and assessment of weathering processes of the Patsio glacier meltwater, Western Himalaya, India. Environmental Earth Sciences, 73(1), 387–397.

113) Smith, M., Emberlin, J., & Kress, A. (2005). Examining high magnitude grass pollen episodes at Worcester, United Kingdom, using back-trajectory analysis. Aerobiologia, 21(2), 85–94.

114) Souchez, R. A., & Lorrain, R. D. (1975). Chemical sorting effect at the base of an alpine glacier. Journal of Glaciology, 14(71), 261–265.

115) Souchez, R. A., & Lorrain, R. D. (1978). Origin of the basal ice layer from Alpine glaciers indicated by its chemistry. Journal of Glaciology, 20(83), 319–328.

116) Srikantia, S. V., & Padhi, R. N. (1963). Geology and structure of a part of Chandra-Bhaga valley. In Lahaul-Spiti District, Punjab. In Proceeding of national symposium on himalayan geology, Calcutta, Geological Society of India, miscellaneous publication (No (Vol. 15, pp. 229–232).

117) Stachnik, Ł., Majchrowska, E., Yde, J. C., Nawrot, A. P., Cichała-Kamrowska, K., Ignatiuk, D., & Piechota, A. (2016). Chemical denudation and the role of sulfide oxidation at Werenskioldbreen, Svalbard. Journal of Hydrology, 538, 177–193.

118) Sundriyal, S., Bhan, U., Selvakumar, S., Singh, R., & Dobhal, D. P. (2021a). Two Decadal Changes in the Major Ions Chemistry of Melt Water Draining from Dokriani Glacier, central Himalaya, India. Journal of the Geological Society of India, 97(3), 308–314.

119) Sundriyal, S., Shukla, T., Tripathee, L., & Dobhal, D. P. (2020). Natural versus anthropogenic influence on trace elemental concentration in precipitation at Dokriani Glacier, central Himalaya, India. Environmental Science and Pollution Research, 27(3), 3462–3472.

120) Sundriyal, S., Shukla, T., Tripathee, L., Dobhal, D. P., Tiwari, S. K., & Bhan, U. (2018). Deposition of atmospheric pollutant and their chemical characterization in snow pit profile at Dokriani Glacier, Central Himalaya. Journal of Mountain Science, 15(10), 2236–2246.

121) Thayyen, R. J. (2015). Ground ice melt in the catchment runoff in the Himalayan cold-arid system. In IGS Symposium on Glaciology in High-Mountain Asia (pp. 1–6).

122) Thayyen, R. J., & Gergan, J. T. (2010a). Role of glaciers in watershed hydrology: a preliminary study of a' Himalayan catchment'. The Cryosphere, 4(1), 115–128.

123) Thayyen, R. J., Gergan, J. T., & Dobhal, D. P. (2007). Role of glaciers and snow cover on headwater river hydrology in monsoon regime—Micro-scale study of Din Gad catchment, Garhwal Himalaya, India. Current Science, 376–382.

124) Tipper, E. T., Bickle, M. J., Galy, A., West, A. J., Pomiès, C., & Chapman, H. J. (2006). The short term climatic sensitivity of carbonate and silicate weathering fluxes: insight from seasonal variations in river chemistry. Geochimica et Cosmochimica Acta, 70(11), 2737–2754.

125) Torres, M. A., Moosdorf, N., Hartmann, J., Adkins, J. F., & West, A. J. (2017). Glacial weathering, sulfide oxidation, and global carbon cycle feedbacks. Proceedings of the National Academy of Sciences, 114(33), 8716–8721.

126) Tranter, M. (2006). Glacial chemical weathering, runoff composition and solute fluxes. Glacier Science and Environmental, change, 71–75.

127) Tranter, M., Brown, G., Raiswell, R., Sharp, M., & Gurnell, A. (1993). A conceptual model of solute acquisition by Alpine glacial meltwaters. Journal of Glaciology, 39(133), 573–581.

128) Tranter, M., Sharp, M. J., Lamb, H. R., Brown, G. H., Hubbard, B. P., & Willis, I. C. (2002a). Geochemical weathering at the bed of Haut Glacier d'Arolla, Switzerland—a new model. Hydrological Processes, 16(5), 959–993.

129) Tripathee, L., Kang, S., Huang, J., Sillanpää, M., Sharma, C. M., Lüthi, Z. L.,& Paudyal, R. (2014). Ionic composition of wet precipitation over the southern slope of central Himalayas, Nepal. Environmental Science and Pollution Research, 21(4), 2677-2687.

130) Tripathee, L., Kang, S., Sharma, C. M., Rupakheti, D., Paudyal, R., Huang, J., & Sillanpää, M. (2016). Preliminary health risk assessment of potentially toxic metals in surface water of the Himalayan. Rivers, Nepal. Bulletin of Environmental Contamination and Toxicology, 97(6), 855–862.

131) Valdiya, K. S. (1980). The two intracrustal boundary thrusts of the Himalaya. Tectonophysics, 66(4), 323–348.

132) Valdiya, K. S. (1999a). Rising Himalaya: advent and intensification. Curr. Sci, 76(4).

133) Valdiya, K. S. (1999b). Tectonic and lithological characterization of Himadri (Great Himalaya) between Kali and Yamuna rivers, central Himalaya. Him. Geol, 20(2), 1–17.

134) Velbel, M. A. (1985). Geochemical mass balances and weathering rates in forested watersheds of the southern Blue Ridge. American Journal of Science, 285(10), 904–930.

135) Viviroli, D., Dürr, H. H., Messerli, B., Meybeck, M., & Weingartner, R. (2007). Mountains of the world, water towers for humanity: Typology, mapping, and global significance. Water Resources Research, 43(7).

136) Wadham, J. L., Cooper, R. J., Tranter, M., & Bottrell, S. (2007). Evidence for widespread anoxia in the proglacial zone of an Arctic glacier. Chemical Geology, 243(1–2), 1–15.

137) Wadham, J. L., Hodson, A. J., Tranter, M., & Dowdeswell, J. A. (1998). The hydrochemistry of meltwaters draining a polythermal based, high Arctic glacier, south Svalbard. I. The Ablation Season. Hydrological Processes, 12(12), 1825–1849.

138) Wadham, J. L., Tranter, M., Hodson, A. J., Hodgkins, R., Bottrell, S., Cooper, R., & Raiswell, R. (2010). Hydro- biogeochemical coupling beneath a large polythermal Arctic glacier: Implications for subice sheet biogeochemistry. Journal of Geophysical Research: Earth Surface, 115(4).

139) Wadham, J. L., Tranter, M., Skidmore, M., Hodson, A. J., Priscu, J., Lyons, W. B., & Jackson, M. (2010a). Biogeochemical weathering under ice: size matters. Global Biogeochemical Cycles, 24(3).

140) Wake, C. P., Mayewski, P. A., Li, Z., Han, J., & Qin, D. (1994). Modern eolian dust deposition in central Asia. Tellus B: Chemical and Physical Meteorology, 46(3), 220–233.

141) Wake, C. P., Mayewski, P. A., Ping, W., Qinzhao, Y., Jiankang, H., & Zichu, X. (1992). Anthropogenic sulfate and Asian dust signals in snow from Tien Shan, northwest China. Annals of Glaciology, 16, 45–52.

142) Wake, C. P., Mayewski, P. A., & Spencer, M. J. (1990). A review of central Asian glaciochemical data. Annals of Glaciology, 14, 301–306.

143) Wake, C. P., Mayewski, P. A., Zichu, X., Ping, W., & Zhongqin, L. (1993). Regional distribution of monsoon and desert dust signals recorded in Asian glaciers. Geophysical Research Letters, 20(14), 1411–1414.

144) West, A. J., Bickle, M. J., Collins, R., & Brasington, J. (2002a). Small-catchment perspective on Himalayan weathering fluxes. Geology, 30(4), 355–358.

145) White, A. F., & Brantley, S. L. (2003). The effect of time on the weathering of silicate minerals: why do weathering rates differ in the laboratory and field? Chemical Geology, 202(3–4), 479–506.

146) Williamson, M. A., & Rimstidt, J. D. (1994). The kinetics and electrochemical rate-determining step of aqueous pyrite oxidation. Geochimica et Cosmochimica Acta, 58(24), 5443–5454.

147) Yadav, J. S., Pratap, B., Gupta, A. K., Dobhal, D. P., Yadav, R. B. S., & Tiwari, S. K. (2019). Spatio-temporal variability of near-surface air temperature in the Dokriani glacier catchment (DGC), central Himalaya. Theoretical and Applied Climatology, 136(3), 1513–1532.

148) Yadav, R. R. (2011). Long-term hydroclimatic variability in monsoon shadow zone of western Himalaya, India. Climate Dynamics, 36(7–8), 1453–1462.

149) Yalcin, K., Wake, C. P., Kreutz, K. J., Germani, M. S., & Whitlow, S. I. (2006). Ice core evidence for a second volcanic eruption around 1809 in the Northern Hemisphere. Geophysical Research Letters, 33(14).

150) Yde, J. C., Riger-Kusk, M., Christiansen, H. H., Knudsen, N. T., & Humlum, O. (2008). Hydrochemical characteristics of bulk meltwater from an entire ablation season, Longyearbreen, Svalbard. Journal of Glaciology, 54(185), 259–272.

151) Zhu, B., Yu, J., Qin, X., Rioual, P., Liu, Z., Zhang, Y., & Xiong, H. (2013). The significance of mid-latitude rivers for weathering rates and chemical fluxes: evidence from northern Xinjiang rivers. Journal of Hydrology, 486, 151–174.

152) Zongxing, L., Yuanqing, H., Hongxi, P., Theakstone, W. H., Ningning, Z., Xianzhong, H., & Jiankuo, D. (2009). Environmental significance of snowpit chemistry in the typical monsoonal temperate glacier region, Baishui glacier no. 1, Mt Yulong, China. Environmental geology, 58(6), 1319-1328.